Appendices

Appendix 1: List of Materials for Limbal Epithelial Cell Culture

3.1.1 Culture of Limbal Explants on Nanofibrous Membranes, page 46		
Product	**Company**	**Catalog Number**
70% Ethanol	Penta	E03801
PBS pH 7.4 (10x)	Gibco	70011-036
Fibronectin	Sigma-Aldrich	10838039001
DMEM/F12 (1:1, GlutaMAX)	Gibco	31331-028
100x Antibiotic-antifungal solution	Gibco	15240-062
12 Well TC-Treated Polystyrene Permeable Support Companion Plate	Falcon	353503

3.1.2 Preparation of Fibrin Gel, page 47				
		Concentration after reconstitution	**Dilute in PBS**	**Final concentration after dilution (ready to use)**
Component 1	Human Fibrinogen (Sealer protein lyophilized Concentrate)	91 mg/ml	1 ml (reconstituted sol.) + 8 ml PBS	Fibrinogen 10mg/ml
Solvent for component 1	Aprotinin solution	3000 KIU/ml		Aprotinin 333 KIU/ ml
Component 2	Human thrombin (Thrombin lyophilized)	500 IU/ml	0.5 ml (reconstituted sol.) + 24.5 ml PBS	Thrombin 10 IU/ml
Solvent for component 2	$CaCl_2$	40 µmol/ml		$CaCl_2$ 0.8 µmol/ml

3.1.4 Explant Culture, page 48		
Product	**Company**	**Catalog Number**
DMEM/F12 (1:1, GlutaMAX)	Gibco	31331-028

100x Antibiotic-antifungal solution	Gibco	15240-062
100nm Cholera Toxin	Sigma	C8052
Human serum	Bio&Sell	HU.SE.0500
Fetal bovine serum	Gibco	10500-064
Insulin-Transferrin-Selenium (100x)	Gibco	41400-045
Hydrocortisone	VUAB Pharma A.S., Roztoky	256084
Adenin hydrochlorid	Sigma	A9795
EGF	Gibco	PH60311L
Tranexamic Acid	Supelco	PHR1812
Well TC-Treated Polystyrene Permeable Support Companion Plate	Falcon	353503

3.1.5 Reverse Transcription-Quantitative Real-Time Polymerase Chain Reaction (RT-qPCR), page 48

Product	**Company**	**Catalog Number**
Dispase II	Gibco	17105-041
TrypLE™ Express	Gibco	12604021
Dual Chamber Cell counting slides	Bio-Rad	1450011
Trypan blue dye 0.40%	Bio-Rad	1450013
TC20™ Automated Cell Counter	Bio-Rad	1450102
Universal 32 R centrifuge	Hettich Zentrifugen	1610
RNeasy® Micro Kit	Qiagen	74004
Eppendorf Biophotometer Spectrophotometer	Eppendorf	6131
iScript cDNA synthesis kit	Bio-Rad	1708890
Hard Shell 96-well PCR plate	Bio-Rad	HSR9901
SsoAdvanced Universal SYBR Green Supermix RT-qPCR Kit	Bio-Rad	1725270
CFX Connect Real-Time PCR Detection System	Bio-Rad	1855201

3.1.5 Reverse Transcription-Quantitative Real-Time Polymerase Chain Reaction (RT-qPCR), page 48

Gene name, Gene symbol	**Forward Primer**	**Reverse Primer**	**Size (bp)**

Hypoxanthine phosphoribosyltransferase 1, *HPRT1*	TCTTTGCTGACCTGCTGGATTAC	GTCTGCATTGTTTTGCCAGTGTC	214
Ribosomal protein L32, *RPL32*	CTCAGACCCCTTGTGAAGCC	TTGCTTCCATAACCAATGTTGG	179
POU class 5 homeobox 1, *OCT4*	AGAAGTGGGTGGAGGAAGCTG	CCAGGTTGCCTCTCACTCG	123
SRY-box transcription factor 2, *SOX2*	GCTAGTCTCCAAGCGACGAAA	GCCTCTCCTTGAAAAATATTGGC	137
Krüppel like factor 4, *KLF4*	CCACACTTGTGATTACGCGG	GAATTTCCATCCACAGCCGT	127
Marker of proliferation Ki-67, *MKI67*	CTTTGGGTGCGACTTGACG	GTCGACCCCGCTCCTTTT	199
Tumor protein p63, *ΔNp63α*	TATCCGCATGCAGGACTCG	GAGCCAGAAGAAAGGACAGCAG	127
ATP binding cassette subfamily G member 2 (Junior blood group), *ABCG2*	GAGCCTACAACTGGCTTAGACTCAA	TGATTGTTCGTCCCTGCTTAGAC	85
ATP-binding cassette sub-family B member 5, *ABCB5*	CAGCAAGGGAAGCAAATGC	GGGTTTCGAACTAAGGCACG	139
Keratin 3, *KRT3*	GGATGTGGACAGTGCCTATATGAA	AGCACCACAGATGTGTCACTGAT	144
Keratin 7, *KRT7*	ATGGAGTGGGAGCCGTGAA	AGCCTTCAGGAGCCCAGG	146
Keratin 8, *KRT8*	CGAGATCGCCACCTACAGGA	CGAGATCGCCACCTACAGGA	116
Keratin *12, KRT12*	GGAGATCGAGCTACAGTCCCA	TCCAGGTTGCTGATGAGCTG	120
Keratin 14, *KRT14*	TCTCCTCTGGATCGCAGTCA	GCCTCAGTTCTTGGTGCGA	131
Keratin 15, *KRT15*	AGGGCCTGAATGAGGAGCTAG	CCTCATCTCTGCCAGCACAC	146
Integrin subunit beta 1, *ITGB1*	ACATTTGAGTGTGGCGCGT	CACACTGTCCGCAGACGC	163
Nerve growth factor receptor, *NGFR*	CGTATTCCGACGAGGCCA	ACCGTGTAATCCAACGGCC	138

CCAAT enhancer binding protein delta, *CEBPD*	GAGAACGAGAAGCTGCACCAG	TGAGGTATGGGTCGTTGCTG	170
Leucine rich repeats and immunoglobulin like domains 1, *LRIG1*	CCGTGGCTAATTGGCAGG	TGTCCTTGCCCACCATAGC	178
Insulin like growth factor binding protein 5, *IGFBP5*	AGCTACCGCGAGCAAGTCAA	TCGGAGATGCGGGTGTGT	125
Actin alpha 2, smooth muscle, *ACTA2*	CTTTGCTGGGGACGATGC	TCCCATTCCCACCATCAC C	85
CD34 molecule, *CD34*	GGCATCTGCCTGGAGCAA	CACCTCAGACTGGGCAAGGA	153
Thy-1 cell surface antigen, *THY1*	TCCCCACCCATCTCCTCC	CGAGGTGTTCTGAGCCAGC	90
Visual system homeobox 2, *VSX2*	AAGAAACGGAAGAAGCGGC	TGGGTAGTGGGCTTCGTTG	91
Fibulin 1, *FBLN1*	CTGCGAATGCAAGACGGG	CAGCGTGTTCTCGCACTTGT	115

Appendix 2: List of Materials for Oral Mucosa Epithelial Cell Culture

3.2.1 Oral Mucosal Tissue Retrieval, page 50		
Product	**Company**	**Catalog Number**
Betadine 100 mg/ml	Egis	32/389/92-S/C
NaCl 0.9% 1000 ml	B. Braun	2305960
BASE•128	Alchimia	BAS 006-00
6-mm biopsy punch	Kai Medical	BP-60F

3.2.5 Preparation of Cell Suspension, page 53		
Product	**Company**	**Catalog Number**
BASE•128	Alchimia	BAS 006-00
PBS pH 7.4 (10x)	Gibco	70011-036
DMEM/F12 (1:1, GlutaMAX)	Gibco	31331-028
100x Antibiotic-antifungal solution	Gibco	15240-062
100nm Cholera Toxin	Sigma	C8052
Human serum	Bio&Sell	HU.SE.0500
Fetal bovine serum	Gibco	10500-064
Insulin-Transferrin-Selenium (100x)	Gibco	41400-045
Hydrocortisone	VUAB Pharma A.S., Roztoky	256084
Adenin hydrochlorid	Sigma	A9795
Triiodothyronine	Sigma	T6397
EGF	Gibco	PH60311L
Tranexamic Acid	Supelco	PHR1812
Dispase II	Gibco	17105-041
0.05% Trypsin-EDTA (1X)	Gibco	25300-054
RNAlater™	Sigma	R0901
Millex-GV Filter, 0.22 µm, PVDF, 13 mm	Merck Millipore	SLGVR13SL
Tissue Culture Plates 24 wells, sterile	VWR	734-2325
Petri dish 35mm, Sterile	Nunc	153066
Petri dish 60mm, Sterile	VWR	10062-890
Cell scraper (11mm blade)	Corning	C5981-100EA

pluriStrainer Mini 70 µm (Cell Strainer)	PluriSelect	43-10070-60
Dual Chamber Cell counting slides	Bio-Rad	1450011
Trypan blue dye 0.40%	Bio-Rad	1450013
TC20™ Automated Cell Counter	Bio-Rad	1450102
Universal 32 R centrifuge	Hettich Zentrifugen	1610

3.2.8 Harvesting Cultured Cells after Cell Confluence, page 55

Product	Company	Catalog Number
PBS pH 7.4 (10x)	Gibco	70011-036
Dispase II	Gibco	17105-041
DMEM/F12 (1:1, GlutaMAX)	Gibco	31331-028
TrypLE™ Express	Gibco	12604-021
Millex-GV Filter, 0.22 µm, PVDF, 13 mm	Merck Millipore	SLGVR13SL
Dual Chamber Cell counting slides	Bio-Rad	1450011
Trypan blue dye 0.40%	Bio-Rad	1450013
TC20™ Automated Cell Counter	Bio-Rad	1450102
Universal 32 R centrifuge	Hettich Zentrifugen	1610
RNeasy® Micro Kit	Qiagen	74004
Eppendorf Biophotometer Spectrophotometer	Eppendorf	6131
iScript cDNA synthesis kit	Bio-Rad	1708890
Hard Shell 96-well PCR plate	Bio-Rad	HSR9901
SsoAdvanced Universal SYBR Green Supermix RT-qPCR Kit	Bio-Rad	1725270
CFX Connect Real-Time PCR Detection System	Bio-Rad	1855201

3.2.4 Hematoxylin and Eosin Staining, page 52

Product	Company	Catalog Number
Hematoxylin Harris	Penta	14680-11000
Eosin Y	Merck	17372-87-1
Ethanol 96% p.a.	Penta	70390-11001
HCl 35%	Penta	7647-01-0
Ethanol 100%	Penta	71250-11001
Solakryl	Penta	2001280115
Xylene	Lach-ner s.r.o.	1330-20-7
Aquatex	Merck	1.08562.0050

OCT cryomount	Penta	00890-EX
Ethanol 70%	Penta	70392-11001
Carbol-xylene	Penta	180407V

3.2.10 Immunofluorescence, page 56

Product	Company	Catalog Number
Tween® 20	Sigma-Aldrich	P1379
Triton X® 100	Roth	3051.3
Normal Goat serum	Cell Signaling Technology	5425
Bovine Serum Albumin	Sigma	A9647
PBS pH 7.4 (10x)	Gibco	70011-036
DAPI	Invitrogen	
Mowiol® 4-88	Aldrich	81381
Superfrost® Plus	Thermo Scientific	J1800AMNZ
Paraformladehyde	Fluka Chemical	76240

3.2.11 Reverse Transcription Quantitative Real-time PCR (RT-qPCR), page 58

Gene name, Gene symbol	Forward Primer	Reverse Primer	Size (bp)
Hypoxanthine phosphoribosyltransferase 1, *HPRT1*	TCTTTGCTGACCTGCTGGATTAC	GTCTGCATTGTTTTGCCAGTGTC	214
Ribosomal protein L32, *RPL32*	CTCAGACCCCTTGTGAAGCC	TTGCTTCCATAACCAATGTTGG	179
POU class 5 homeobox 1, *OCT4*	AGAAGTGGGTGGAGGAAGCTG	CCAGGTTGCCTCTCACTCG	123
SRY-box transcription factor 2, *SOX2*	GCTAGTCTCCAAGCGACGAAA	GCCTCTCCTTGAAAAATATTGGC	137
Krüppel like factor 4, *KLF4*	CCACACTTGTGATTACGCGG	GAATTTCCATCCACAGCCGT	127
Nanog homeobox, *NANOG*	CAGAACTGTGTTCTCTTCCACCC	CCATTGCTATTCTTCGGCCA	198
Paired box 6, *PAX6*	GCCAGGGCAACCTACGC	TCTATTTCTTTGCAGCTTCCGC	139
Marker of proliferation Ki-67, *MKI67*	CTTTGGGTGCGACTTGACG	GTCGACCCCGCTCCTTTT	199
Proliferating cell nuclear antigen, *PCNA*	TCTGCAAGTGGAGAACTTGGAA	TTCAGGTACCTCAGTGCAAAAGTTAG	131
Tumor protein p63, *ΔNp63α*	TATCCGCATGCAGGACTCG	GAGCCAGAAGAAAGGACAGCAG	127

ATP binding cassette subfamily G member 2 (Junior blood group), *ABCG2*	GAGCCTACAACTGGCTTAGACTCAA	TGATTGTTCGTCCCTGCTTAGAC	85
Keratin 3, *KRT3*	GGATGTGGACAGTGCCTATATGAA	AGCACCACAGATGTGTCACTGAT	144
Keratin 7, *KRT7*	ATGGAGTGGGAGCCGTGAA	AGCCTTCAGGAGCCCAGG	146
Keratin 8, *KRT8*	CGAGATCGCCACCTACAGGA	AGCTCAGACCACCTGCATAGC	116
Keratin *12, KRT12*	GGAGATCGAGCTACAGTCCCA	TCCAGGTTGCTGATGAGCTG	120
Keratin 13, *KRT13*	GAAGATCCGTGACTGGCACC	TCCAGGATGACCCGGTTGT	135
Keratin 14, *KRT14*	TCTCCTCTGGATCGCAGTCA	GCCTCAGTTCTTGGTGCGA	131
Keratin 17, *KRT17*	GGATGCCCACCTGACTCAGTA	GATGACCTTGCCATCCTGGA	91
Keratin 15, *KRT15*	AGGGCCTGAATGAGGAGCTAG	CCTCATCTCTGCCAGCACAC	146
Keratin 19, *KRT19*	CGAGCTAGAGGTGAAGATCCG	TGTCGATCTGCAGGACAATCC	152
Aldehyde dehydrogenase 3 family member A1, *ALDH3A1*	GAGATCTTCGGGCCTGTGC	CCACCCCACCACTGGATG	160
Nestin, *NESTIN*	GGCTGCGGGCTACTGAAA	AGCGATCTGGCTCTGTAGGC	80
Integrin subunit beta 1, *ITGB1*	ACATTTGAGTGTGGCGCGT	CACACTGTCCGCAGACGC	163
Nerve growth factor receptor, *NGFR*	CGTATTCCGACGAGGCCA	ACCGTGTAATCCAACGGCC	138
Leucine rich repeats and immunoglobulin like domains 1, *LRIG1*	CCGTGGCTAATTGGCAGG	TGTCCTTGCCCACCATAGC	178
Insulin like growth factor binding protein 5, *IGFBP5*	AGCTACCGCGAGCAAGTCAA	TCGGAGATGCGGGTGTGT	125

Appendix 3: Interleukin-13 increases the stemness of limbal epithelial stem cells cultures

PLOS ONE

RESEARCH ARTICLE

Interleukin-13 increases the stemness of limbal epithelial stem cells cultures

Peter Trosan[1,2☯*], **Joao Victor Cabral**[1☯], **Ingrida Smeringaiova**[1], **Pavel Studeny**[3], **Katerina Jirsova**[1]

1 Laboratory of the Biology and Pathology of the Eye, First Faculty of Medicine, Institute of Biology and Medical Genetics, Charles University and General University Hospital in Prague, Prague, Czech Republic, **2** Department of Ophthalmology, Rostock University Medical Center, Rostock, Germany, **3** Ophthalmology Department of 3rd Medical Faculty and University Hospital Kralovske Vinohrady, Prague, Czech Republic

☯ These authors contributed equally to this work.
* peter.trosan@med.uni-rostock.de

OPEN ACCESS

Citation: Trosan P, Cabral JV, Smeringaiova I, Studeny P, Jirsova K (2022) Interleukin-13 increases the stemness of limbal epithelial stem cells cultures. PLoS ONE 17(8): e0272081. https://doi.org/10.1371/journal.pone.0272081

Editor: Alexander V. Ljubimov, Cedars-Sinai Medical Center, UNITED STATES

Received: November 29, 2021

Accepted: July 12, 2022

Published: August 2, 2022

Data Availability Statement: All data underlying the findings described in the paper are fully available at the address: osf.io/fkuzw.

Funding: This work was supported by Norway Grants and Technology Agency of the Czech Republic within the KAPPA Programme (project TO01000099), by project Ministry of Education, Youth and Sports BBMRI_CZ LM2018125, and by Bundesministerium für Bildung und Forschung (BMBF) (FKZ 01IO1803). Institutional support (Charles University, Prague) was provided by program Cooperatio: Medical Diagnostics and

Abstract

This study aimed to determine the effect of interleukin-13 (IL13) on the stemness, differentiation, proliferation, clonogenicity, and morphology of cultured limbal epithelial cells (LECs). Human limbal explants were used to culture LECs up to the second passage (P0-P2) with or without IL13 (IL13+ and IL13-, respectively). Cells were analyzed by qPCR (for the expression of ΔNp63α, BMI-1, keratin (K) 3, K7, K12, K14, K17, mucin 4, and MKI67) and immunofluorescence staining for p63α. The clonogenic ability was determined by colony-forming assay (CFA), and their metabolic activity was measured by WST-1 assay. The results of the CFA showed a significantly increased clonogenic ability in P1 and P2 cultures when LECs were cultured with IL13. In addition, the expression of putative stem cell markers (ΔNp63α, K14, and K17) was significantly higher in all IL13+ cultures compared to IL13-. Similarly, immunofluorescence analysis showed a significantly higher percentage of p63α positive cells in P2 cultures with IL13 than without it. LECs cultures without IL13 lost their cuboidal morphology with a high nucleocytoplasmic ratio after P1. The use of IL13 also led to significantly higher proliferation in P2, which can be reflected by a higher ability to reach confluence in P2 cultures. On the other hand, IL13 had no effect on corneal epithelial cell differentiation (K3 and K12 expression), and the expression of the conjunctival marker K7 significantly increased in all IL13+ cultures compared to the respective cell culture without IL13. This study showed that IL13 enhanced the stemness of LECs by increasing the clonogenicity and the expression of putative stem cell markers of LECs while maintaining their stem cell morphology. We established IL13 as a culture supplement for LESCs, which increases their stemness potential in culture, even after the second passage, and may lead to the greater success of LESCs transplantation in patients with LSCD.

Introduction

The corneal epithelium undergoes continuous renewal throughout life but has a limited capacity to renew itself [1]. Maintenance of the epithelium is provided by a population of limbal

Basic Medical Sciences (JVC, KJ, PT). The funders had no role in study design, data collection and analysis, decision to publish, or preparation of the manuscript.

Competing interests: The authors have declared that no competing interests exist.

epithelial stem cells (LESCs), which reside in the basal layer of the limbus, the transition zone between the cornea and the conjunctiva [2]. LESCs are slow cycling and divide asymmetrically to self-renew and differentiate to maintain the corneal epithelium [3,4]. The limbus provides a unique environment—niche, which is morphologically complex with dense innervation and vascularization [5,6]. The niche of stem cells plays a crucial role in cell division, proliferation, differentiation, migration, and maintaining their stemness. It consists of cells, the extracellular matrix, cytokines, and growth factors [7]. As already demonstrated, various growth factors could induce LESCs proliferation and migration [8–11], regulation of apoptosis [12], or differentiation [13]. Because the properties of stem cells are unique, it is challenging to mimic their environment outside the niche. Therefore, the usage of LESCs for a more prolonged culture and its possible application in treatment are limited.

It is crucial for scientific and therapeutic use to search for endogenous factors that could prolong the culture of LESCs. Supplementation of culture medium with NGF extended the life span of LESCs cultures *in vitro* and increased the expression of LESCs' putative markers *ΔNp63α* and *ABCG2* [14]. The expression of the *p63* gene is crucial for the stemness of LESCs [15]. While *TP63* transactivated isoforms (TAp63) participate in senescence and metabolism [16], the β and μ isoforms of *ΔNp63* gene play a role in epithelial differentiation during corneal regeneration, and the α variant is responsible for maintaining the stem/progenitor cells [15]. A higher percentage of the stem cell marker p63 in the sheets of transplanted limbal epithelial cells (LECs) was shown to be related to the success rate of transplantation in patients with limbal stem cell deficiency (LSCD) [17].

Our previous work found a positive effect of interleukin-13 (IL13) on proliferative activity and *ΔNp63α* gene expression in the conjunctival epithelium generated from limbal explants [18]. The effect of IL13 on increasing the expression of the *ΔNp63α* gene in conjunctival cultures leads to the idea of its role in maintaining stemness and using it as part of the medium for the culture of LESCs from limbal explants.

As a T helper 2-type cytokine, which regulates the responses of lymphocytes, myeloid cells, and nonhematopoietic cells [19], IL13 is considered one of the anti-inflammatory interleukins. The effect of IL13 on LESCs or stem cells in general is not widely studied. It is essential during early myelopoiesis when, together with the stem cell factor (SCF), it induces the proliferation of Lin-Sca-1+ progenitor cells and, together with the granulocyte-macrophage-SCF, enhances their colony formation [20]. Similarly as with IL4, IL13 can activate the STAT6 signaling pathway [19], which leads to increased clonogenic potential of prostate stem-like cells [21]. Recently, secreted IL13 was found to promote intestinal stem cell self-renewal by initiating the Foxp1 transcription factor expression, associated with the β-catenin signaling pathway responsible for maintaining their stemness [22]. Together with our observation of the role of IL13 in the stemness of conjunctival epithelial cells, it makes IL13 a promising stem cell research target. In this study, we investigated the role of IL13 in the stemness, differentiation, clonogenicity, and proliferation of LESCs.

Materials and methods

Donor corneal tissue

The study adhered to the tenets set out in the Declaration of Helsinki. Donor tissue procurement met all Czech legal requirements, including the absence of the donor in the national register of persons opposed to postmortem withdrawal of tissues and organs. On the use of the corneoscleral rim based on Czech legislation on specific health services (Law Act No. 372/2011 Coll.), informed consent is not required if the presented data are anonymized in the form. Forty corneoscleral rims were obtained from cadaver donor corneas within 24 h after death

and stored in Eusol-C preservation medium (Alchimia, Padova, Italy) until transplantation. The mean donor age ± standard deviation (SD) was 59.3 ± 9.9 (range 41–75 years).

Preparation of limbal explants and cell culture

The donor corneoscleral rims were washed three times in Dulbecco's modified Eagle's medium (DMEM)/F12 (1:1, GlutaMAX) containing 1% of 100× Antibiotic-Antimycotic (AA, Thermo Fisher Scientific, Waltham, MA, USA). Then each corneoscleral rim was cut into 12 pieces (approximately 2 × 3 mm) and washed three times in DMEM/F12 medium with 1% AA. Six explants were placed directly on the plastic bottom of the 24-well plate (one explant per well), and six pieces were placed on Thermanox plastic cell culture coverslips (Nunc, Thermo Fisher Scientific, Rochester, NY, USA) present on the bottom of the wells. Cultures grown on coverslips were used for immunostaining, and the explant grown on plastic for all other experiments. Each explant was covered with 50 μl of complete medium consisting of 1:1 DMEM/F12, 10% FBS, 1% AA, 10 ng/ml recombinant EGF, 0.5% insulin-transferrin-selenium (Thermo Fisher Scientific), 5 μg/ml hydrocortisone, 10 μg/ml adenine hydrochloride and 10 ng/ml cholera toxin (Sigma-Aldrich, Darmstadt, Germany) and maintained at 37˚C in 5% CO_2. Complete medium was changed every day until cell outgrowth was seen. The tissue was then covered with 250 μl of complete medium, which was changed three times a week until the cells were 90–100% confluent. Half of the donor explants were cultured in a complete medium supplemented with 10 ng/ml recombinant human IL13 (BioLegend, San Diego, CA, USA). Similarly, after passage, cells were cultured in a complete medium with (IL13+) or without IL13 (IL13-). When primary cultures (P0) and cells after passage 1 (P1) were 90–100% confluent, cells were passaged using TrypLE Express (Gibco, Thermo Fisher Scientific). After detaching the culture, cells were seeded again on the plastic bottom or Thermanox coverslip in 24-well plates at concentrations of 1.5×10^4 cells per well. The rest of the cells were stored in Trizol (Molecular Research Center, Cincinnati, OH, USA) for subsequent RNA isolation. All experiments were carried out on P0, P1, and P2 cells and repeated at least three times.

Morphology, cell growth, and cell viability

Expanded LECs were monitored, and the beginning of cell outgrowth, confluence, cell morphology, viability and contamination by fibroblast-like cells were evaluated under an inverted microscope (Olympus CX41, Olympus, Tokyo, Japan). After each passage, cell viability was defined by staining with 0.4% trypan blue (Gibco, Thermo Fisher Scientific). Both unstained live cells and stained dead cells were counted with a hemocytometer and calculated as follows: viability (%) = live cells/ (live + dead cells) × 100. The percentage of successfully cultured rims was calculated as from how many corneoscleral rims the cell culture reached confluence to the total number of rims. The percentage of fibroblast-like cells contamination was calculated as how many cultures had contamination to the overall number of cultures. Culture is taken here as cell culture from one explant. From one rim 3 explants cultures were cultured with IL13 and 3 without. If one culture had fibroblast-like cell contamination, just other two were passaged to subsequent culture.

Preparation of mouse 3T3 feeder layer

The 3T3 mouse fibroblasts were cultured in DMEM supplemented with 10% FBS and 1% AA and kept at 37˚C and 5% CO_2. At 80–90% confluence, 3T3 cells were treated with 12 μg/ml mitomycin-C Kyowa (NORDIC Pharma, Prague, Czech Republic) for 2 h at 37 ˚C under 5% CO_2 to arrest cell growth. After incubation, cells were washed with PBS three times, detached

with TrypLE Express for 2 to 4 min, and seeded in a 6-well plate at a density of 3 x 10^5 cells per well. Cells were used within 24 h of preparation.

Colony-forming assay (CFA)

After reaching at least 80% confluence, the cell cultures were passaged to obtain a single-cell suspension. After P1 and P2, 1000 cultured cells were seeded in 6-well plates containing growth-arrested 3T3 mouse fibroblasts. All experiments were carried out at least in triplicate for each donor and condition (i.e., IL13- and IL13+). The LECs were kept at 37 ˚C and 5% CO_2, and after 12 days of culture, colonies were fixed with cold methanol for 30 min at -20˚C. Subsequently, the cells were rehydrated with PBS and stained for 5 min at 37˚C with 2% rhodamine B (Sigma-Aldrich). After that, rhodamine B was removed, and the colonies were washed with tap water until optimal staining intensity was achieved. The plates were photographed and manually computed by using Fiji image processing software (https://imagej.net/Fiji). Only bright-purple colonies were counted, small dots were excluded. The colony growth was monitored during the colony-formation phase under a microscope. The total colony-forming efficiency (CFE) (%) was calculated using the following equation:

$$CFE\ (\%) = \frac{number\ of\ colonies}{number\ of\ seeded\ cells}\ x\ 100$$

Immunocytochemistry

The cells for immunocytochemistry (ICC) cultured on Thermanox coverslips were at 90 −100% confluency fixed in 4% paraformaldehyde for 20 min at room temperature. Immunocytochemical staining was performed for the p63α isotype encoded by the tumor protein P63 gene, *TP63*. After fixation, the cell membranes were permeabilized with 0.33% Triton X-100 (Sigma-Aldrich) diluted in PBS, followed by a 1 h incubation at room temperature with primary p63α antibody (Cell Signalling Technology, Danvers, MA, USA; cat. No: 4892) diluted in 0.1% bovine serum albumin. The cells were then rinsed three times in 0.5% Tween 20 and incubated for 1 h at room temperature with the Alexa Fluor 594 conjugated goat anti-rabbit IgG secondary antibody (Life Technologies, Eugene, OR, USA; cat. No. A11037). After rinsing three times in 0.5% Tween 20, followed by rinsing in PBS, cells were mounted with Vecta-Shield-DAPI (4′ 6-diamidino-2-phenylindole) (Vector Laboratories, Burlingame, CA, USA) to counterstain nuclear DNA. Cell samples were examined by fluorescence microscopy (Nikon ECLIPSE Ni-U, Nikon) at ×100 and ×200 magnifications. At least 1000 cells were evaluated to calculate the percentage of positive cells.

Quantitative real-time polymerase chain reaction (qPCR)

The expression of the *GAPDH* (glyceraldehyde-3-phosphate dehydrogenase), *ΔNp63α*, *BMI-1*, *K3*, *K7*, *K12*, *K14*, *K17*, *mucin 4* (*Muc4*), and *MKI67* genes was detected by qPCR. Cells were collected after each passage (P0-P2), transferred to Eppendorf tubes containing 500 μl of TRI Reagent (Molecular Research Center, Cincinnati, OH, USA), and total RNA was extracted according to the manufacturer's instructions, followed by reverse transcription, which has been described previously [18]. Briefly, 1 μg of RNA was treated with deoxyribonuclease I (Promega, Madison, WI, USA) and used for reverse transcription (RT). First-strand complementary DNA (cDNA) was synthesized using M-MLV (Moloney murine leukemia virus) reverse transcriptase and random primers (Promega) in a total reaction volume of 25 μl.

The qPCR was performed in a CFX Connect Real-Time PCR Detection System (Bio-Rad, Hercules, CA, USA). The sequences of the primers used are summarized in Table 1. The

Table 1. Primers used for quantitative real-time PCR.

Gene (human)	Sequence (5′→3′)	GenBank accession number	Product size (bp)
GAPDH	F: GAAGGGGTCATTGATGGCAAC R: GGGAAGGTGAAGGTCGGAGTC	NM_001289746.1	108
ΔNp63α	F: GAGGTTGGGCTGTTCATCAT R: GAGGAGAATTCGTGGAGCTG	NM_001114980.1	174
BMI-1	F: GCTCGCATTCATTTTCTGCT R: ACACACATCAGGTGGGGATT	NM_005180.8	163
K3	F:GGATGTGGACAGTGCCTATATG R: AGATAGCTCAGCGTCGTAGAG	NM_057088.2	106
K7	F: AGGATGTGGTGGAGGACTTC R: CTTGCTCATGTAGGCAGCAT	NM_005556.3	116
K12	F: CCAGGTGAGGTCAGCGTAGAA R: CCTCCAGGTTGCTGATGAGC	NM_005556.3	352
K14	F: TTCTGAACGAGATGCGTGAC R: GCAGCTCAATCTCCAGGTTC	NM_000526.4	189
K17	F: GCTGCTACAGCTTTGGCTCT R: GACGGGCATTGTCAATCTGT	NM_000422.2	315
MUC4	F: TCCGTGTCCTGCTGGATAACC R: GTTGCGGCTCAGGAGGACTC	NM_018406.6	104
MKI67	F: CTTTGGGTGCGACTTGACG R: GTCGACCCCGCTCCTTTT	NM_002417	199

https://doi.org/10.1371/journal.pone.0272081.t001

sequence specificity of all primers was confirmed via BLAST (http://www.ncbi.nlm.nih.gov/blast/). Conventional reverse transcription PCR was performed to confirm that only a single band was obtained. The PCR products were electrophoresed on 1% agarose gels containing GelRed Nucleic Acid Gel Stain (Biotium, Fremont, CA, USA). The qPCR parameters included initial denaturation at 95 ˚C for 2 min, 40 cycles of denaturation at 95 ˚C for 5 s, and annealing at 60 ˚C for 30 s. Fluorescence was monitored at 55 to 95 ˚C at 0.5 ˚C intervals for 5 s. Each experiment was carried out in triplicate. A relative quantification model was used to calculate the expression of the target gene expression compared to *GAPDH*, used as the endogenous control.

Determination of the proliferation activity

The proliferation activity of living cells was determined by the WST-1 assay, as described before [23]. In brief, the LECs (15 x 10^3 cells/ well) were cultured in a complete DMEM medium with or without IL13 in a 96-well tissue culture plate (VWR, Radnor, PA, USA) for 7 days at 37˚C in an atmosphere of 5% CO_2. WST-1 reagent (Roche, Mannheim, Germany) was added to each well (10 μl/100 μl of medium), and plates were incubated for another 1 h to form formazan. A formazan-containing medium (100 μl) was transferred from each well into a new 96-well tissue culture plate. The absorbance was measured using a Tecan Infinite M200 (Tecan, Mannedorf, Switzerland) at a wavelength of 450 nm.

Statistical analysis

Statistical analysis was performed with GraphPad Prism (GraphPad Software, La Jolla, CA, USA). Descriptive statistics are reported as N (number of values), mean ± SD, or the median with quartile range. Data sets were analyzed by Mann–Whitney U nonparametric test. P-values < 0.05 were considered statistically significant.

Results

Limbal epithelial cell growth and morphology

LECs P0 cultures started to outgrow from limbal explants mostly on the fifth day, and 90–100% confluence was achieved after 14 days regardless of the presence of IL13 (Fig 1A). P1 and P2 cultures reached confluence significantly earlier than P0, but there was no difference whether the cells were cultured with or without IL13 (Fig 1D). The cell viability after passaging was comparable between the cultures (Fig 1E). The percentage of successful cultures decreased

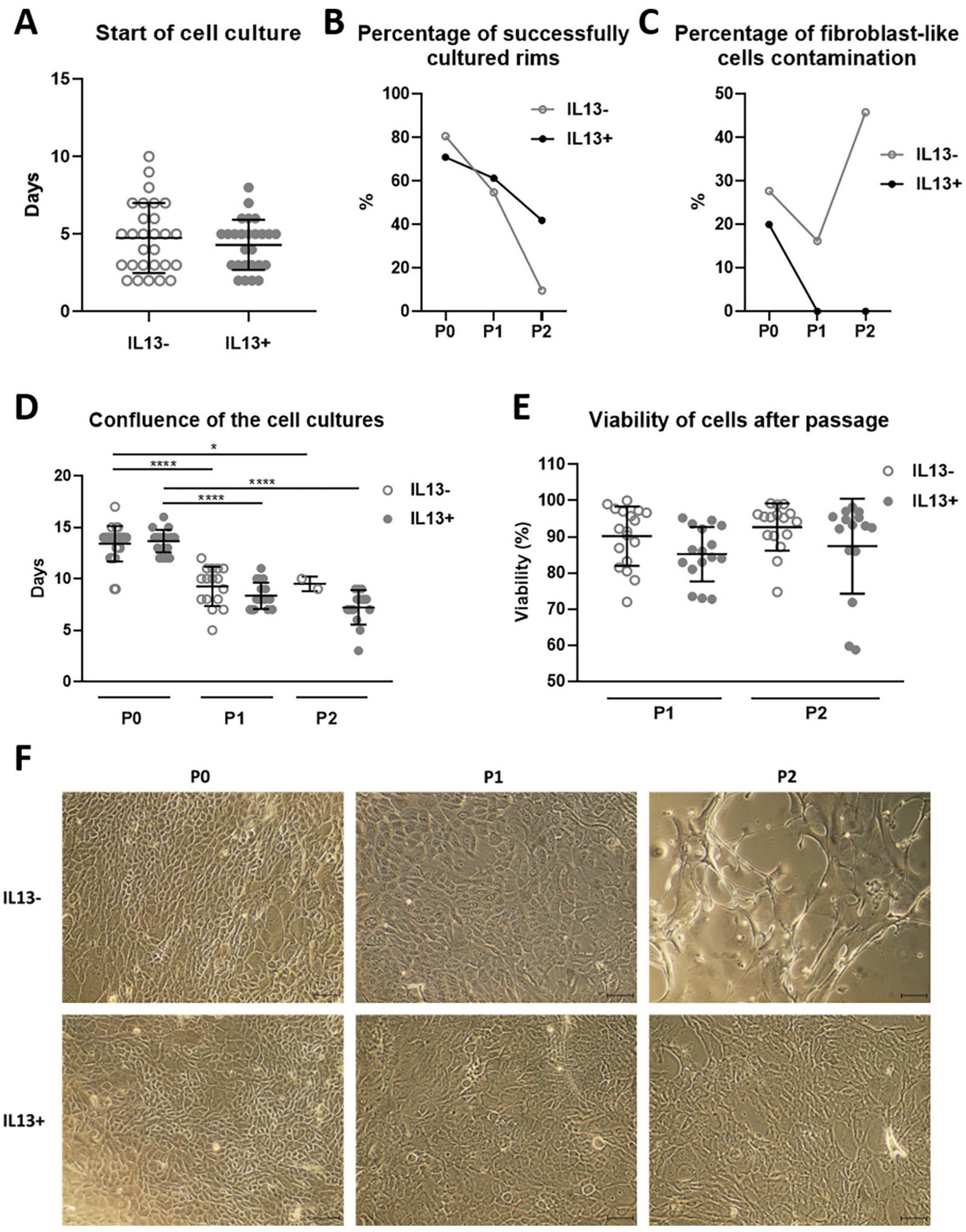

Fig 1. The growth and morphology of IL13- and IL13+ cell cultures. (A) The beginning of the outgrowth of LEC cultures from day 0 (D) to reaching full confluence in P0, P1, and P2 cultures. (B) The percentage of successfully cultured corneoscleral rims. (C) The percentage of fibroblast-like cells contamination in cell cultures. (E) Percentages of cell viability after the first and second passages. (F) Cell morphology was observed at the end of cultivation of P0, P1, and P2 cultures under an inverted phase-contrast microscope. Scale bars: 50 μm.

https://doi.org/10.1371/journal.pone.0272081.g001

throughout the cell culture from P0 to P1 and P2 (Fig 1B). The most noticeable difference was after P2, where 9.7% of IL13- cultures reached confluence, compared to 42% in the IL13 + group. This fact is also reflected in the morphology of cells. Typical cuboidal morphology of

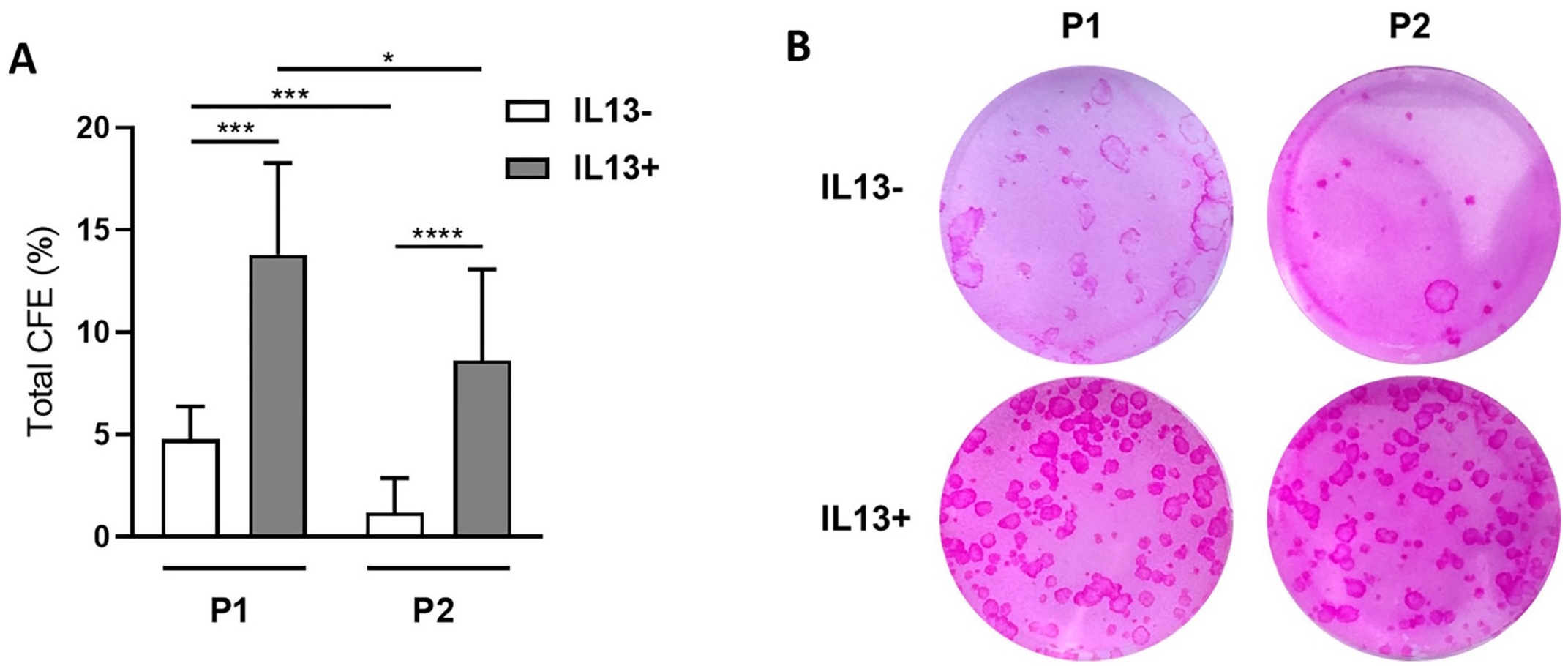

Fig 2. Comparison of total CFE. After the first and second passages (P1 and P2), cells were cultured with growth-arrested 3T3 mouse fibroblasts to compare their growth capacity under IL13- and IL13+ conditions. (A) Distribution of total CFE percentages of the P1 and P2 groups. Each bar represents the mean ± SD from 7 to 13 determinations. The asterisks represent a statistically significant difference between the examined groups (*$P \leq 0.05$, ***$P \leq 0.001$, ****$P \leq 0.0001$). (B) The colonies were stained with 2% rhodamine B.

https://doi.org/10.1371/journal.pone.0272081.g002

LECs with a high nucleocytoplasmic ratio was visible in all cultures, except P2 IL13- cultures, where cells were more flattened or fibroblast-like morphology with a low nucleocytoplasmic ratio (Fig 1F). The contamination by fibroblast-like cells was higher in the P0 group without than P0 with IL13 (27.7% and 20% respectively). Cell cultures without IL13 had a low percentage of contamination in P1 (16.2%) but increased in P2 (45.8%). On the contrary, the fibroblast-like cell contamination was not observed in P1 and P2 cultures with IL13 (Fig 1C).

CFA

The CFA was performed for P1 and P2 cultures (Fig 2). A significantly higher growth potential was observed in the P1 and P2 IL13+ groups (mean 13.79% and 8.63% respectively) than the P1 and P2 IL13- cultures (mean 4.78% and 1.19% respectively), $P<0.001$ and $P<0.0001$ respectively. The decrease of the number of colonies was between both passages and IL13 groups, more significant in IL13- than in IL13+ cultures ($P< 0.001$ vs. $P<0.05$).

Expression of limbal stem cell markers

The *ΔNp63α* gene expression was significantly higher in all cultures (P0, P1, and P2) with IL13 compared to the cells cultured without it ($P<0.001$, $P<0.001$, $P<0.01$, respectively). A consistent decrease of *ΔNp63α* gene expression was observed during the LECs culture with significance between P0-P1 and P1-P2 cultures in the IL13- (both $P<0.01$) and IL13+ ($P< 0.05$, $P<0.001$ respectively) groups. A slightly higher expression of the *BMI-1* gene was observed in P0 IL13+ cultures compared to IL13- cells with no statistical significance. The *BMI-1* expression values in P1 and P2 cultures were comparable. The gene expressions of *K14* were significantly higher in the IL13+ groups P0 ($P<0.05$) and P1 ($P<0.001$) than controls without IL13. The expression decreased significantly between P0 and P1 cultures without IL13 ($P<0,05$). A decreased *K17* gene expression tendency was found throughout the cell culture with statistical significance between the P0 IL13+ culture and the P1 and P2 IL13+ groups, respectively (both

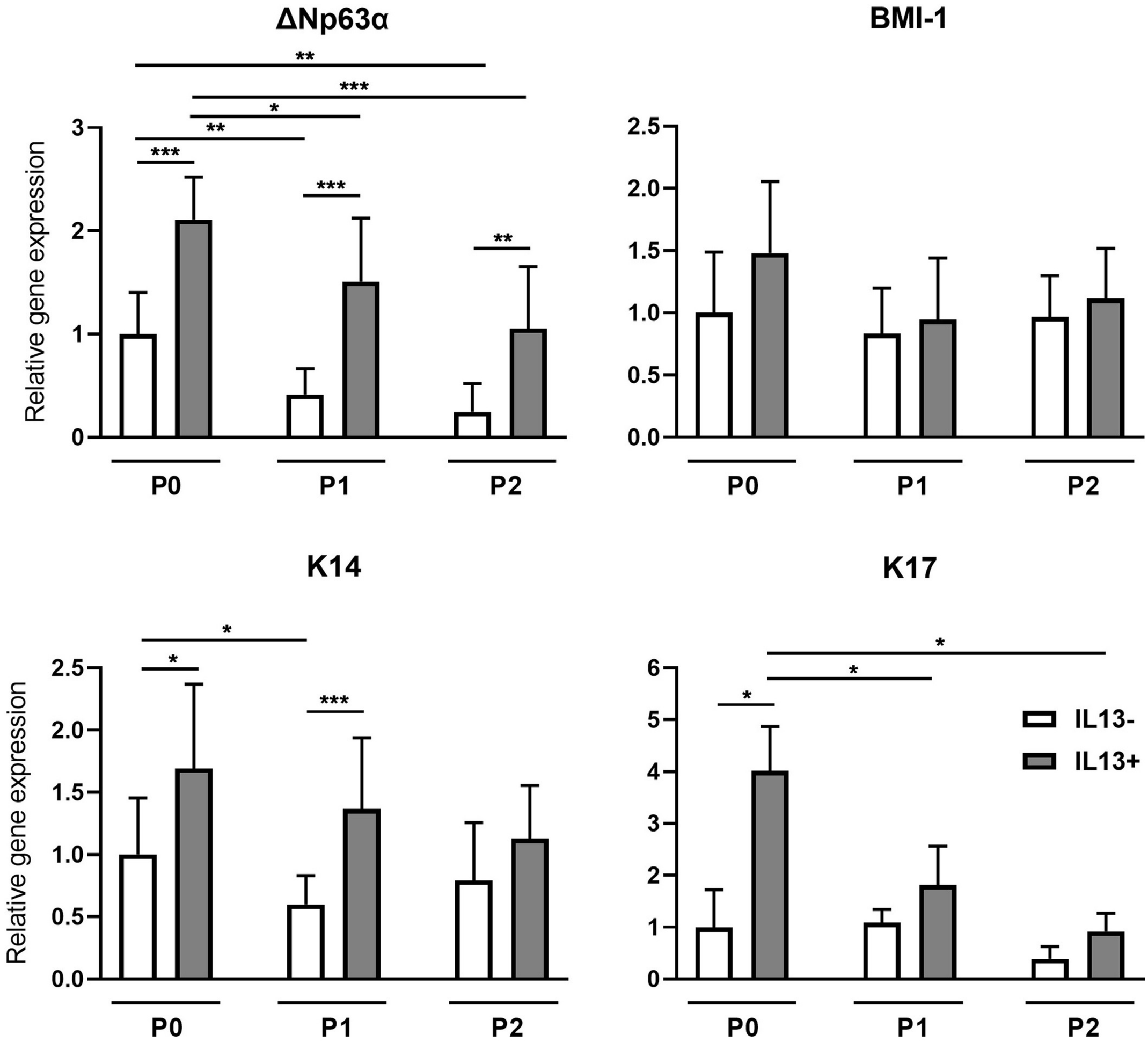

Fig 3. Relative gene expression of *ΔNp63α*, *BMI-1*, *K14*, and *K17* in IL13- and IL13+ cell cultures. Cells originating from limbal explants (P0) and passaged cells (P1 and P2) were analyzed at the end of the culture for *p63α*, *BMI-1*, *K14*, and *K17* gene expression by qPCR. Each bar represents the mean ± SD of three to ten determinations. The asterisks represent statistically significant difference between the examined groups (*P < 0.05, **P ≤ 0.01, ***P ≤ 0.001).

https://doi.org/10.1371/journal.pone.0272081.g003

P<0.05). The expression of the *K17* gene was significantly higher in samples with IL13 in P0 (P<0.05) compared to samples without IL13 (Fig 3).

Immunocytochemical staining for p63

Cells positive for the p63 protein were detected in all cultures and conditions (Fig 4A). The percentage of p63 positive cells significantly decreased during cell culture without IL13 (mean values 94.86%, 91.65%, and 75.55% for P0, P1, and P2 cultures, respectively; P<0.05). Cell cultures with IL13 had a similar expression of p63 in all passages (mean values 96.23%, 95.54%,

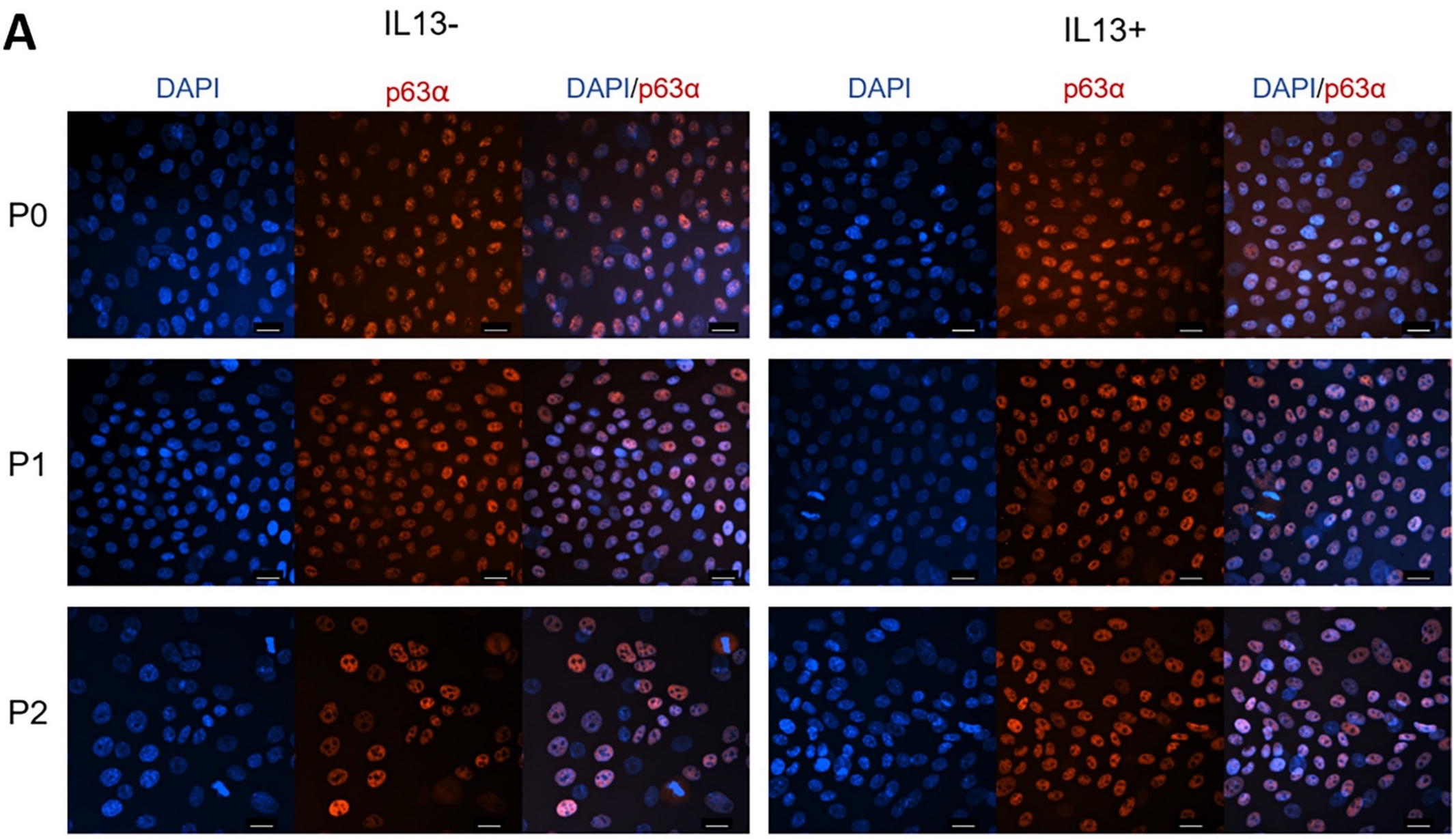

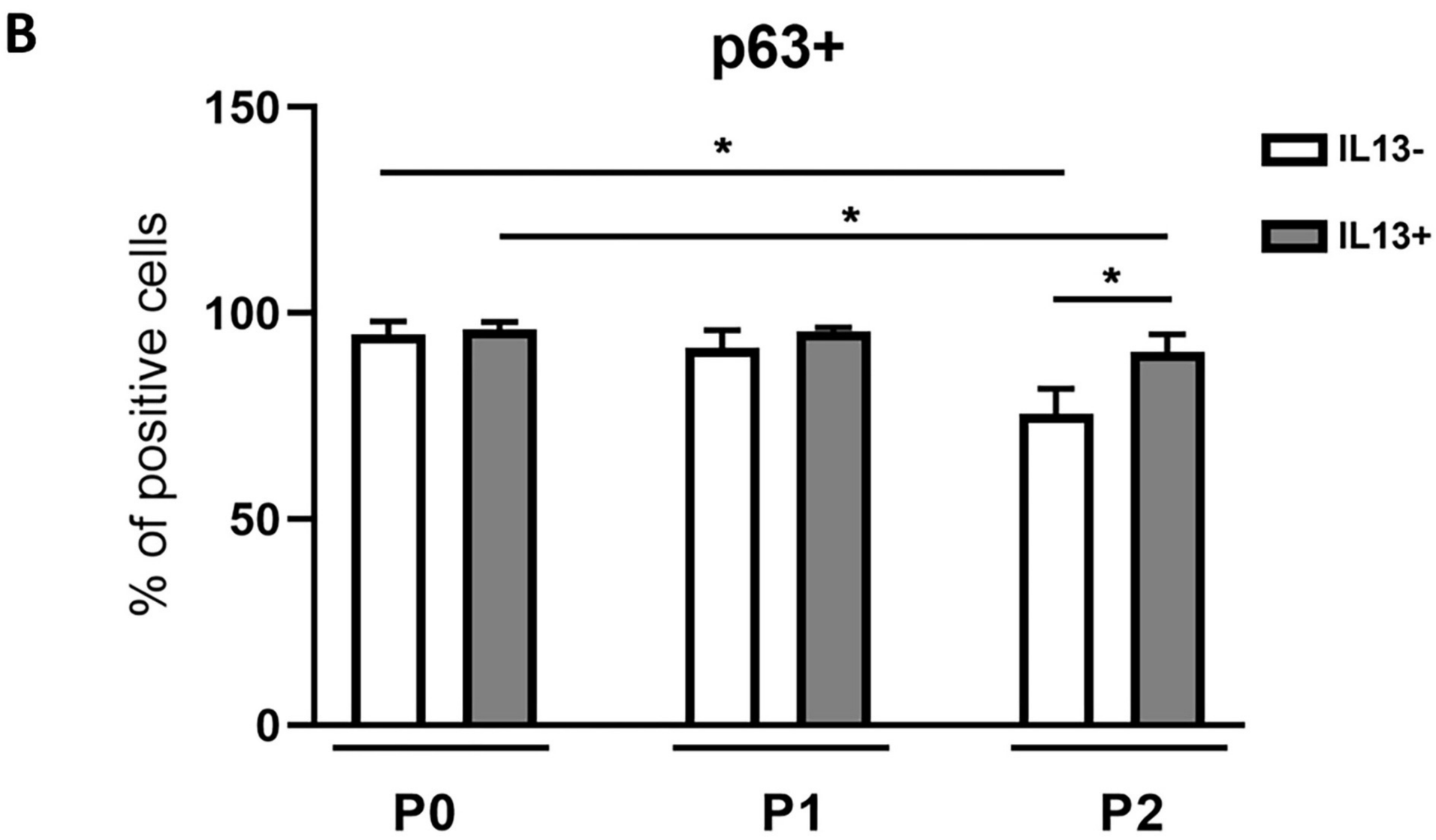

Fig 4. Immunostaining for the putative limbal stem cell marker p63α in IL13- and IL13+ cell cultures. (A) Cells were analyzed by immunofluorescent staining for p63α (red) at the end of P0-P2 cultures. Nuclei were counterstained with DAPI (blue). Scale bars: 20 μm. (B) Distribution of percentages in the P0, P1, and P2 groups for p63α staining. Each bar represents the mean ± SD of three to eight determinations. The asterisks represent a statistically significant difference between the examined groups ($^{*}P \leq 0.05$).

https://doi.org/10.1371/journal.pone.0272081.g004

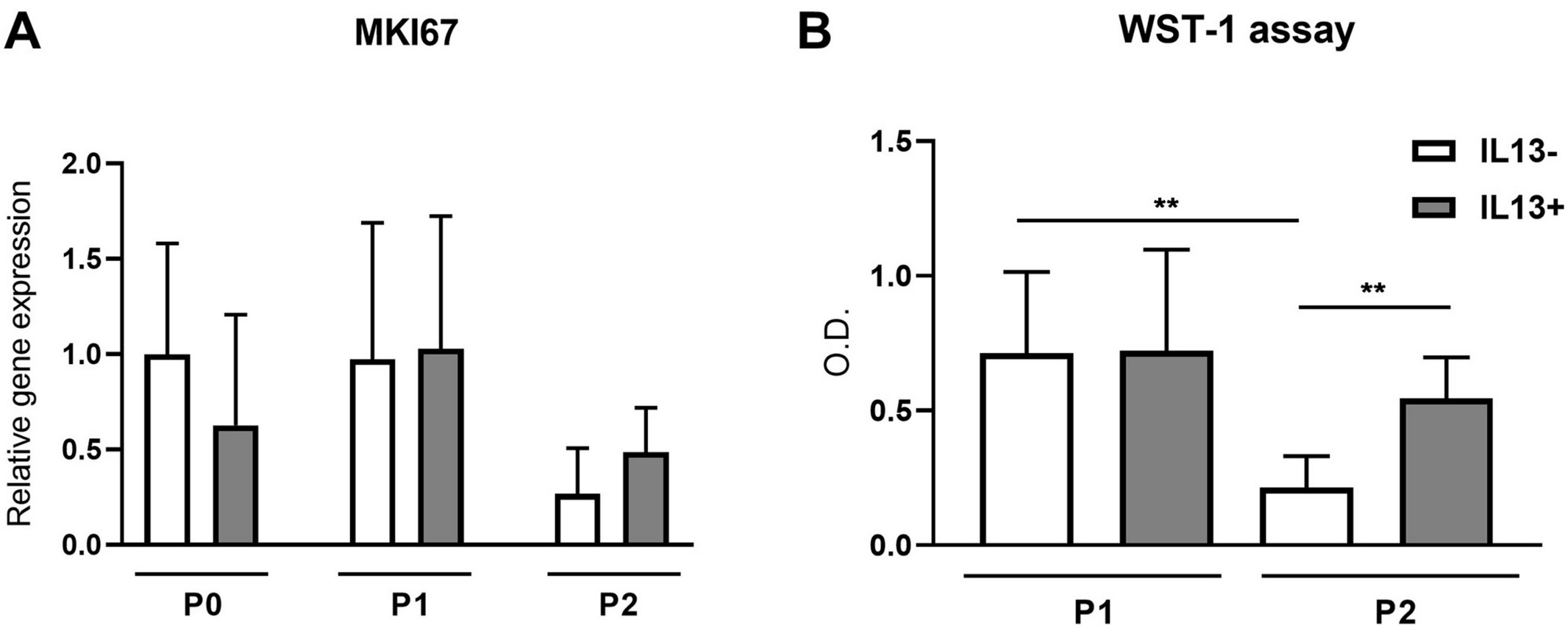

Fig 5. Relative gene expression of *MKI67* and WST-1 assay in IL13- and IL13+ cell cultures. (A) Cells originating from limbal explants (P0) and passaged cells (P1 and P2) at the end of culture were analyzed for *MKI67* gene expression by qPCR. Each bar represents the mean ± SD of five to ten determinations. (B) Measurement of cell proliferation after the first and second passages (P1 and P2). The WST-1 reagent was added to the cell cultures for 1 h to form formazan. The absorbance was measured at a wavelength of 450 nm via optical density. Each bar represents the mean ± SD of eight to ten determinations. The asterisks represent a statistically significant difference between the examined groups (**P ≤ 0.01).

https://doi.org/10.1371/journal.pone.0272081.g005

and 90.69% for P0, P1, and P2 cultures, respectively). A significantly higher percentage of p63 + cells were measured in P2 IL13+ compared to P2 IL13- culture (P<0.05) (Fig 4B).

LECs proliferation and metabolic activity

The proliferation of cultured LECs was determined by gene expression analysis of *MKI67* and WST-1 assay (Fig 5). No significant difference was observed between the evaluated groups for *MKI67* gene expression. No difference was found between IL13+ and IL13- groups in P1, but significantly higher proliferation was determined in P2 IL13+ compared to P2 IL13- (P<0.01) according to WST-1 assay. The significant decrease of the proliferation activity was measured between P1 and P2 cultures without IL13 (P<0.01).

Presence of differentiation markers

K3 and *K12* genes specific for the corneal epithelium were expressed in all groups at very low levels with no difference and significance. Conjunctival *K7* gene expression was higher in all IL13+ cell passages compared to IL13- cultures, significantly in P0 and P1 (both P<0.05). The *MUC4* gene was expressed in all groups with a significant decrease between passages P0 and P2 and between P1 and P2 in IL13- conditions (P<0.05) (Fig 6).

Discussion

In this study, we explore the potential of IL13 to improve the properties of cultured LECs, particularly in terms of their stemness and use for the treatment of LSCD. Our results showed that IL13 significantly increases stemness of LECs after P1 and P2, as shown by the CFA, by the expression of putative stem cell markers (*ΔNp63α*, *K14*, and *K17*), and by immunocytochemistry (p63α). Besides the increase in stemness, there was no change in the morphology, but cell proliferation was significantly higher after P2 cultures with IL13 compared to without IL13.

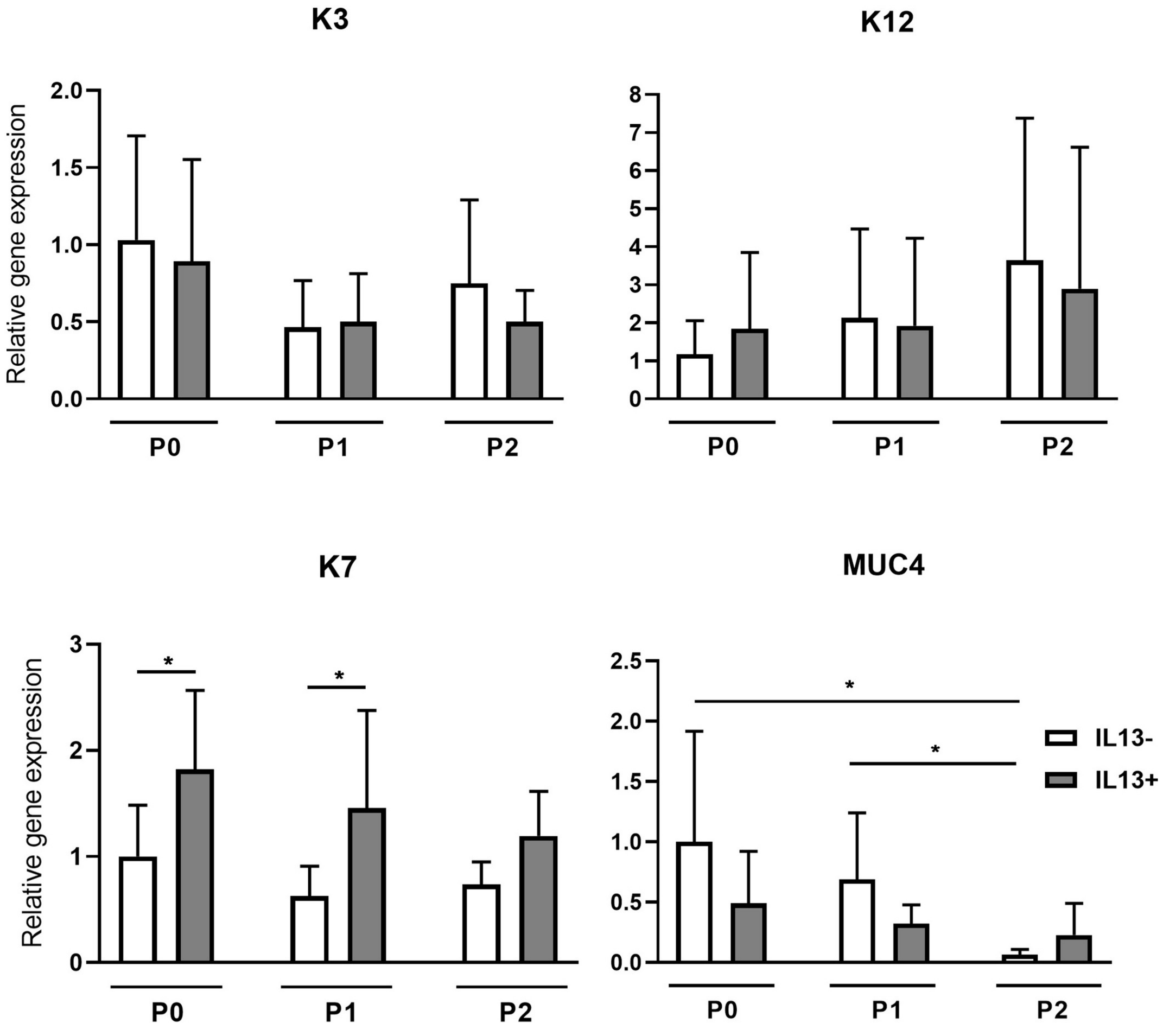

Fig 6. Relative gene expression of *K3*, *K12*, *K7*, and *MUC4* in IL13- and IL13+ cell cultures. Cells originating from limbal explants (P0) and passaged cells (P1 and P2) at the end of culture were analyzed for the expression of *K3*, *K12*, *K7*, and *MUC4* genes by qPCR. Each bar represents the mean ± SD of four to ten determinations. The asterisks represent a statistically significant difference between the examined groups (*$P < 0.05$).

https://doi.org/10.1371/journal.pone.0272081.g006

The clonogenic activity of our LESCs cultures without IL13 was about 5% after the first passage, decreasing to 1% after the second passage. This percentage was higher than the clonogenic activity in conjunctival cultures or limbal explants in previous studies [18,24]. Cultures with IL13 had significantly higher clonogenic capacity after both passages than the related passage of cultures without IL13. The higher clonogenic activity of IL13+ cultures corresponds to increased gene expression of the putative stem cell marker p63α. Previously, it was reported that coexpression of C/EBPΔ, BMI-1, and ΔNp63α identified mitotically quiescent limbal stem cells, which generate holoclones in culture [25].

Furthermore, human holoclone-forming cells have been shown to be only located in the limbus [26,27], and that more than 3% of p63 positive cells from total clonogenic cells in the

culture led to successful transplantation in patients with LSCD. Therefore, clonogenic activity is an important indicator of stem cells, as the competence for the continued proliferation of stem cells in tissues is required for normal tissues' continued integrity and function [28]. The time-dependent decrease in clonogenicity is consistent with the observation of other studies; a 4-day culture of LECs led to differentiation and loss of almost all the capacity for colony formation [14]. The loss of clonogenic properties in transient amplifying cells during culture was also found by Pellegrini et al. [26]. Moreover, a decreased number of cells with p63 stemness factor was observed during a more extended culture of LECs from limbal explants [29]. It looks like a typical stem cell process. The clonogenic activity decreased rapidly in our LECs cultures from 5% after P1 to 1% after P2. The preservation of clonogenicity and stemness due to IL13 also corresponds to the cuboidal morphology of cultured cells that had a high nucleo-cytoplasmic ratio during all cultures. On the contrary, LESCs cultures without IL13 lost their morphology after the second passage, consistent with other works [14,18]. Fibroblast-like cells contamination was lower or not present in cultures with IL13, and the epithelial phenotype was predominant compared to cultures without IL13. Still, more studies are necessary to analyze whether IL13 inhibits fibroblasts' outgrowth directly or the lower contamination is because of higher stemness in the IL13 cultures.

Our gene expression analysis showed that LECs culture with IL13 increased the expression of K14, K17, and most importantly, ΔNp63α stem cell markers, which are generally used to indicate stemness in LESCs cultures [30–33]. However, according to immunohistochemistry, the percentage of p63 positive cells showed a significant difference between cultures with or without IL13 only in P2, in which a slight increase in p63 positive cells was observed in IL13 + cells compared to IL13- culture. The discrepancy between qPCR and immunostaining findings has been previously found [34,35]. It can be explained by immunostaining analysis showing only the number of positive cells and not the amount of protein expressed. In addition, the antibody is less specific than the qPCR primers due to the six isoforms of the *p63* gene and the minor differences between them.

Generally, LESCs are slow-cycling during homeostasis and highly proliferative in case of injury [36]. Our gene expression analysis of the *MKI67* gene, which is involved in cell proliferation, showed weak expression and no difference between cultures with or without IL13 in all passages. Joyce et al. showed in the study of the expression of MKI67 in the human cornea by indirect immunofluorescence localization that most LECs did not present this marker of cell proliferation [37]. A similar observation was found in the study of limbal explant cultures, in which epithelial cells were positive for MKI67 in the first week of culture, but most expression disappeared by 3 weeks when cells migrating from explants reached confluence [29]. They hypothesized that MKI67 expression indicates the proliferative status of cells in a certain time but not the proliferation capacity of cells, as they showed a decrease in MKI67 staining in cells from confluent cultures [29]. This is in accordance with the weak gene expression of MKI67 in our cultures, as we measured the expression after the passage when cells were about to reach the confluence. Therefore, we also used another measurement of cell proliferation, the WST-1 assay, which showed no difference in cell proliferation between P1 and P2 IL13+ cultures. However, a substantially higher proliferation of IL13+ than IL13- cultures after the second passage indicates their potential to be used as a graft even after passage. This observation follows the weak potential of LECs after P2 without IL13 to reach confluence.

The gene expression of corneal epithelial markers K3 and K12 did not differ between the IL13- and IL13+ cultures. The expressions of these genes were weak, and we did not observe any changes leading to differentiation into the corneal epithelial phenotype. In contrast to our findings, some works showed 60–80% positivity of K3 and K12 in LESCs cultures [24,38]. The low expression of corneal epithelial factors can be explained as a positive effect of IL13, as the

culture cells did not differentiate into the corneal epithelial phenotype but retained their stemness. Nevertheless, it is unclear whether cells with a differentiated corneal epithelial phenotype in the graft are more important for transplant success than the presence of a niche with cells with varying degrees of differentiation [39].

Here we show that culture influenced by IL13 led to a higher differentiation into conjunctival phenotype, as we measured a higher gene expression of the *K7* gene in all cultures (P0-P2). K7 is considered a marker of the conjunctival epithelium [40]. The same differentiation potential of IL13 was observed in conjunctival cultures from limbal explants [18]. Interestingly, the expression of another conjunctival marker, MUC4, was not affected by the addition of IL13 and decreased significantly during passages. Because conjunctival cells have also been used for the successful treatment of LSCD, the presence of K7 is unlikely to adversely affect the quality of the graft. Our previous results with conjunctival epithelial cells showed that partial differentiation to the conjunctival phenotype was expected [18]. However, unlike corneal conjunctivalization, which includes a vascularized pannus that overgrows on the cornea in LSCD-affected eyes, these transplanted conjunctival epithelial cells do not have any associated fibrous or vascular tissue [41].

IL13 is essential during early myelopoiesis. However, its role in the stemness of LESCs or other cell types was unknown. The first findings were made in conjunctival cell cultures from limbal explants, where IL13 maintained the stemness of the cultures by increasing their clonal capacity and p63α expression [18]. The detailed signaling pathway for this mechanism is unclear. A similar observation of maintaining stemness via IL13 –IL13R (IL13 receptor) was recently described in intestinal stem cells (ISCs) [22]. They found that the circular RNA molecule circPan3 bounds the mRNA encoding the cytokine IL13R subunit IL13Rα1 in ISCs to increase the stability of the receptor. IL13 then binds to IL13R, which initiates the expression of the transcription factor Foxp1. Foxp1 is associated with the β-catenin signaling pathway, causing activation of this pathway and maintenance of ISCs. The deletion of circPan3 in ISCs led to impaired stem cell self-renewal capacity and regeneration of the intestinal epithelium [22]. IL13 can induce through IL4Rα present in the human corneal epithelial cells the expression of various genes, such as *HAS3*, encoding hyaluronan synthases; hyaluronan in the extracellular matrix has been shown to control epithelial proliferation and regeneration [42,43]. The Wnt/β-catenin signaling is also present in the ocular surface epithelium and plays an important role in regulating LESCs proliferation [41]; further investigation of this signaling pathway would better explain the whole mechanism of IL13 in LESCs.

This study showed that IL13 enhanced the stemness of LESCs by increasing the clonogenicity and the expression of putative stem cell markers of LECs while maintaining their stem cell morphology. We established IL13 as a culture supplement for LESCs, which increases their stemness potential in culture, even after the second passage, and may lead to greater success of LECs transplantations in patients with LSCD.

Author Contributions

Conceptualization: Peter Trosan, Joao Victor Cabral, Katerina Jirsova.

Data curation: Peter Trosan, Joao Victor Cabral.

Formal analysis: Joao Victor Cabral, Katerina Jirsova.

Funding acquisition: Katerina Jirsova.

Investigation: Peter Trosan, Joao Victor Cabral, Ingrida Smeringaiova, Pavel Studeny, Katerina Jirsova.

Methodology: Peter Trosan, Joao Victor Cabral, Ingrida Smeringaiova.

Project administration: Katerina Jirsova.

Supervision: Katerina Jirsova.

Validation: Peter Trosan, Joao Victor Cabral, Pavel Studeny, Katerina Jirsova.

Visualization: Peter Trosan.

Writing – original draft: Peter Trosan, Joao Victor Cabral.

Writing – review & editing: Katerina Jirsova.

References

1. Ebato B, Friend J, Thoft RA. Comparison of limbal and peripheral human corneal epithelium in tissue culture. Invest Ophthalmol Vis Sci. 1988 Oct; 29(10):1533–1537. PMID: 3170124
2. Schermer A, Galvin S, Sun TT. Differentiation-related expression of a major 64K corneal keratin in vivo and in culture suggests limbal location of corneal epithelial stem cells. J Cell Biol. 1986 Jul; 103(1):49–62. https://doi.org/10.1083/jcb.103.1.49 PMID: 2424919
3. Cotsarelis G, Cheng SZ, Dong G, Sun TT, Lavker RM. Existence of slow-cycling limbal epithelial basal cells that can be preferentially stimulated to proliferate: implications on epithelial stem cells. Cell. 1989 Apr 21; 57(2):201–209. https://doi.org/10.1016/0092-8674(89)90958-6 PMID: 2702690
4. Castro-Muñozledo F, Gómez-Flores E. Challenges to the study of asymmetric cell division in corneal and limbal epithelia. Exp Eye Res. 2011 Jan; 92(1):4–9. https://doi.org/10.1016/j.exer.2010.11.002 PMID: 21056036
5. Van Buskirk EM. The anatomy of the limbus. Eye (Lond). 1989 Jan 1; 3 (Pt 2):101–108. https://doi.org/10.1038/eye.1989.16 PMID: 2695343
6. Meyer PA. The circulation of the human limbus. Eye (Lond). 1989; 3 (Pt 2):121–127. https://doi.org/10.1038/eye.1989.19 PMID: 2695346
7. Zhang Y, Sun H, Liu Y, Chen S, Cai S, Zhu Y, et al. The limbal epithelial progenitors in the limbal niche environment. Int J Med Sci. 2016 Oct 18; 13(11):835–840. https://doi.org/10.7150/ijms.16563 PMID: 27877075
8. Gospodarowicz D, Mescher AL, Brown KD, Birdwell CR. The role of fibroblast growth factor and epidermal growth factorin the proliferative response of the corneal and lens epithelium. Exp Eye Res. 1977 Dec; 25(6):631–649. https://doi.org/10.1016/0014-4835(77)90142-7 PMID: 304011
9. Daniels JT, Limb GA, Saarialho-Kere U, Murphy G, Khaw PT. Human corneal epithelial cells require MMP-1 for HGF-mediated migration on collagen I. Invest Ophthalmol Vis Sci. 2003 Mar; 44(3):1048–1055. https://doi.org/10.1167/iovs.02-0442 PMID: 12601028
10. Sotozono C, Inatomi T, Nakamura M, Kinoshita S. Keratinocyte growth factor accelerates corneal epithelial wound healing in vivo. Invest Ophthalmol Vis Sci. 1995 Jul; 36(8):1524–1529. PMID: 7601632
11. Lee HK, Lee JH, Kim M, Kariya Y, Miyazaki K, Kim EK. Insulin-like growth factor-1 induces migration and expression of laminin-5 in cultured human corneal epithelial cells. Invest Ophthalmol Vis Sci. 2006 Mar; 47(3):873–882. https://doi.org/10.1167/iovs.05-0826 PMID: 16505019
12. Kakazu A, Chandrasekher G, Bazan HEP. HGF protects corneal epithelial cells from apoptosis by the PI-3K/Akt-1/Bad- but not the ERK1/2-mediated signaling pathway. Invest Ophthalmol Vis Sci. 2004 Oct; 45(10):3485–3492. https://doi.org/10.1167/iovs.04-0372 PMID: 15452053
13. Trosan P, Svobodova E, Chudickova M, Krulova M, Zajicova A, Holan V. The key role of insulin-like growth factor I in limbal stem cell differentiation and the corneal wound-healing process. Stem Cells Dev. 2012 Dec 10; 21(18):3341–3350. https://doi.org/10.1089/scd.2012.0180 PMID: 22873171
14. Kolli S, Bojic S, Ghareeb AE, Kurzawa-Akanbi M, Figueiredo FC, Lako M. The Role of Nerve Growth Factor in Maintaining Proliferative Capacity, Colony-Forming Efficiency, and the Limbal Stem Cell Phenotype. Stem Cells. 2019; 37(1):139–149. https://doi.org/10.1002/stem.2921 PMID: 30599086
15. Pellegrini G, Dellambra E, Golisano O, Martinelli E, Fantozzi I, Bondanza S, et al. p63 identifies keratinocyte stem cells. Proc Natl Acad Sci USA. 2001 Mar 13; 98(6):3156–3161. https://doi.org/10.1073/pnas.061032098 PMID: 11248048
16. Di Iorio E, Barbaro V, Ruzza A, Ponzin D, Pellegrini G, De Luca M. Isoforms of DeltaNp63 and the migration of ocular limbal cells in human corneal regeneration. Proc Natl Acad Sci USA. 2005 Jul 5; 102(27):9523–9528. https://doi.org/10.1073/pnas.0503437102 PMID: 15983386

17. Rama P, Matuska S, Paganoni G, Spinelli A, De Luca M, Pellegrini G. Limbal stem-cell therapy and long-term corneal regeneration. N Engl J Med. 2010 Jul 8; 363(2):147–155. https://doi.org/10.1056/NEJMoa0905955 PMID: 20573916

18. Stadnikova A, Trosan P, Skalicka P, Utheim TP, Jirsova K. Interleukin-13 maintains the stemness of conjunctival epithelial cell cultures prepared from human limbal explants. PLoS One. 2019 Feb 11; 14 (2):e0211861. https://doi.org/10.1371/journal.pone.0211861 PMID: 30742646

19. Junttila IS. Tuning the Cytokine Responses: An Update on Interleukin (IL)-4 and IL-13 Receptor Complexes. Front Immunol. 2018 Jun 7; 9:888. https://doi.org/10.3389/fimmu.2018.00888 PMID: 29930549

20. Jacobsen SE, Okkenhaug C, Veiby OP, Caput D, Ferrara P, Minty A. Interleukin 13: novel role in direct regulation of proliferation and differentiation of primitive hematopoietic progenitor cells. J Exp Med. 1994 Jul 1; 180(1):75–82. https://doi.org/10.1084/jem.180.1.75 PMID: 7516418

21. Nappo G, Handle F, Santer FR, McNeill RV, Seed RI, Collins AT, et al. The immunosuppressive cytokine interleukin-4 increases the clonogenic potential of prostate stem-like cells by activation of STAT6 signalling. Oncogenesis. 2017 May 29; 6(5):e342. https://doi.org/10.1038/oncsis.2017.23 PMID: 28553931

22. Zhu P, Zhu X, Wu J, He L, Lu T, Wang Y, et al. IL-13 secreted by ILC2s promotes the self-renewal of intestinal stem cells through circular RNA circPan3. Nat Immunol. 2019 Jan 14; 20(2):183–194. https://doi.org/10.1038/s41590-018-0297-6 PMID: 30643264

23. Trosan P, Javorkova E, Zajicova A, Hajkova M, Hermankova B, Kossl J, et al. The Supportive Role of Insulin-like Growth Factor-I in the Differentiation of Murine Mesenchymal Stem Cells into Corneal-like Cells. Stem Cells Dev. 2016 Apr 6; 25(11):874–881. https://doi.org/10.1089/scd.2016.0030 PMID: 27050039

24. López-Paniagua M, Nieto-Miguel T, de la Mata A, Dziasko M, Galindo S, Rey E, et al. Comparison of functional limbal epithelial stem cell isolation methods. Exp Eye Res. 2016 May; 146:83–94. https://doi.org/10.1016/j.exer.2015.12.002 PMID: 26704459

25. Barbaro V, Testa A, Di Iorio E, Mavilio F, Pellegrini G, De Luca M. C/EBPdelta regulates cell cycle and self-renewal of human limbal stem cells. J Cell Biol. 2007 Jun 18; 177(6):1037–1049. https://doi.org/10.1083/jcb.200703003 PMID: 17562792

26. Pellegrini G, Golisano O, Paterna P, Lambiase A, Bonini S, Rama P, et al. Location and clonal analysis of stem cells and their differentiated progeny in the human ocular surface. J Cell Biol. 1999 May 17; 145 (4):769–782. https://doi.org/10.1083/jcb.145.4.769 PMID: 10330405

27. Majo F, Rochat A, Nicolas M, Jaoudé GA, Barrandon Y. Oligopotent stem cells are distributed throughout the mammalian ocular surface. Nature. 2008 Nov 13; 456(7219):250–254. https://doi.org/10.1038/nature07406 PMID: 18830243

28. Franken NAP, Rodermond HM, Stap J, Haveman J, van Bree C. Clonogenic assay of cells in vitro. Nat Protoc. 2006; 1(5):2315–2319. https://doi.org/10.1038/nprot.2006.339 PMID: 17406473

29. Joseph A, Powell-Richards AOR, Shanmuganathan VA, Dua HS. Epithelial cell characteristics of cultured human limbal explants. Br J Ophthalmol. 2004 Mar; 88(3):393–398. https://doi.org/10.1136/bjo.2003.018481 PMID: 14977776

30. Kramerov AA, Saghizadeh M, Maguen E, Rabinowitz YS, Ljubimov AV. Persistence of reduced expression of putative stem cell markers and slow wound healing in cultured diabetic limbal epithelial cells. Mol Vis. 2015 Dec 30; 21:1357–1367. PMID: 26788028

31. Utheim O, Islam R, Lyberg T, Roald B, Eidet JR, de la Paz MF, et al. Serum-free and xenobiotic-free preservation of cultured human limbal epithelial cells. PLoS One. 2015 Mar 3; 10(3):e0118517. https://doi.org/10.1371/journal.pone.0118517 PMID: 25734654

32. Zhao B, Allinson SL, Ma A, Bentley AJ, Martin FL, Fullwood NJ. Targeted cornea limbal stem/progenitor cell transfection in an organ culture model. Invest Ophthalmol Vis Sci. 2008 Aug; 49(8):3395–3401. https://doi.org/10.1167/iovs.07-1263 PMID: 18441310

33. Saghizadeh M, Dib CM, Brunken WJ, Ljubimov AV. Normalization of wound healing and stem cell marker patterns in organ-cultured human diabetic corneas by gene therapy of limbal cells. Exp Eye Res. 2014 Dec; 129:66–73. https://doi.org/10.1016/j.exer.2014.10.022 PMID: 25446319

34. López-Paniagua M, Nieto-Miguel T, de la Mata A, Galindo S, Herreras JM, Corrales RM, et al. Consecutive expansion of limbal epithelial stem cells from a single limbal biopsy. Curr Eye Res. 2013 May; 38 (5):537–549. https://doi.org/10.3109/02713683.2013.767350 PMID: 23405945

35. Brejchova K, Trosan P, Studeny P, Skalicka P, Utheim TP, Bednar J, et al. Characterization and comparison of human limbal explant cultures grown under defined and xeno-free conditions. Exp Eye Res. 2018 Jun 19; 176:20–28. https://doi.org/10.1016/j.exer.2018.06.019 PMID: 29928900

36. Lehrer MS, Sun TT, Lavker RM. Strategies of epithelial repair: modulation of stem cell and transit amplifying cell proliferation. J Cell Sci. 1998 Oct; 111 (Pt 19):2867–2875. https://doi.org/10.1242/jcs.111.19.2867 PMID: 9730979

37. Joyce NC, Navon SE, Roy S, Zieske JD. Expression of cell cycle-associated proteins in human and rabbit corneal endothelium in situ. Invest Ophthalmol Vis Sci. 1996 Jul; 37(8):1566–1575. PMID: 8675399

38. Li Y, Yang Y, Yang L, Zeng Y, Gao X, Xu H. Poly(ethylene glycol)-modified silk fibroin membrane as a carrier for limbal epithelial stem cell transplantation in a rabbit LSCD model. Stem Cell Res Ther. 2017 Nov 7; 8(1):256. https://doi.org/10.1186/s13287-017-0707-y PMID: 29116027

39. Calonge M, Nieto-Miguel T, de la Mata A, Galindo S, Herreras JM, López-Paniagua M. Goals and Challenges of Stem Cell-Based Therapy for Corneal Blindness Due to Limbal Deficiency. Pharmaceutics. 2021 Sep 16; 13(9). https://doi.org/10.3390/pharmaceutics13091483 PMID: 34575560

40. Jirsova K, Dudakova L, Kalasova S, Vesela V, Merjava S. The OV-TL 12/30 clone of anti-cytokeratin 7 antibody as a new marker of corneal conjunctivalization in patients with limbal stem cell deficiency. Invest Ophthalmol Vis Sci. 2011 Jul 29; 52(8):5892–5898. https://doi.org/10.1167/iovs.10-6748 PMID: 21693612

41. Ang LPK, Tanioka H, Kawasaki S, Ang LPS, Yamasaki K, Do TP, et al. Cultivated human conjunctival epithelial transplantation for total limbal stem cell deficiency. Invest Ophthalmol Vis Sci. 2010 Feb; 51 (2):758–764. https://doi.org/10.1167/iovs.09-3379 PMID: 19643956

42. Kakizaki I, Itano N, Kimata K, Hanada K, Kon A, Yamaguchi M, et al. Up-regulation of hyaluronan synthase genes in cultured human epidermal keratinocytes by UVB irradiation. Arch Biochem Biophys. 2008 Mar 1; 471(1):85–93. https://doi.org/10.1016/j.abb.2007.12.004 PMID: 18158910

43. Ueta M, Sotozono C, Kinoshita S. Expression of interleukin-4 receptor α in human corneal epithelial cells. Jpn J Ophthalmol. 2011 Jul; 55(4):405–410. https://doi.org/10.1007/s10384-011-0030-6 PMID: 21617960

Appendix 4: Ex vivo cultivated oral mucosal epithelial cell transplantation for limbal stem cell deficiency: a review

Cabral *et al. Stem Cell Research & Therapy* (2020) 11:301
https://doi.org/10.1186/s13287-020-01783-8

Stem Cell Research & Therapy

REVIEW Open Access

Ex vivo cultivated oral mucosal epithelial cell transplantation for limbal stem cell deficiency: a review

Joao Victor Cabral[1], Catherine Joan Jackson[2,3,4], Tor Paaske Utheim[2,4,5] and Katerina Jirsova[1*]

Abstract

Destruction or dysfunction of limbal epithelial stem cells (LESCs) leads to unilateral or bilateral limbal stem cell deficiency (LSCD). Fifteen years have passed since the first transplantation of ex vivo cultivated oral mucosal epithelial cells (COMET) in humans in 2004, which represents the first use of a cultured non-limbal autologous cell type to treat bilateral LSCD. This review summarizes clinical outcomes from COMET studies published from 2004 to 2019 and reviews results with emphasis on the culture methods by which grafted cell sheets were prepared.

Keywords: Cultivated oral mucosal epithelial cell, Limbal stem cell deficiency, Oral mucosal epithelial cells, Tissue regeneration

Background

Damage to the limbus can lead to a decrease in limbal epithelial stem cells (LESCs) and dysfunctional homeostasis of the corneal epithelium. This failure, termed limbal stem cell deficiency (LSCD) [1–3], leads to disruption of the barrier function and invasion of conjunctival cells onto the corneal surface [4, 5]. Conjunctivalization is followed by vascularization, chronic inflammation, photophobia, recurrent pain, and decreased vision [4, 6–8]. LSCD is classified as partial or total and may occur unilaterally or bilaterally [9].

Conjunctival limbal autograft (CLAU) and cultivated limbal epithelium transplantation (CLET) are procedures often used in the treatment of unilateral LSCD [10, 11]. However, patients with bilateral total LSCD do not have limbal tissue available for use in either CLAU or CLET. Thus, options for a source of LESCs are limited to living-related or cadaveric donors and entail use of immunosuppression to prevent rejection [12].

In 2004, Nakamura and co-workers performed the first transplantation of autologous oral epithelial cells cultured ex vivo on human amniotic membrane (AM) to offer an alternative to use of allogenic tissue and avoid immunosuppression [13]. The treatment of LSCD using ex vivo cultivated oral mucosal epithelial cell transplantation (COMET) minimizes the risk of graft rejection and has the added advantage that it can be repeated if necessary. However, neo-angiogenesis following transplantation is a drawback associated with this procedure [13]. This review summarizes clinical outcomes from COMET case series from 2004 to 2019 and reviews the methods used in preparation of transplanted cell sheets.

General analysis of studies

The review was prepared by searching the Ovid MEDLINE database using search terms: limbus corneae, limbus, limbal stem cell deficiency, corneal epithelium, cornea, mouth mucosa, and transplantation. We found 24 studies published over the past fifteen years [13–36].

* Correspondence: katerina.jirsova@lf1.cuni.cz
[1]Laboratory of the Biology and Pathology of the Eye, Institute of Biology and Medical Genetics, First Faculty of Medicine, Charles University and General University Hospital in Prague, Prague, Czech Republic
Full list of author information is available at the end of the article

A case report of one patient (one eye) was excluded from this review [37].

COMET has been performed in Japan [13–19, 23–25, 27, 29, 30], Taiwan [20, 21, 28], India [22], France [26], the UK [31], Poland [32], Thailand [33], Iran [34], South Korea [35], and China [36]. In total, 343 eyes of 315 patients (64% men and 36% women) were included. The age range was from eight to 86 years, the mean age was 46.5 (± 18.6) and 50.8 (± 21.5) years for males and females, respectively. About 26% of male and 23% of female patients were younger than 30 years, while about 28% and approximately 45%, respectively, were older than 60 years.

Three hundred and twenty LSCD eyes were classified as totally deficient, eight eyes as partial [32, 33]. One study classified all 5 eyes as severe LSCD [21]. Nine studies included patients with bilateral LSCD [13–16, 19, 26, 31, 33, 34], two studies included both bilateral and unilateral cases [22, 30], and one study enrolled only patients with unilateral LSCD [25].

Patients and surgery

Etiology

The most common etiology of LSCD is corneal burn (146/343 eyes; 42.6%) resulting from chemical, thermal or unspecified causes, followed by Stevens-Johnson syndrome (SJS) (92/343 eyes; 26.8%) (Fig. 1 and Table 1). Ocular cicatricial pemphigoid (OCP) and pseudo-ocular cicatricial pemphigoid (pOCP) together composed the third most common cause of LSCD receiving COMET (44/343 eyes; 12.8%).

Diagnosis

Diagnosis of LSCD is based on the following clinical features: irregular corneal surface with loss of light reflex, corneal epithelial opacity, loss of limbal palisades of Vogt, fluorescein staining, epithelial thinning in a vortex pattern, corneal neovascularization, peripheral pannus, persistent epithelial defect (PED), corneal stroma scarring, and opacification [6, 38].

Corneal conjunctivalization can be confirmed clinically using in vivo confocal microscopy (IVCM) to define the phenotype of cells on the cornea (conjunctival epithelial cells are hyperreflective with bright nuclei and ill-defined borders, whereas corneal epithelial cells are well-defined with bright borders and dark cytoplasm) [39]. Conjunctival tissue contains goblet cells (GCs) and blood vessels, which can also be seen using IVCM [39]. Impression cytology (IC) is another method used to detect GCs on the corneal surface [4]. In case of GC absence due to severe ocular surface damage, conjunctival (but not corneal) mucins (mucin 1) [40] or keratins (keratin 7, -13, and -15) can be detected using immunocytochemistry [41–43]. Clinical features were used in diagnosis of LSCD in 18/24 studies [13–16, 19, 22–27, 29–33, 35, 36], five of these studies also used IC (Table 1) [19, 23, 31, 33, 36].

Pre-operative considerations

Some studies reported previous surgeries, including AM transplantation (38 eyes) [13, 15, 20–22, 28, 30, 35], and penetrating keratoplasty (PKP) (8 eyes) [14–16, 20, 21, 34, 35], or other (57 eyes) [29, 36]. Moreover, 21 eyes had previously undergone CLAU or allograft transplantation [13–15,

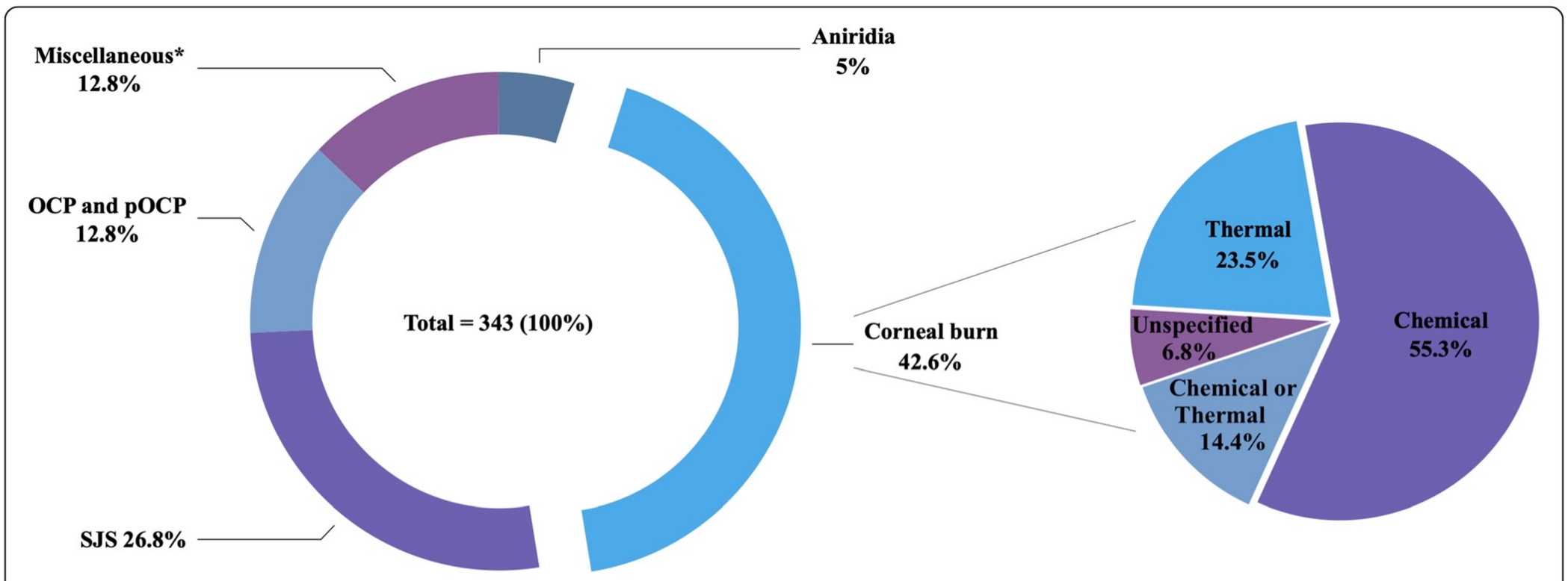

Fig. 1 Etiology of limbal stem cell deficiency (LSCD). Percentages are according to the number of eyes. OCP, ocular cicatricial pemphigoid; pOCP, pseudo-ocular cicatricial pemphigoid; SJS, Stevens-Johnson syndrome. *Miscellaneous (%): trachoma (1.45), post keratitis (1.45), idiopathic (1.2), Lyell syndrome (1.2), rosacea keratitis (0.9), congenital aniridia (0.6), contact lens hypoxia + congenital aniridia (0.6), neuroparalytic keratitis (0.6), Behcet's disease (0.6), graft-versus-host disease (0.6), squamous cell carcinoma (0.6), gelatinous drop-like dystrophy (0.3), multiple eye surgery (0.3), advanced pterygium (0.3), ocular trauma (0.3), contact lens hypoxia (0.3), cystinosis (0.3), severe Groenouw dystrophy (0.3), hepatitis C (0.3), radiation keratopathy (0.3), Salzmann's corneal degeneration (0.3), and drug toxicity (0.3)

Table 1 Summary of clinical studies

Author, year	Etiology	No. of eyes/No. of patients	Dry eye assessment pre-operatively
Nakamura et al., 2004 [13]	SJS × 3, chemical burns × 3	6/4	Yes
Nishida et al., 2004 [14]	SJS × 1, OCP × 3	4/4	Yes
Inatomi et al., 2006 a [15]	SJS × 7, chemical injury × 5, thermal injury × 1, pOCP × 1, idiopathic × 1	15/12	Yes
Inatomi et al., 2006 b [16]	SJS × 1, chemical injury × 1	2/2	Yes
Ang et al., 2006 [17]	SJS × 7, thermal injury × 1, chemical injury × 1, OCP × 1	10/10	Yes
Nakamura et al., 2007 [18]	SJS × 3, chemical injury × 3	6/5	NA
Satake et al., 2008 [19]	SJS × 2, pOCP × 2	4/4	NA
Chen et al., 2009 [20]	Chemical burn × 3, thermal burn × 1	4/4	NA
Ma et al., 2009 [21]	Chemical burn × 3, thermal burn × 2	5/5	NA
Priya et al., 2011 [22]	SJS × 1, chemical injury × 9	10/10	Yes
Satake et al., 2011 [23]	SJS × 12, chemical or thermal injury × 11, OCP × 9, pOCP × 7, gelatinous drop-like dystrophy × 1	40/36	Yes
Nakamura et al., 2011 [24]	SJS × 11, chemical or thermal injury × 1, OCP × 4, squamous cell carcinoma × 2, graft-versus-host disease × 1	19/17	Yes
Takeda et al., 2011 [25]	Chemical burn × 1, thermal burn × 2	3/3	NA
Burillon et al., 2012 [26]	Corneal burn × 9, neuroparalytic keratitis × 2, rosacea keratitis × 3, Lyell syndrome × 4, severe trachoma × 1, contact lens hypoxia × 1, congenital aniridia × 1, cystinosis × 1, severe Groenouw dystrophy × 1, hepatitis C × 1, contact lens hypoxia + congenital aniridia × 2	26/25	Unclear[a]
Hirayama et al., 2012 [27]	Chemical injury × 12, pOCP × 12 (trachoma × 4, Behcet's disease × 2, thermal burn × 1 and post keratitis × 5), SJS × 4, OCP × 4	32/32	Partially (27/32)
Chen et al., 2012 [28]	Chemical burn × 4, thermal burn × 2	6/6	NA
Sotozono et al., 2013 [29]	SJS × 21, OCP × 10, chemical or thermal injury × 7, idiopathic × 3, radiation keratopathy × 1, graft-versus-host disease × 1, congenital aniridia × 1, Salzmann's corneal degeneration × 1, drug toxicity × 1	46/40	Unclear[a]
Sotozono et al., 2014 [30]	SJS × 3, thermal injury × 3, chemical injury × 2, OCP × 2	10/9	Unclear[a]
Kolli et al., 2014 [31]	Chemical burn × 2	2/2	Partially (1/2)
Dobrowolski et al., 2015 [32]	Aniridia × 17	17/13	NA
Prabhasawat et al., 2016 [33]	SJS × 10, chemical burn × 7, multiple eye surgery × 1, advanced pterygium × 1, ocular trauma × 1	20/18	Yes
Baradaren-Rafii et al., 2017 [34]	Chemical burn × 14	14/14	Yes
Kim et al., 2018 [35]	SJS × 6, OCP × 1, chemical burn × 1	8/8	NA
Wang et al., 2019 [36]	Chemical injury × 16, thermal injury × 18	34/32	NA

LSCD limbal stem cell deficiency, *NA* not available, *OCP* ocular cicatricial pemphigoid, *pOCP* pseudo-ocular cicatricial pemphigoid, *SJS* Stevens-Johnson syndrome

[a]These studies mentioned that dry eye patients received artificial tears in the post-operative management, but it was not stated whether dry eye was assessed in all patients

18–22, 35]. In total, 148 earlier surgeries were reported. Thus, the number of eyes previously treated was 119, more than a third (34.7%) of the total number of eyes included in this review [13–16, 18–22, 28–30, 34–36].

Prognostic factors

The presence of pre-operative epithelial defects and/or poor tear production may affect successful outcome [23, 44, 45]. Thus, numerous studies included assessment of dry eye in the pre-operative evaluation (Table 1) [13–17, 22–24, 27, 31, 33, 34]. DeSousa et al. recommend that adnexal abnormalities, including the health and function of the eyelids, fornix, and tear film, be assessed and improved prior to surgery to ensure the best chance of epithelial healing [46]. Conjunctival swab has revealed the presence of pathogenic organisms, which is likely due to a poor ocular surface and absence of a tear film. Therefore, performing a conjunctival swab culture before COMET to ensure a receptive ocular surface is suggested [47]. A complete oral exam is also recommended as successful culture of oral mucosal epithelial cells (OMECs) sheets may be affected by poor oral hygiene and smoking [15, 34].

Surgery

Surgical technique was similar in all studies. First, the conjunctival tissue was removed from the corneal surface, up to 3 mm away from the limbus to expose the corneal stroma [14, 17, 26]. Dissection of symblepharon was performed where necessary, and in some cases, AM was grafted onto the bare sclera to reconstruct the conjunctival fornix [17, 29, 30, 35]. In several cases, the subconjunctival space was treated with Mitomycin C [13, 15–17, 19, 22, 24, 27, 33]. A cultured OMEC sheet measuring from 14 [32] to 23.4 mm [14] diameter was transferred onto the corneal surface. Most of the studies used sutures to secure the graft in place [13, 15–34, 36]. Sutures were not used if the cell sheet was carrier-free [14, 26, 27, 35]. A study also used tissue adhesive glue [33], one used fibrin glue plus temporary tarsorrhaphy [35], and another used lateral tarsorrhaphy [34].

After surgery, AM [31] or therapeutic contact lenses (CLs) [13–36] were typically applied for 1 month [20, 29, 30] or for up to 3 months [24, 36] to protect the graft. One study reported adverse events attributed to hypoxia caused by extended use of CLs [26].

Post-operative considerations

Post-operative management varied considerably across the studies. A moist ocular surface post-COMET has been shown to be an important criterion for success [14, 24]. This was achieved by frequent application of preservative-free artificial tears [14, 19, 23, 26, 27, 32–34, 36], autologous serum eye drops [19, 21, 23, 31–33, 35, 36], or water-retaining hyaluronic acid [19, 23, 35]. One study occluded the lacrimal punctum to increase tear retention [14]. Topical antibiotics were applied in all studies, generally from 2 weeks [32, 33] up to 6 months [22]. Post-operative inflammation was controlled by topical steroids alone [27, 31–33] or in combination with systemic steroids [13, 14, 17, 19, 21–24, 26, 29, 30, 34–36]. The length of the treatment varied from 1 week [14, 26] up to 2 months [13, 21, 34]. Two studies tapered the dose-dependent on the patient response [29, 30]. In some studies, immunosuppression in the form of cyclosporine [17, 24, 29, 30] or cyclophosphamide [13, 21] was used to control post-operative inflammation, and topical tacrolimus [34] was used to decrease the risk of allograft rejection following PKP.

Characteristics of the culture protocol used in clinical studies

Biopsy

The smallest tissue sample was ~ 4.7 mm^2, obtained by using a 3-mm diameter biopsy punch [31], the largest ranged from 120 to 200 mm^2 (Table 2) [35]. Fourteen studies used tissue from the buccal mucosa [14, 19, 21–23, 26–33, 36], and two from the lip [34, 35].

Culture methods

Cell suspension was the most common culture system (23 studies), in which single OMECs were released from tissue using enzymatic treatment (Table 3) [13–30, 32–36]. All but one [33] of the cell suspension cultures reported standard use of 3T3 mouse fibroblasts in coculture, as a feeder layer [13–30, 32, 34–36]. The explant method was investigated in one study, where culture of the biopsy on AM demonstrated faster growth compared to culture on a feeder layer [31]. In vitro work has also shown that OMEC sheets maintain a comparable epithelial stem cell phenotype when cultured on autologous dermal fibroblasts compared with use of 3T3 mouse fibroblasts [48]. Culture time was typically 2 to 3 weeks; the shortest was 1 week [32]. Good manufacturing practice (GMP) regulations were followed in four studies from Japan [29, 30], South Korea [35], and the UK [31].

Medium

Dulbecco Modified Eagle's Medium with HAM F12 mixture (DMEM/F12) was used in more than half of the studies; in ten of these, the DMEM/F12 ratio was 1:1 [13, 15, 16, 18, 19, 22, 23, 25, 27, 34], and in three of them 3:1 (Table 3) [31, 35, 36]. Other studies used supplemented hormonal epithelial medium (SHEM) [20, 28], keratinocyte growth medium (KGM) [17, 24], or serum-free keratinocyte growth medium (KBM-2) [33].

Fetal bovine serum (FBS, or FCS when referred to as "fetal calf serum") was used in nine studies [13, 16, 19–

Table 2 Size and location of oral mucosal biopsy used in COMET

Studies	Biopsy size (mm^2)	Location of biopsy
[13]	2–3	NA
[14]	9	Buccal mucosa
[15]	2–3	NA
[16]	3–5	NA
[17]	2–3	NA
[18]	NA	NA
[19]	50.24[a]	Buccal mucosa (inferior)
[20]	36	NA
[21]	36	Buccal mucosa
[22]	8	Buccal mucosa
[23]	50.24[a]	Buccal mucosa (inferior)
[24]	NA	NA
[25]	NA[c]	NA
[26]	9	Buccal mucosa (cheek)
[27]	50.24[a]	Inferior buccal mucosa
[28]	36	Buccal mucosa
[29]	9.42[b]	Buccal mucosa
[30]	9.42[b]	Buccal mucosa
[31]	4.71[c]	Buccal mucosa (cheek, 20 mm behind the angle of the mouth)
[32]	3–5	Buccal mucosa (inferior)
[33]	100	Buccal mucosa
[34]	NA	Labial mucosa (behind the lip)
[35]	120–200	Labial mucosa (inside the inferior lip)
[36]	16	Buccal mucosa (cheek)

NA not available
Area of an [a]8-, [b]6-, or [c]3-mm diameter biopsy punch

21, 28, 34–36], five used autologous serum (AS) [17, 22, 23, 27, 31], and four used FBS and AS (Table 3) [15, 29, 30, 32]. Only one was serum-free [33]. Use of AS eliminates exposure to xenogeneic compounds contained in animal serum. One study compared use of AS with FBS and found that cell sheet morphology and expression of structural proteins were similar in both groups [17]. Preliminary in vitro work has also shown that AS promotes similar expression of putative stem cells markers in cultured OMEC sheets compared to use of FBS [31]. The two patients receiving AS feeder-free cultured OMEC sheets in this study had significant improvement in corneal epithelium integrity, pain relief, and visual acuity (VA) [31].

Airlifting

Fifteen studies (258 eyes) used airlifting to promote formation of a stratified epithelium (Table 3) [13, 15–19, 23–25, 27, 29, 30, 32, 34, 36]. Airlifting produced more stratification with four to nine layers compared to two to five in non-air-lifted OMEC sheets. Stratification promotes cell-cell adhesion between superficial epithelial cells via tight junction formation, which helps to prevent loss of the transplant due to blinking [49]. On the other hand, highly differentiated air-lifted sheets have lower proliferative function, which is consistent with a decrease in p63α-expressing stem cells [50].

Substrate

AM was the most common culture substrate (Table 3). Eighteen studies used denuded AM (epithelial layer removed) [13, 15–22, 24, 26, 29, 30, 32–34, 36], and one used intact AM [31]. Of the remaining studies, two used either denuded AM or fibrin-coated culture inserts [23, 27], two used temperature-responsive cell-culture inserts [14, 26], and one study did not employ a substrate [35].

Carrier

Most studies employed AM as a culture substrate and OMECs were transferred directly on the same substrate

Table 3 Summary of culture methods used in OMEC sheet preparation

Ref.	Culture system	Substrate	Feeder layer	Nutrient	Air lifting	% SC	Medium	GMP	Carrier	Culture time (days)
[13]	S	dAM	3T3	10% FBS	Y	–	DMEM/F12 (1:1)	N	dAM	14–21
[14]	S	CellSeed[b]	3T3	NA	N	2.1 ± 0.9	NA	N	Carrier-free*	14
[15]	S	dAM	3T3	10% FBS/10% AS	Y	–	DMEM/F12 (1:1)	N	dAM	15–16
[16]	S	dAM	3T3	10% FBS[a]	Y	–	DMEM/F12 (1:1)[a]	N	dAM[a]	14
[17]	S	dAM	3T3	5% AS	Y	–	KGM	N	dAM	15–16
[18]	S[a]	dAM[a]	3T3[a]	U[d]	Y[a]	–	DMEM/F12 (1:1)[a]	N[a]	dAM	U[d]
[19]	S	dAM	3T3	10% FBS	Y	–	DMEM/F12 (1:1)[a]	N	dAM	> 14
[20]	S	dAM	3T3	5% FBS	N	–	SHEM	N	dAM	14–21[a]
[21]	S	dAM	3T3	5% FBS	N	–	U	N	dAM	14–21[a]
[22]	S	dAM	3T3	10% AS	N	2.0 ± 1.0	DMEM/F12 (1:1)	N	dAM	18–21
[23]	S	Fibrin[c]/ dAM	3T3	4% AS	Y	–	DMEM/F12 (1:1)	N	U	NA
[24]	S	dAM	3T3	5% Serum	Y	–	KGM	N	dAM[a]	15–16
[25]	S[a]	dAM	3T3	U[d]	Y	–	DMEM/F12 (1:1)[a]	N	dAM	15–16
[26]	S	CellSeed[b]	3T3	NA	N	3.4 ± 2.06	NA	N	Carrier-free**	U[e]
[27]	S	Fibrin[c]/ dAM	3T3	4% AS	Y	–	DMEM/F12 (1:1)	N	Fibrin group: carrier-free*** AM group: denuded AM	8–16 (Fibrin)/NA (dAM)
[28]	S	dAM	3T3	5% FBS	N	–	SHEM	N	dAM	14–21[a]
[29]	S[a]	dAM[a]	3T3	10%[a] FBS/5%[b] AS	Y	–	U[d]	Y	dAM[a]	8–9
[30]	S[a]	dAM[a]	3T3	10%[a] FBS/%[c] AS	Y	–	U[d]	Y	dAM[a]	8–9
[31]	E	iAM	N	AS	U	~ 12	DMEM/F12 (3:1)	Y	iAM	21
[32]	S	dAM	3T3	10% FBS/10% AS	Y	–	DMEM/F12	N	dAM	7
[33]	S	dAM	N	Serum-free	N	–	KBM-2	N	dAM	14–21
[34]	S[a]	dAM	3T3[a]	10% FBS[a]	Y	–	DMEM/F12 (1:1)[a]	N	dAM	14–21
[35]	S	BM-free	3T3	10% FBS	N	NA	DMEM/F12 (3:1)	Y	Carrier-free****	7–12
[36]	S	dAM	3T3	5% FBS	Y	–	DMEM/F12 (3:1)	N	dAM	U[f]

AM amniotic membrane, *AS* autologous serum, *BM-free* biomaterial-free, *dAM* denuded amniotic membrane, *iAM* intact amniotic membrane, *E* explant, *FBS* fetal bovine serum, *DMEM/F12* Dulbecco modified Eagle's medium (DMEM) with HAM F12 mixture, *GMP* good manufacturing practice, *KGM* keratinocyte growth medium, *KBM-2* serum-free Keratinocyte Growth medium, *N* no, *NA* not available, *S* suspension, *SHEM* supplemented hormonal epithelial medium, *U* unclear, *Y* yes, *3T3* 3T3 murine fibroblasts, *%SC* percentage of transplanted stem cells

[a]According to the referenced protocol in the paper
[b]CellSeed, temperature-responsive cell-culture inserts (CellSeed Inc., Tokyo, Japan)
[c]Fibrin-coated inserts
[d]Conflicting data among the referenced studies
[e]For at least 4 days after the confluence
[f]For at least 5 days after the confluence and then air-lifted for 1 to 2 days
*Supporter
**Polyvinylidene fluoride (PVDF) ring
***Filter paper
****Support mesh

(Table 3). Two studies using temperature-responsive cell-culture inserts transferred cells on a supporter [14] or polyvinylidene fluoride membrane rings [26], which were removed after transfer to the cornea. A filter paper ring was used to transfer cell sheets grown on a fibrin substrate [27]. A support mesh was used in one study employing substrate-free culture [35].

Phenotype of cultured cells and presence of stem cells in culture

Immunohistochemistry and RT-PCR have shown that cultured OMECs are positive for keratin (K)3, K4, and K13 [13, 14, 17, 21, 26, 31–33], the latter is not expressed in the corneal epithelium [51]. OMECs also express markers of corneal differentiation connexin 43, laminin 5 [52, 53], and putative stem cell markers ß1-integrin, p75, p63, ABCG2, C/EBPδ [52, 54]. They do not express corneal-specific K12 and transcription factor PAX6 [22, 31]. However, heterogeneous populations of progenitor cells and mature epithelial cells in oral mucosal epithelium are similar to normal in vivo corneal epithelium; thus, its feasibility as a functional ocular surface epithelium [55, 56].

It has been shown that the presence of at least 3% stem cells (defined as ΔNp63α-positive cells) is associated with clinical success in the treatment of LSCD using CLET [57]. It is likely that the percentage of stem cells in grafted OMEC sheets also influences COMET success. Nishida et al. showed p63 expression in the basal layer of OMEC cultures used in the successful treatment of four patients with LSCD (Table 3) [14]. Analysis of putative stem cell markers (ΔNp63α, ABCG2, and C/EBPδ) in transplants have shown that OMEC and limbal cells have similar expression levels [31]. Four studies employed the colony-forming efficiency (CFE) assay to show the presence of stem cells in OMEC sheets (Table 3) [14, 22, 26, 31]. To date, any correlation between stem cell content in OMEC sheets before transplantation and clinical success using COMET remains to be investigated.

Follow-up and clinical outcome

The shortest reported follow-up period was 1 month [35]; two studies had less than 1 year [26, 35], ten studies 1 to 2 years [13–17, 19, 22, 30, 32, 36], and nine studies between 2 and 3 years [20, 21, 23, 25, 27, 29, 31, 33, 34]. Only two studies had a follow-up time longer than 3 years [24, 28], in which the longest was 7.5 years (Table 4) [24].

Success rate

Clinical success was most consistently defined in terms of a stable ocular surface. Secondary objectives reported were improved VA and best-corrected VA (BCVA). Post-graft investigations rarely included IVCM [16, 21] or IC [19]. Satake et al. used IC to show that in 2/4 eyes, the oral mucosa phenotype persisted for up to 16 months post-operatively, and in some cases the assessed epithelium displayed a mixture of oral mucosal and conjunctival cells [19].

In total, 70.8% (172/243) of eyes receiving COMET achieved a stable ocular surface and were defined as successful (Table 4; see Fig. 2 for detailed results per etiology). This percentage is lower compared to transplantation of cultured limbal epithelial cells (LECs) (75%) [58]. Moreover, one study directly compared COMET to transplantation of allogeneic cultured limbal epithelial transplantation (ACLET) and reported 71.4% (30/42) eyes in the ACLET group achieved a stable ocular surface, versus 52.9% (18/34) eyes in the COMET group. The authors attributed the significantly higher success using ACLET to the lower incidence of post-operative PED, superior LEC proliferation and differentiation, and the ability of LECs to more readily form a stable corneal epithelium [36].

Visual improvement

VA improvement was reported in all but two of the studies (Fig. 2 and Table 4), and 225/331 (68.2%) eyes had some improvement. An improvement in the BCVA of at least two lines was noted in 172/271 (63.5%) eyes (data from 20 studies). The absent or incomplete description of methodology for VA/BCVA measurement prevented an accurate comparison of results between studies. VA inconsistently measured either before or after subsequent surgeries, such as PKP, was another major confounding factor.

Survival of oral mucosal epithelial cells after grafting

Nakamura et al. have shown that post-COMET specimens exhibit a decrease in the number of epithelial layers from 5 to 6 in successful grafts to 2 to 5 disorganized epithelial layers in unsuccessful grafts [18]. The phenotype of COMET grafts (assessed from corneal buttons retrieved after a secondary procedure, mostly PKP) was also investigated in order to characterize the differences between successful (four samples) and unsuccessful (two samples) graft phenotypes [18]. Successful cases showed the presence of K3, a marker common to oral and corneal epithelium, in all specimens; K12, a corneal-specific keratin, presented only occasional staining in one case. K4 and K13, markers of oral mucosal epithelium, were present in both successful and failed samples. In failed specimens, one presented occasional staining for K3, but both were negative for K12. MUC5AC, a conjunctival goblet cell marker [59], was present only in both failed cases and found absent in successful cases [18].

Other studies have also assessed the expression profile post-COMET, but only in successful cases. Results were similar to Nakamura et al., showing positive staining for K3, K4, K13 and negative staining for MUC5AC [16, 20, 31, 35]. Additionally, Kim et al. showed that the corneal-specific keratin, K12, was present in all four successful COMET specimens [35]. Two other studies have indicated occasional K12 staining, shown in 2/6 specimens [16, 20]. These results suggest that the epithelium post-

Table 4 Clinical results, complications, and follow-up

Ref.	Complications	Stable ocular surface, ***n/N*** (%)	VA improvement, ***n/N*** (%)	Improvement in at least 2 lines of BCVA, ***n/N*** (%)	Mean follow-up ± SD (range) in months
[13]	Corneal epithelial defect/bacterial infection × 2	6/6 (100)	6/6 (100)	6/6 (100)	13.8 ± 2.9 (11–17)
[14]	No complications	4/4 (100)	4/4 (100)	4/4 (100)	14 (13–15)
[15]	Epithelial defect × 5	13/15 (86.7)	12/15 (80)	12/15 (80)	20 (3–34)
[16]	No complication	2/2 (100)	2/2 (100)	2/2 (100)	22.5 (19–26)
[17]	Bacterial infection × 1, epithelial defects × 4	10/10 (100)	9/10 (90)	9/10 (90)	12.6 ± 3.9 (8–19)
[18]	Bacterial infection × 1, recurrent small epithelial defects × NA	4/6 (66.7)	NA	NA	NA
[19]	Increased intraocular pressure × 1	4/4 (100)	4/4 (100)	4/4 (100)	16 (6–24)
[20]	NA	NA	4/4 (100)	4/4 (100)	31 (27–35)
[21]	Microperforation × 1, PED × 1	NA	5/5 (100)	5/5 (100)	29.6 ± 3.6 (26–34)
[22]	Corneal graft rejection × 2	5/10 (50)	5/10 (50)	3/10 (30)	18.6 (1–38)
[23]	PED × 19, stromal melting or perforation × 8, corneal infection 3 (bacterial infection × 2, recurrence of epithelial herpes simplex × 1), glaucoma × 8 (3 were new), evisceration × 2	23/40 (57.5)	23,6/40 (59)	NA [d]	25.5 (6–54.9)
[24]	PED × 7, bacterial infection × 1, ocular hypertension × 3	NA	18/19 (95)	15/19 (79)	55 ± 17 (36–90)
[25]	Recurrence of entropion × 1, epithelial defect × 1, Symblepharon 1	2/3 (66.7)[a]	NA	NA	30 (11–50)
[26]	Symblepharon × 1, Pain and graft complication × 1, inflammation × 2, corneal graft rejection × 1, keratitis × 1, increased IOP × 1, corneal perforation × 1, Meibomian cyst × 1, pain and corneal recurrence × 1	NA[b]	17/23 (73.91) [c]	16/23 (69.5)[c]	11.83 (NA)
[27]	Small epithelial defect × 1, PED × 10, ocular hypertension × 3	Substrate-free: 10/16 (62.5) AM: 6/16 (37.5) Total: 16/32 (50)	Substrate-free: 11/16 (68.8) AM: 7/16 (43.8) Total: 18/32 (56.3)	Substrate-free: 11/16 (68.8) AM: 7/16 (43.8) Total: 18/32 (56.3)	25.26 ± 10.8 (14.45–36.08) (substrate-free)[e] 33.73 ± 17 (16,68–50.79) (AM)
[28]	Glaucoma × 1	6/6 (100)	6/6 (100)	6/6 (100)	36.7 + 17 (16–56)
[29]	Hepatic dysfunction × 1, drug-induced allergy × 1, PED × 16, corneal stromal melting × 2, keratitis × 1, endophthalmitis × 1, infiltration × 3, increased IOP × 4	NA	26/46 (56.52)	25/46 (54.3)	28.7 (6.2–85.6)
[30]	Epithelial defect × 3, increased IOP × 2, bacterial infection × 1	10/10 (100)	2/10 (20)	2/10 (20)	22.79 (5.6–39.7)
[31]	Central corneal epithelial defect × 1	2/2 (100)	2/2 (100)	2/2 (100)	31 (21–41)
[32]	Stromal scarring or conjunctival vascularization or stromal vascularization × 3, epithelial defect × 4	13/17 (76.5)	15/17 (88.2)	15/17 (88.2)	16 (12–18)
[33]	PED × 1, perforation × 1	15/20 (75)	14/20 (70)[d]	NA	31.9 ± 12.1 (8–50)
[34]	Epithelial defect × 3, PED × 1, bacterial keratitis × 1, increased IOP × 2, endothelial graft rejection × 4	13/14 (92.9)	14/14 (100)	14/14 (100)	28.2 ± 8.0 (14–40)
[35]	Central epithelial defect × 1, symblepharon × 1, PED × 1, primary failure × 1, recurrence of an epithelial defect × 2	6/8 (75)	5/8 (62.5)	5/8 (62.5)	9.96 ± 4.7 (2.07–15, 8)[f]
[36]	Epithelial defect × 3, PED × 9, increased IOP × 2, stroma melting × 5	18/34 (52.94)	14/34 (41.17)	5/34 (14.7)	16.1 ± 5.8 (range NA)
	Total	172/243 (70.78)	225.6/331 (68.15)	172/271 (63.46)	

n/N number of eyes/total number of eyes, *BCVA* best-corrected visual acuity, *IOP* intraocular pressure, *NA* not available, *PED* persistent epithelial defect, *VA* visual acuity

[a]100% after repeated transplantation

[b]There was a success rate of 16/25 (64%), but it is based on a composition of criteria, not on a stable ocular surface per se

[c]It excluded from the results two patients who had serious adverse events

[d]There is no mention if visual improvement was at least of two lines

[e]Follow-up was originally given in weeks as it follows: 109.8 ± 47 weeks (substrate-free) and 146.6 ± 74.1 weeks (AM)

[f]Follow-up was originally given in days as it follows: 303 ± 144 (63–482) days

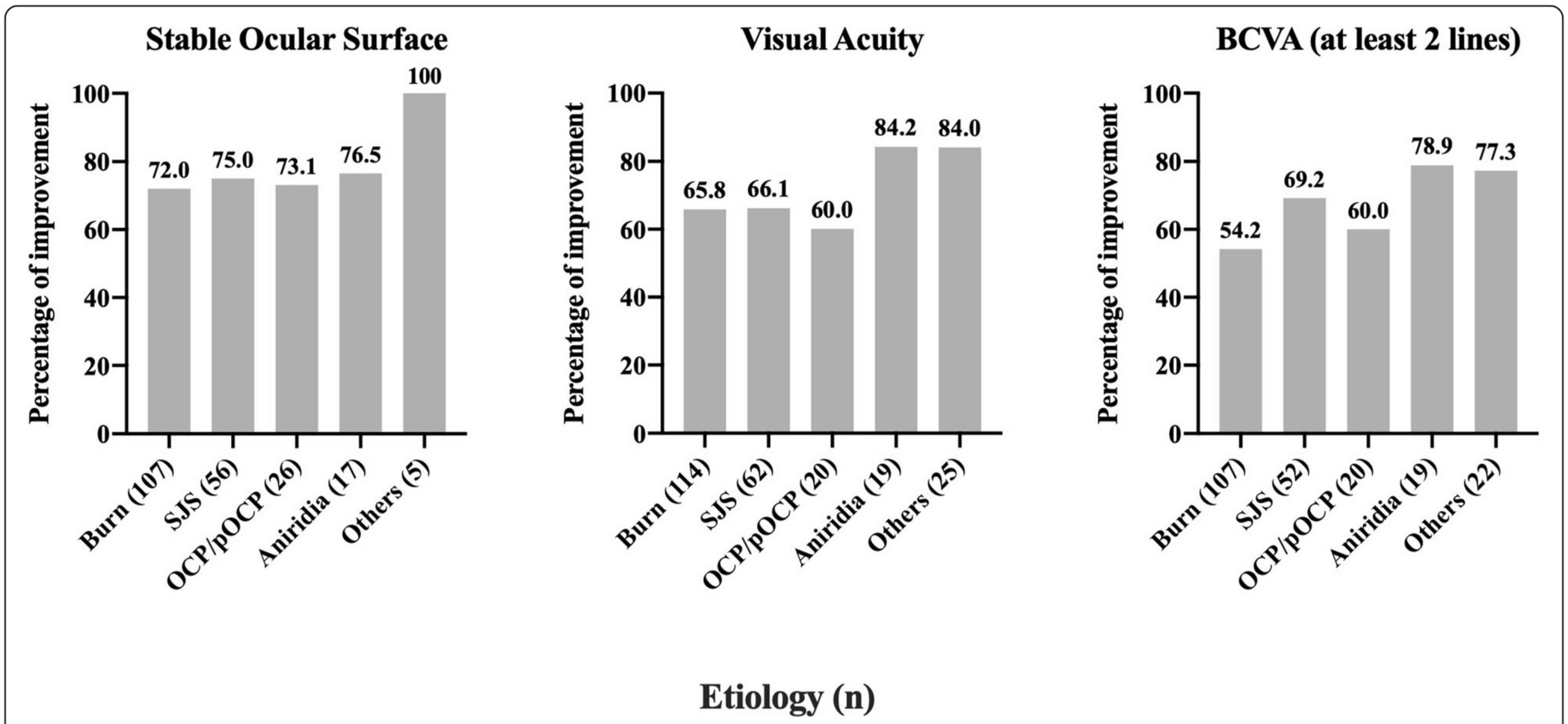

Fig. 2 Results per etiology. OCP, ocular cicatricial pemphigoid; pOCP, pseudo-ocular cicatricial pemphigoid; SJS, Stevens-Johnson syndrome. Others: advanced pterygium, Behcet's disease, contact lens hypoxia, contact lens hypoxia + congenital aniridia, cystinosis, drug toxicity, gelatinous drop-like dystrophy, graft-versus-host disease, hepatitis C, idiophatic, Lyell syndrome, multiple eye surgery, neuroparalytic keratitis, ocular trauma, post keratitis, radiation keratopathy, rosacea keratitis, Salzmann's corneal degeneration, severe Groenouw dystrophy, squamous cell carcinoma, and trachoma

COMET exhibits signs of both corneal-like (K12[+]) as well as oral mucosal epithelium phenotype (K13[+]). Detection of K3[+], K4[+], K12[+], K13[+], and MUC5AC[−] in clinically successful grafts shows that cultivated OMECs survive transplantation and continue to contribute to ocular surface integrity [18, 35].

However, without clear detection of cell origin (donor/host) [60–62] it is difficult to determine clearly whether cultivated OMECs were transdifferentiated into the corneal lineage or whether the presence of corneal epithelial cells represents expansion and migration of remaining corneal cells. In vivo study on rats has shown that transplanted oral mucosal cell sheets were able to survive and retain stem/progenitor cells for at least 8 weeks post-operatively, which results in the long-term success of transplantation of cultured OMECs in LSCD patients [63]. It has been suggested that restoration of a non-inflammatory environment post-operatively may be sufficient to allow repopulation of any remaining corneal cells to the ocular surface and/or resumption of normal homeostatic function by residual limbal stem cells [64].

Success of stem cell transplantation and the long-term survival of the graft in ocular surface therapy not only depends on the features of transplanted cells, but also on the surrounding microenvironment, as it provides the necessary signals required for cell maintenance and growth [48, 65]. Huang et al. speculate that transplanted OMECs might be regulated by signals originating from healthy stroma and differentiate toward the corneal phenotype, while simultaneously maintaining the oral phenotype [56]. However, identification of the key factors necessary to promote transdifferentiation of OMECs to the corneal phenotype still requires further research.

Post-operative complications

The most common complications described following COMET were epithelial defects (52.8%; 36.1% PED), increased intraocular pressure or glaucoma (15%), stromal melting or perforation (9.4%), and infection (7.2%) (Fig. 3). For comparison, a review summarizing transplantation of cultured LECs (889 eyes) reported that the most common complications post-surgery were bleeding (8.7%), inflammation (7.5%), and blepharitis and epitheliopathy (4%) [58]. Epithelial defects making up more than half of the complications could reflect the often more serious nature of the bilateral LSCD diagnosis that demands an alternative treatment such as COMET.

Of note, there was no consensus on the definition of PED. For instance, Nakamura et al. considered epithelial defects to be persistent if they lasted for more than 4 weeks [24], while Hirayama et al. [27] defined PED occurring after 1 week following failure of conventional therapy. In a retrospective comparative study (76 eyes) a higher incidence of post-operative PED was reported in eyes receiving COMET (9/34 eyes) compared to those receiving ACLET (3/42 eyes) [36]. Several studies pointed to an association between incidence of post-operative with pre-operative PED [15, 23, 36]. It has also

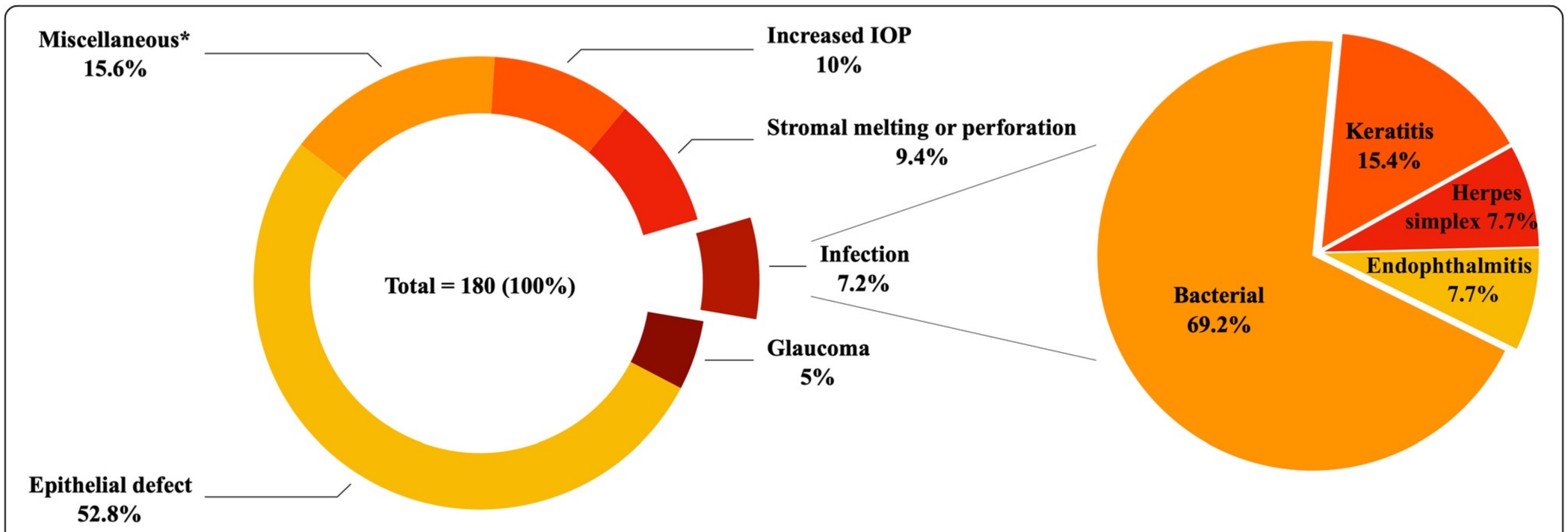

Fig. 3 Post-operative complications. IOP intraocular pressure. *Miscellaneous (%): symblepharon (2.2), endothelial graft rejection (2.2), corneal graft rejection (1.7), stromal scarring or conjunctival/stromal vascularization (1.7), infiltration (1.7), inflammation (1.1), evisceration (1.1), entropion (0.6), primary failure (0.6), hepatic dysfunction (0.6), drug-induced allergy (0.6), pain and graft complication (0.6), Meibomian cyst (0.6), and pain and corneal recurrence (0.6)

been shown that the transplanted epithelium exhibits decreased barrier function following COMET [19].

Baradaran-Rafii et al. suggest that PKP is inevitable in most cases of LSCD involving chemical burns due to the presence of significant corneal opacification [34]. Patients receiving PKP had improved visual function and the authors recommended performing PKP several months post-COMET to achieve the best chance of success [34].

Although most studies noted neovascularization post-transplantation [13–15, 17, 20, 21, 24, 26–28, 32–34, 36], they did not define this as a complication of the procedure. Corneal peripheral neovascularization occurred slowly in most cases, during the first post-operative year [33]. However, the central corneal area was usually spared, and neovascularization usually ceased to progress after 1 year, remaining stable thereafter [14, 33] or gradually abating with time [15, 24]. In the one retrospective study comparing ACLET and COMET, the incidence of neovascularization, corneal conjunctivalization, and improvement in symblepharon was similar between the two groups [36].

Nishida et al. pointed out that stromal vascularization observed beneath COMET transplants on the periphery of the cornea should be differentiated from subepithelial neovascularization that accompanies conjunctival ingrowth, which occurs several months post-transplantation [14]. The peripheral neovascularization seen after COMET may be caused by the lack of antiangiogenic factors, such as the soluble vascular endothelial growth factor (VEGF) receptor, fms-like tyrosine kinase-1 (sFlt-1), tissue inhibitor of metalloproteinase-3 (TIMP-3) and thrombospondin-1 (TSP-1) [28, 66, 67] or by an increase in fibroblast growth factor-2 (FGF-2) [68]. Initial in vitro work suggests that OMEC sheets produced in a culture system where 3T3 fibroblast cells are replaced with limbal niche cells as a feeder layer are less likely to induce postsurgical neovascularization [69].

Effect of preparation method on clinical success

We found that OMEC sheet preparation was relatively standardized; most studies used buccal tissue biopsy, DMEM/F12 culture medium, AM as a substrate and air lifting during culture. Several studies compared OMEC culture methods. The two elements that were directly compared were use of AS versus FBS in the culture medium [17] and use of substrate-free culture versus AM as a substrate [27]. Both AS and substrate-free culture have the advantage of minimizing patient exposure to potential contaminants. Clinical results so far suggest comparative or improved corneal epithelial integrity and VA with use of AS and substrate-free culture compared to the use of FBS and AM. However, larger defined comparative studies are necessary before conclusions can be drawn.

Hirayama et al. reported improved success (10/16; 62.5%) in patients receiving substrate-free OMEC sheets compared to those receiving OMEC cultured on AM (6/16; 37.5%) (Table 4) [27]. Improvement in BCVA was also superior in the substrate-free group with 11/16 (68.8%) showing improvement compared to 7/16 (43.8%). Both methods resulted in a stable ocular surface. However, graft survival was significantly improved in the carrier-free group. This may be attributed to direct contact of transplanted OMECs with stromal keratocytes and promotion of proliferation and differentiation of cells in the transplant [70].

Conclusions

OMECs are to date the most common choice of non-limbal autologous cells in the treatment of LSCD. COMET is a promising treatment modality for LSCD,

with a stable ocular surface reported in 70.8% (172/243) of LSCD eyes, and visual improvement achieved in 68.2% (225.6/331) based on published cases from the past 15 years (2004–2019).

Variation in methodologies (LSCD diagnosis, cell-culture protocols, transplantation technique, post-operative management, and measurement of VA) among the studies did not allow a precise comparative analysis of results. The use of unified tools for characterization of pre-operative status, as well as standardized assessment of outcomes would allow better comparison of studies.

Abbreviations

AM: Amniotic membrane; AS: Autologous serum; ACLET: Allogeneic cultured limbal epithelial transplantation; BCVA: Best-corrected visual acuity; CFE: Colony-forming efficiency; CLAU: Conjunctival limbal autograft; CLET: Cultivated limbal epithelium transplantation; CLs: Contact lenses; COMET: Ex vivo cultivated oral mucosal epithelial cell transplantation; DMEM/F12: Dulbecco Modified Eagle's Medium (DMEM) with HAM F12 mixture; FBS: Fetal bovine serum; FCS: Fetal calf serum; GCs: Goblet cells; GMP: Good manufacturing practice; KBM-2: Serum-free keratinocyte growth medium; KGM: Keratinocyte growth medium; IC: Impression cytology; IVCM: In vivo confocal microscopy; LECs: Limbal epithelial cells; LESCs: Limbal epithelial stem cells; LSCD: Limbal stem cell deficiency; OCP: Ocular cicatricial pemphigoid; OMECs: Oral mucosal epithelial cells; pOCP: Pseudo-ocular cicatricial pemphigoid; PED: Persistent epithelial defect; PKP: Penetrating keratoplasty; sFlt-1: fms-like tyrosine kinase-1; SHEM: Supplemented hormonal epithelial medium; SJS: Stevens-Johnson syndrome; TIMP-3: Tissue inhibitor of metalloproteinase-3; TSP-1: Thrombospondin-1; VA: Visual acuity; VEGF: Vascular endothelial growth factor

Acknowledgements

Not applicable.

Authors' contributions

JVC, TPU, and KJ contributed to the design and implementation of the research. JVC and KJ contributed to the analysis of the results. JVC, CJJ, and KJ wrote the manuscript. All authors read and approved the final manuscript.

Authors' information

Not applicable.

Funding

Institutional support was provided by Progres-Q25 (JVC, KJ). This study was supported by research projects BBMRI_CZ LM 2018125 and EF16_013/0001674.

Availability of data and materials

Not applicable.

Ethics approval and consent to participate

Not applicable.

Consent for publication

Not applicable.

Competing interests

The authors declare that they have no competing interests.

Author details

[1]Laboratory of the Biology and Pathology of the Eye, Institute of Biology and Medical Genetics, First Faculty of Medicine, Charles University and General University Hospital in Prague, Prague, Czech Republic. [2]Department of Medical Biochemistry, Oslo University Hospital, Oslo, Norway. [3]Department of Oral Biology, Faculty of Dentistry, University of Oslo, Oslo, Norway. [4]Department of Plastic and Reconstructive Surgery, Oslo University Hospital, Oslo, Norway. [5]Department of Ophthalmology, Sørlandet Hospital Trust Arendal, Arendal, Norway.

Received: 21 February 2020 Revised: 26 May 2020
Accepted: 18 June 2020 Published online: 21 July 2020

References

1. Schwartz GS, LoVerde L, Gomes J, Holland EJ. Classification and staging of ocular surface disease. In: Mark J. Mannis, Edward J. Holland., editors. Cornea. 4th ed. Elsevier; 2017. p. 1668–1680.
2. Chen JJ, Tseng SC. Abnormal corneal epithelial wound healing in partial-thickness removal of limbal epithelium. Invest Ophthalmol Vis Sci. 1991; 32(8):2219–33.
3. Kruse FE, Chen JJ, Tsai RJ, Tseng SC. Conjunctival transdifferentiation is due to the incomplete removal of limbal basal epithelium. Invest Ophthalmol Vis Sci. 1990;31(9):1903–13.
4. Puangsricharern V, Tseng SC. Cytologic evidence of corneal diseases with limbal stem cell deficiency. Ophthalmology. 1995;102(10):1476–85.
5. Huang AJ, Tseng SC. Corneal epithelial wound healing in the absence of limbal epithelium. Invest Ophthalmol Vis Sci. 1991;32(1):96–105.
6. Dua HS, Azuara-Blanco A. Limbal stem cells of the corneal epithelium. Surv Ophthalmol. 2000;44(5):415–25.
7. Dua HS, Joseph A, Shanmuganathan VA, Jones RE. Stem cell differentiation and the effects of deficiency. Eye (Lond). 2003;17(8):877–85.
8. Tseng SC. Staging of conjunctival squamous metaplasia by impression cytology. Ophthalmology. 1985;92(6):728–33.
9. Dua HS, Saini JS, Azuara-Blanco A, Gupta P. Limbal stem cell deficiency: concept, aetiology, clinical presentation, diagnosis and management. Indian J Ophthalmol. 2000;48(2):83–92.
10. Kenyon KR, Tseng SC. Limbal autograft transplantation for ocular surface disorders. Ophthalmology. 1989;96(5):709–22 discussion 722.
11. Pellegrini G, Traverso CE, Franzi AT, Zingirian M, Cancedda R, De Luca M. Long-term restoration of damaged corneal surfaces with autologous cultivated corneal epithelium. Lancet. 1997;349(9057):990–3.
12. Zhao Y, Ma L. Systematic review and meta-analysis on transplantation of ex vivo cultivated limbal epithelial stem cell on amniotic membrane in limbal stem cell deficiency. Cornea. 2015;34(5):592–600.
13. Nakamura T, Inatomi T, Sotozono C, Amemiya T, Kanamura N, Kinoshita S. Transplantation of cultivated autologous oral mucosal epithelial cells in patients with severe ocular surface disorders. Br J Ophthalmol. 2004;88(10): 1280–4.
14. Nishida K, Yamato M, Hayashida Y, Watanabe K, Yamamoto K, Adachi E, et al. Corneal reconstruction with tissue-engineered cell sheets composed of autologous oral mucosal epithelium. N Engl J Med. 2004;351(12):1187–96.
15. Inatomi T, Nakamura T, Koizumi N, Sotozono C, Yokoi N, Kinoshita S. Midterm results on ocular surface reconstruction using cultivated autologous oral mucosal epithelial transplantation. Am J Ophthalmol. 2006; 141(2):267–75.
16. Inatomi T, Nakamura T, Kojyo M, Koizumi N, Sotozono C, Kinoshita S. Ocular surface reconstruction with combination of cultivated autologous oral mucosal epithelial transplantation and penetrating keratoplasty. Am J Ophthalmol. 2006;142(5):757–64.
17. Ang LPK, Nakamura T, Inatomi T, Sotozono C, Koizumi N, Yokoi N, et al. Autologous serum-derived cultivated oral epithelial transplants for severe ocular surface disease. Arch Ophthalmol. 2006;124(11):1543–51.
18. Nakamura T, Inatomi T, Cooper LJ, Rigby H, Fullwood NJ, Kinoshita S. Phenotypic investigation of human eyes with transplanted autologous cultivated oral mucosal epithelial sheets for severe ocular surface diseases. Ophthalmology. 2007;114(6):1080–8.
19. Satake Y, Dogru M, Yamane G-Y, Kinoshita S, Tsubota K, Shimazaki J. Barrier function and cytologic features of the ocular surface epithelium after autologous cultivated oral mucosal epithelial transplantation. Arch Ophthalmol. 2008;126(1):23–8.
20. Chen H-CJ, Chen H-L, Lai J-Y, Chen C-C, Tsai Y-J, Kuo M-T, et al. Persistence of transplanted oral mucosal epithelial cells in human cornea. Invest Ophthalmol Vis Sci. 2009;50(10):4660–8.
21. Ma DHK, Kuo MT, Tsai YJ, Chen HCJ, Chen XL, Wang SF, et al. Transplantation of cultivated oral mucosal epithelial cells for severe corneal burn. Eye (Lond). 2009;23(6):1442–50.
22. Priya CG, Arpitha P, Vaishali S, Prajna NV, Usha K, Sheetal K, et al. Adult human buccal epithelial stem cells: identification, ex-vivo expansion, and transplantation for corneal surface reconstruction. Eye (Lond). 2011;25(12): 1641–9.

23. Satake Y, Higa K, Tsubota K, Shimazaki J. Long-term outcome of cultivated oral mucosal epithelial sheet transplantation in treatment of total limbal stem cell deficiency. Ophthalmology. 2011;118(8):1524–30.
24. Nakamura T, Takeda K, Inatomi T, Sotozono C, Kinoshita S. Long-term results of autologous cultivated oral mucosal epithelial transplantation in the scar phase of severe ocular surface disorders. Br J Ophthalmol. 2011;95(7):942–6.
25. Takeda K, Nakamura T, Inatomi T, Sotozono C, Watanabe A, Kinoshita S. Ocular surface reconstruction using the combination of autologous cultivated oral mucosal epithelial transplantation and eyelid surgery for severe ocular surface disease. Am J Ophthalmol. 2011;152(2):195–201 e1.
26. Burillon C, Huot L, Justin V, Nataf S, Chapuis F, Decullier E, et al. Cultured autologous oral mucosal epithelial cell sheet (CAOMECS) transplantation for the treatment of corneal limbal epithelial stem cell deficiency. Invest Ophthalmol Vis Sci. 2012;53(3):1325–31.
27. Hirayama M, Satake Y, Higa K, Yamaguchi T, Shimazaki J. Transplantation of cultivated oral mucosal epithelium prepared in fibrin-coated culture dishes. Invest Ophthalmol Vis Sci. 2012;53(3):1602–9.
28. Chen H-CJ, Yeh L-K, Tsai Y-J, Lai C-H, Chen C-C, Lai J-Y, et al. Expression of angiogenesis-related factors in human corneas after cultivated oral mucosal epithelial transplantation. Invest Ophthalmol Vis Sci. 2012;53(9):5615–23.
29. Sotozono C, Inatomi T, Nakamura T, Koizumi N, Yokoi N, Ueta M, et al. Visual improvement after cultivated oral mucosal epithelial transplantation. Ophthalmology. 2013;120(1):193–200.
30. Sotozono C, Inatomi T, Nakamura T, Koizumi N, Yokoi N, Ueta M, et al. Cultivated oral mucosal epithelial transplantation for persistent epithelial defect in severe ocular surface diseases with acute inflammatory activity. Acta Ophthalmol. 2014;92(6):e447–53.
31. Kolli S, Ahmad S, Mudhar HS, Meeny A, Lako M, Figueiredo FC. Successful application of ex vivo expanded human autologous oral mucosal epithelium for the treatment of total bilateral limbal stem cell deficiency. Stem Cells. 2014;32(8):2135–46.
32. Dobrowolski D, Orzechowska-Wylegala B, Wowra B, Wroblewska-Czajka E, Grolik M, Szczubialka K, et al. Cultivated oral mucosa epithelium in ocular surface reconstruction in aniridia patients. Biomed Res Int. 2015;2015:281870.
33. Prabhasawat P, Ekpo P, Uiprasertkul M, Chotikavanich S, Tesavibul N, Pornpanich K, et al. Long-term result of autologous cultivated oral mucosal epithelial transplantation for severe ocular surface disease. Cell Tissue Bank. 2016;17(3):491–503.
34. Baradaran-Rafii A, Delfazayebaher S, Aghdami N, Taghiabadi E, Bamdad S, Roshandel D. Midterm outcomes of penetrating keratoplasty after cultivated oral mucosal epithelial transplantation in chemical burn. Ocul Surf. 2017;15(4):789–94.
35. Kim YJ, Lee HJ, Ryu JS, Kim YH, Jeon S, Oh JY, et al. Prospective clinical trial of corneal reconstruction with biomaterial-free cultured oral mucosal epithelial cell sheets. Cornea. 2018;37(1):76–83.
36. Wang J, Qi X, Dong Y, Cheng J, Zhai H, Zhou Q, et al. Comparison of the efficacy of different cell sources for transplantation in total limbal stem cell deficiency. Graefes Arch Clin Exp Ophthalmol. 2019;257(6):1253–63.
37. Gaddipati S, Muralidhar R, Sangwan VS, Mariappan I, Vemuganti GK, Balasubramanian D. Oral epithelial cells transplanted on to corneal surface tend to adapt to the ocular phenotype. Indian J Ophthalmol. 2014;62(5):644–8.
38. Le Q, Xu J, Deng SX. The diagnosis of limbal stem cell deficiency. Ocul Surf. 2018;16(1):58–69.
39. Dua HS, Miri A, Alomar T, Yeung AM, Said DG. The role of limbal stem cells in corneal epithelial maintenance: testing the dogma. Ophthalmology. 2009;116(5):856–63.
40. Barbaro V, Ferrari S, Fasolo A, Pedrotti E, Marchini G, Sbabo A, et al. Evaluation of ocular surface disorders: a new diagnostic tool based on impression cytology and confocal laser scanning microscopy. Br J Ophthalmol. 2010;94(7):926–32.
41. Jirsova K, Dudakova L, Kalasova S, Vesela V, Merjava S. The OV-TL 12/30 clone of anti-cytokeratin 7 antibody as a new marker of corneal conjunctivalization in patients with limbal stem cell deficiency. Invest Ophthalmol Vis Sci. 2011;52(8):5892–8.
42. Poli M, Janin H, Justin V, Auxenfans C, Burillon C, Damour O. Keratin 13 immunostaining in corneal impression cytology for the diagnosis of limbal stem cell deficiency. Invest Ophthalmol Vis Sci. 2011;52(13):9411–5.
43. Yoshida S, Shimmura S, Kawakita T, Miyashita H, Den S, Shimazaki J, et al. Cytokeratin 15 can be used to identify the limbal phenotype in normal and diseased ocular surfaces. Invest Ophthalmol Vis Sci. 2006;47(11):4780–6.
44. Ilari L, Daya SM. Long-term outcomes of keratolimbal allograft for the treatment of severe ocular surface disorders. Ophthalmology. 2002;109(7):1278–84.
45. Shimazaki J, Shimmura S, Fujishima H, Tsubota K. Association of preoperative tear function with surgical outcome in severe Stevens-Johnson syndrome. Ophthalmology. 2000;107(8):1518–23.
46. DeSousa J-L, Daya S, Malhotra R. Adnexal surgery in patients undergoing ocular surface stem cell transplantation. Ophthalmology. 2009;116(2):235–42.
47. Gunasekaran S, Dhiman R, Vanathi M, Mohanty S, Satpathy G, Tandon R. Ocular surface microbial flora in patients with chronic limbal stem cell deficiency undergoing cultivated oral mucosal epithelial transplantation. Middle East Afr J Ophthalmol. 2019;26(1):23–6.
48. Sharma SM, Fuchsluger T, Ahmad S, Katikireddy KR, Armant M, Dana R, et al. Comparative analysis of human-derived feeder layers with 3T3 fibroblasts for the ex vivo expansion of human limbal and oral epithelium. Stem Cell Rev Rep. 2012;8(3):696–705.
49. Kinoshita S, Koizumi N, Nakamura T. Transplantable cultivated mucosal epithelial sheet for ocular surface reconstruction. Exp Eye Res. 2004;78(3):483–91.
50. Massie I, Levis HJ, Daniels JT. Response of human limbal epithelial cells to wounding on 3D RAFT tissue equivalents: effect of airlifting and human limbal fibroblasts. Exp Eye Res. 2014;127:196–205.
51. Ramirez-Miranda A, Nakatsu MN, Zarei-Ghanavati S, Nguyen CV, Deng SX. Keratin 13 is a more specific marker of conjunctival epithelium than keratin 19. Mol Vis. 2011;17:1652–61.
52. Utheim OA, Pasovic L, Raeder S, Eidet JR, Fostad IG, Sehic A, et al. Effects of explant size on epithelial outgrowth, thickness, stratification, ultrastructure and phenotype of cultured limbal epithelial cells. PLoS One. 2019;14(3):e0212524.
53. Yamaguchi M, Ebihara N, Shima N, Kimoto M, Funaki T, Yokoo S, et al. Adhesion, migration, and proliferation of cultured human corneal endothelial cells by laminin-5. Invest Ophthalmol Vis Sci. 2011;52(2):679–84.
54. Kolli S, Bojic S, Ghareeb AE, Kurzawa-Akanbi M, Figueiredo FC, Lako M. The role of nerve growth factor in maintaining proliferative capacity, colony-forming efficiency, and the limbal stem cell phenotype. Stem Cells. 2019;37(1):139–49.
55. Sen S, Sharma S, Gupta A, Gupta N, Singh H, Roychoudhury A, et al. Molecular characterization of explant cultured human oral mucosal epithelial cells. Invest Ophthalmol Vis Sci. 2011;52(13):9548–54.
56. Huang F, Qiu J, Xue Q, Cai R, Zhang C. Phenotypes and transdifferentiation of transplanted oral mucosal epithelial cells for limbal stem cell deficiency; 2019.
57. Rama P, Matuska S, Paganoni G, Spinelli A, De Luca M, Pellegrini G. Limbal stem-cell therapy and long-term corneal regeneration. N Engl J Med. 2010;363(2):147–55.
58. Utheim TP. Limbal epithelial cell therapy: past, present, and future. Methods Mol Biol. 2013;1014:3–43.
59. Gipson IK, Inatomi T. Mucin genes expressed by the ocular surface epithelium. Prog Retin Eye Res. 1997;16(1):81–98.
60. Shimazaki J, Kaido M, Shinozaki N. Evidence of long-term survival of donor-derived cells after limbal allograft transplantation. … & visual science; 1999.
61. Henderson TR, Findlay I, Matthews PL, Noble BA. Identifying the origin of single corneal cells by DNA fingerprinting: part II-- application to limbal allografting. Cornea. 2001;20(4):404–7.
62. Sharpe JR, Daya SM, Dimitriadi M, Martin R, James SE. Survival of cultured allogeneic limbal epithelial cells following corneal repair. Tissue Eng. 2007;13(1):123–32.
63. Soma T, Hayashi R, Sugiyama H, Tsujikawa M, Kanayama S, Oie Y, et al. Maintenance and distribution of epithelial stem/progenitor cells after corneal reconstruction using oral mucosal epithelial cell sheets. PLoS One. 2014;9(10):e110987.
64. Liang L, Sheha H, Li J, Tseng SCG. Limbal stem cell transplantation: new progresses and challenges. Eye (Lond). 2009;23(10):1946–53.
65. Wan P-X, Wang B-W, Wang Z-C. Importance of the stem cell microenvironment for ophthalmological cell-based therapy. World J Stem Cells. 2015;7(2):448–60.
66. Kanayama S, Nishida K, Yamato M, Hayashi R, Maeda N, Okano T, et al. Analysis of soluble vascular endothelial growth factor receptor-1 secreted from cultured corneal and oral mucosal epithelial cell sheets in vitro. Br J Ophthalmol. 2009;93(2):263–7.
67. Sekiyama E, Nakamura T, Kawasaki S, Sogabe H, Kinoshita S. Different expression of angiogenesis-related factors between human cultivated corneal and oral epithelial sheets. Exp Eye Res. 2006;83(4):741–6.

68. Kanayama S, Nishida K, Yamato M, Hayashi R, Sugiyama H, Soma T, et al. Analysis of angiogenesis induced by cultured corneal and oral mucosal epithelial cell sheets in vitro. Exp Eye Res. 2007;85(6):772–81.
69. Duan C-Y, Xie H-T, Zhao X-Y, Xu W-H, Zhang M-C. Limbal niche cells can reduce the angiogenic potential of cultivated oral mucosal epithelial cells. Cell Mol Biol Lett. 2019;24:3.
70. Wilson SE, Mohan RR, Mohan RR, Ambrósio R, Hong J, Lee J. The corneal wound healing response. Prog Retin Eye Res. 2001;20(5):625–37.

Publisher's Note

Appendix 5: The healing dynamics of non-healing wounds using cryo-preserved amniotic membrane

Received: 24 August 2021 | Revised: 25 October 2021 | Accepted: 26 October 2021

DOI: 10.1111/iwj.13719

ORIGINAL ARTICLE

IWJ WILEY

The healing dynamics of non-healing wounds using cryo-preserved amniotic membrane

Alzbeta Svobodova[1] | **Vojtech Horvath**[2] | **Ingrida Smeringaiova**[3] | **Joao Victor Cabral**[3] | **Martina Zemlickova**[4] | **Radovan Fiala**[5] | **Jan Burkert**[5,6] | **Denisa Nemetova**[6] | **Petr Stadler**[2] | **Jaroslav Lindner**[1] | **Jan Bednar**[3] | **Katerina Jirsova**[3,6]

[1]2nd Department of Surgery—Department of Cardiovascular Surgery, First Faculty of Medicine, Charles University and General University Hospital in Prague, Prague, Czech Republic

[2]Department of Vascular Surgery, Na Homolce Hospital, Prague, Czech Republic

[3]Laboratory of the Biology and Pathology of the Eye, Institute of Biology and Medical Genetics, First Faculty of Medicine, Charles University, Prague, Czech Republic

[4]Clinic of Dermatovenerology, General Teaching Hospital and First Faculty of Medicine, Charles University, Prague, Czech Republic

[5]Department of Cardiovascular Surgery, Motol University Hospital, Prague, Czech Republic

[6]Department of Transplantation and Tissue Bank, Motol University Hospital, Prague, Czech Republic

Correspondence
Assoc. Prof. Katerina Jirsova, Ph.D., Laboratory of the Biology and Pathology of the Eye, Institute of Biology and Medical Genetics, First Faculty of Medicine, Charles University, Albertov 4 128 00 Prague, Czech Republic.
Email: katerina.jirsova@lf1.cuni.cz

Funding information
Ministerstvo Zdravotnictví Ceské Republiky, Grant/Award Number:

Abstract

We evaluated the effect of the application of cryo-preserved amniotic membrane on the healing of 26 non-healing wounds (18 patients) with varying aetiologies and baseline sizes (average of 15.4 cm^2), which had resisted the standard of care treatment for 6 to 456 weeks (average 88.8 weeks). Based on their average general responses to the application of cryo-preserved AM, we could differentiate three wound groups. The first healed group was characterised by complete healing (100% wound closure, maximum treatment period 38 weeks) and represented 62% of treated wounds. The wound area reduction of at least 50% was reached for all wounds in this group within the first 10 weeks of treatment. Exactly 19% of the studied wounds responded partially to the treatment (partially healed group), reaching less than 25% of closure in the first 10 weeks and 90% at maximum for extended treatment period (up to 78 weeks). The remaining 19% of treated wounds did not show any reaction to the AM application (unhealed defects). The three groups have different profiles of wound area reduction, which can be used as a guideline in predicting the healing prognosis of non-healing wounds treated with a cryo-preserved amniotic membrane.

Key Messages

- we evaluated the effect of the application of cryo-preserved amniotic membrane on the healing of non-healing wounds
- twenty-six wounds (18 patients) of various aetiologies and baseline sizes with a history of long preceding resistance to standard care were treated for an extended time period (up to 78 weeks)
- we showed that the amniotic membrane application had a profitable effect promoting a complete healing of 62% of treated, previously non-healing defects

NV18-08-00106; Ministry of Education, Youth and Sport of the Czech Republic, Grant/Award Number: BBMRI_CZ LM2018125; Univerzita Karlova v Praze, Grant/Award Number: Progres-Q25

- analysis of our results also suggests that the dynamics of healing process can be used as a predictor of the outcome of the treatment

KEYWORDS

cryo-preserved amniotic membrane, healing dynamics, non-healing wounds

1 | INTRODUCTION

The general term 'chronic wounds' envelopes a heterogeneous group of wounds exhibiting specific healing process physiology different from the acute ones. They typically require a considerably long healing time and are characterised by tissue renewal by granulation.[1] The period required for a wound to be classified as chronic has been defined in the range of 4 weeks up to more than 3 months.[2] As the nomenclature 'chronic wound' is not clear, the European Wound Management Association (EWMA) proposed to use the term 'non-healing wounds' (NHWs),[3] which will be used herein. Common features of NHW include persistent infections, the formation of drug-resistant microbial biofilms, and loss of dermal/epidermal cells ability to respond to reparative stimuli.[4] NHWs are associated with numerous pathological conditions: diabetes mellitus (DM), peripheral artery disease (PAD), chronic venous insufficiency, post-traumatic wounds, or postsurgical wound dehiscence. Apart from the pathological effects, the NHWs have an important impact on the quality of life of affected subjects in the sense of elimination or discrimination from society, limited mobility, and productivity.[5]

The current standard of care (SOC) for treating NHW includes surgical debridement, infection control, appropriate dressing, and treatment of primary pathology. Despite the development of many types of wound dressings, the healing of NHW is often challenging to achieve. Using SOC, closure rates for NHW range from 21% to 35%, and the recurrence rate is high.[6] The increase in the healing efficiency and reduction of the recurrence rate, the healing time, and the costs are thus the objectives of the new approaches to NHW care. The use of different forms of biological dressings, particularly placental derivatives, has been accepted as a promising tool in regenerative medicine.[7-10] Most frequently, they are based on amniochorionic (ACM) or amniotic membrane (AM). For decades the ACM and AM have been recognised for their wound healing stimulation properties and their negligible immunogenicity, making them an attractive choice for biological wound dressing. AM application has been adapted particularly in the ocular surface healing, and in the last decade, its efficiency is broadly confirmed in other surgical procedures in dermatology, plastic surgery, genitourinary medicine, and otolaryngology.[8,11-13]

AM application promotes several effects supporting wound healing, namely anti-inflammatory, anti-fibrotic, anti-microbial, neurotrophic, and analgesic. Besides that, AM influences angiogenesis. AM grafting does not lead to immunological rejection, and there is no need for any immunosuppressive treatment.[13-16] Therefore, the AM grafts are considered a safe substrate, promoting proper granulation and epithelisation, assuring better hydration of the wound bed while suppressing excessive fibrosis. Many studies have reported the healing benefits of AM applied to NHW; improved healing rates (percentage of completely healed wounds) and significantly shortened healing times have been documented.

Systematic studies of the effect of the AM or ACM effect date back to the early 80s of the last century.[17] Often such studies report different healing success rates and wound closure progress, depending on the procedure of AM or ACM preparation (cryo-preserved, dried, or lyophilised),[18] AM application frequency,[19] type of wound treated (diabetic, venous, or arterial ulcer, surgical wound, dehiscence),[20] and the treatment and application approach selected.[7,21,22]

The complete healing rate of NHW because of AM's beneficial effect is reported to be anywhere between 20%[23] and 100%,[24] indicating the existence of non-negligible proportions of subjects who will not respond to the AM treatment. However, it is still unclear whether it is possible to identify such individuals already at the early treatment period (although some indications exist[25]). Because of the elevated cost of AM treatment, this information can be an important economic factor when opting for AM application after SOC failure.

In the present work, we studied the effect of cryo-preserved AM application on NHW of various aetiologies (venous, arterial, postoperative, diabetic) and various sizes (from 0.5 to 98 cm^2), which had previously resisted SOC for more than 6 weeks (average 88.8). By evaluating the healing progress, we aimed to determine the efficiency of the AM treatment and analyse whether the dynamics of the wound closure can be used as a predictor/estimator for the efficacy of the AM treatment of NHW.

2 | MATERIALS AND METHODS

The study followed the Ethics Committee standards of four participating institutions (1st Medical Faculty of Charles University, General University Hospital, University Hospital Motol, and Na Homolce Hospital, all in Prague) and adhered to the tenets set out in the Declaration of Helsinki.

3 | SUBJECTS

The patients for the study were selected according to the following criteria: Inclusion criteria: age ≥18 years, the presence of resistant NHW with the duration of more than 6 weeks, wound of maximum size of 150 cm^2 extending through the full thickness of the skin but not reaching to the tendon or bone. Exclusion criteria: Tendon or bone exposure in the wound, allergy to antibiotics used in solution for AM decontamination, transcutaneous oximetry value below 30 mmHg for patients with DM, known history of AIDS or HIV, ankle brachial index (ABI) <0.5, for all patients except those with DM, suspicious for cancer or history of radiation at wound site, severe (uncontrolled) systemic disease, or planned surgical intervention in the next 6 months.

Patients willing to participate in the study and complying with the criteria signed an informed consent form. Eighteen patients were enrolled in the study (13 men, 5 women) with a total of 26 wounds (multiple wounds in some patients). The average age of the patients was 62.6 years (26 to 85). The treated wound size varied between 0.5 and 98 cm^2 with an average of 15.4 ± 20.2 cm^2. The wound resistance to treatments preceding the enrolment into the study spanned from 6 to 456 weeks with an average of 88.8 weeks. The demographic data of patients are summarised in Table 1.

4 | AM GRAFTS PREPARATION

All placenta donors signed informed consent and were checked negative for hepatitis B and C, syphilis, and HIV, and C-reactive protein was < 20 mg/L. Placentas were obtained from full-term deliveries by elective caesarean section in the Motol University Hospital, Prague, and before processing visually inspected for injuries, visible pathologies, or comorbidities. Then they were immediately placed in a sterile container, overlaid with decontamination solution BASE•128 (Alchimia, Ponte San Nicolò, Italy), and stored at room temperature for 20 hours. The placentas were subsequently processed in aseptic conditions. They were repeatedly cleansed using physiological solution (0.9% NaCl), AM sheets were peeled off by blunt dissection, and blood clots were removed. AM was then overlaid with DMEM (c.n. 32 430 027, Thermo Fisher Scientific) supplemented with antibiotics (Piperacillin/Tazobactam, Amphotericin B, Vancomycin, and Gentamicin) and stored for at least 2 hours to complete the decontamination. Next, the AM sheets were rinsed in physiological solution, stretched on Sanatyl support (Tylex, Letovice, Czech Republic), and sectioned into patches of the desired size. Finally, AM pieces were placed in containers filled with storage medium (50% glycerol in DMEM) (glycerol, Dr Kulich Pharma, Czech Republic) and stored at −80°C. Tissues with negative microbiology tests and negative repeated serology examination performed after 6 months were released after 6 months for grafting.

5 | AM DRESSING APPLICATION AND THE WOUND TREATMENT PROCEDURE

All patients followed up a standard visit protocol. The study visits were scheduled every 7 days and included photodocumentation of the healing process, evaluation of subjective pain perception and completion of patients quality of life questionnaire, the treatment of the wound and surrounding skin, application of AM, and secondary fixation dressing application. The initial AM application frequency was set to weekly (every visit), but it was modulated later according to the evolution of the healing progress. Wound care procedure was standardised for all centres similarly: wound debridement, rinsing with saline, cultivation collection (each 4 weeks, or if necessary), and disinfectant solution application. After thawing, the AM was removed from the storage solution and washed with saline (2 × 5 minutes) in a sterile container. The AM graft was applied with at least 5 mm overlap, and complete contact with the wound surface was assured. After verifying appropriate graft adhesion, a fixation with foam cover (Mepilex XT, Mölnlycke Health, Sweden) was formed with an overlap of at least 2 cm and fixed with a bandage. In patients with venous insufficiency, a compression bandage was added. Wound dressing was left for 3 to 5 days, depending on the condition of the wound. In case of need of redressing at home, the patients were equipped with the necessary material and were eventually assisted by home care agency.

6 | HEALING PROCESS EVALUATION

The wound healing progress was regularly monitored during the scheduled visits for wound treatment and

TABLE 1 Demographic data

Patient number	Age	Sex	DM	Smoker	Comorbidities	Defect number	Location	Aetiology
P1	77	M	N	N	atrial fibrillation	D1	right calf	venous
P2	60	M	Y	N	hypertension, hyperlipidaemia, renal insufficiency, atrial fibrillation, st.p. AVR	D2	left calf	venous
						D3	left calf	venous
P3	72	M	N	N	hypertension, atrial fibrillation, renal insufficiency	D4	left calf	venous
						D5	left calf	venous
						D6	left calf	venous
						D7	left calf	venous
P4	64	M	N	N	renal insufficiency	D8	right calf	venous
						D9	right calf	venous
P5	72	M	N	N	hypertension	D10	right ankle	venous/ arterial
						D11	right ankle	venous/ arterial
P6	56	F	N	Y	hypertension, peripheral artery disease	D12	left calf	defect after fasciotomy
P7	33	M	N	Y	hypertension	D13	right lower leg	venous
P8	60	M	N	N	hypertension	D14	right leg	venous
P9	66	F	N	Y	hypertension	D15	left ankle	venous
P10	65	M	Y	N	hypertension	D16	right leg	arterial
P11	85	F	Y	N	hypertension, peripheral arterial disease, anaemia	D17	left ankle	venous
P12	26	F	N	N	hypertension, hyperlipidaemia, st.p. AVR, st.p. CABG	D18	sternum	dehiscence
P13	45	M	N	N	hypertension	D19	left ankle	venous
						D20	left ankle	venous
P14	68	F	Y	N	X	D21	right ankle	venous
P15	67	M	Y	N	hypertension, hyperlipidaemia	D22	left calf	venous
						D23	left calf	venous
P16	67	M	N	N	X	D24	right ankle	venous
P17	74	M	Y	Y	hypertension, peripheral artery disease, chronic renal failure, anaemia, st.p. CABG	D25	left calf	defect after fasciotomy
P18	69	M	N	Y	hypertension	D26	left ankle	arterial

Abbreviations: DM, diabetes mellitus; st.p. AVR, status post aortic valve replacement; st.p. CABG, status post coronary artery bypass grafting.

dressing renewal. The wound size and the state were photo-documented with a scale indicating the patient ID number, the defect number, and the visit date placed in the closest proximity of the wound to assure the image unique identifier and proper image scaling. The wound size was determined by manual tracing of the wound border on calibrated images with automatic determination of the area size using NIS-Elements software (Laboratory Imaging, The Czech Republic). Wound area reduction, WAR = 100*(Baseline size − Current size)/Baseline size): the parameter was used to evaluate the healing progress, expressing the wound area's percentage at a given treatment period relative to the original size.

The wound was considered as healed (H) only when 100% reepithelialisation was achieved. Wounds with WAR between 50 and 99% were considered as partially healed (PH). Not achieving a reduction in the area by at least 50% was judged as failure to heal (unhealed defects [UH]), in accordance with the most often used criterion.[26] The average wound closure profiles for the H and PH group were fitted with asymptotic function ($y = a - b.c^x$) using ORIGIN50 software. For the unhealed (UH) group, only an approximate linear fit was performed because of the scattered character of the average.

Other than the wound itself, the perception of pain related to the wound was also monitored. The pain

FIGURE 1 Examples of wound closing. A, healed (H) wound (D15, venous leg ulcer); B, partially healed (PH) wound (D19, venous leg ulcer); C, wound with no reaction (D25, defect after fasciotomy). W0: the wound state after 24, 456, and 100 weeks of outpatient care with SOC treatment for A, B, and C, respectively. W: number of weeks of treatment with AM

TABLE 2 Defects' characteristics and outcome data

Patient number	Defect number	Time from onset (w)	Baseline size (cm^2)	Treatment duration (w)	Wound closure (%)	End status	Number of visits	Number of AM applications
P1	D1	315	2.6	9	100	H	10	9
P2	D2	36	16.8	32	100	H	31	15
	D3	36	4.5	17	100	H	17	11
P3	D4	7	28.1	16	100	H	15	11
	D5	7	1.0	6	100	H	5	2
	D6	7	2.4	6	100	H	6	4
	D7	7	13.8	36	100	H	36	15
P4	D8	13	6.2	31	100	H	31	14
	D9	13	2.9	35	100	H	31	15
P5	D10	6	1.3	12	100	H	11	4
	D11	250	5.2	38	100	H	37	19
P6	D12	6	48.7	33	100	H	29	29
P7	D13	53	5.3	36	100	H	34	30
P8	D14	12	0.5	14	100	H	14	14
P9	D15	24	10.7	13	100	H	8	8
P10	D16	8	6.0	5	100	H	6	4
P11	D17	52	98.0	74	79	PH	74	69
P12	D18	20	14.4	44	50	PH	38	32
P13	D19	456	22.9	78	64	PH	67	46
	D20	456	13.9	78	74	PH	67	45
P14	D21	50	7.1	49	90	PH	39	39
P15	D22	117	30.5	6	−28	UH	6	4
	D23	117	5.6	11	18	UH	11	9
P16	D24	100	5.0	19	−3	UH	19	12
P17	D25	100	33.6	18	−22	UH	13	9
P18	D26	40	12.7	17	−34	UH	13	11

level was evaluated using the 0 to 10 scale, 0 equal none, 10—unbearable.

7 | RESULTS

Of 18 patients (26 defects), 10 responded to the AM treatment by complete healing of all wounds (H group, 16 defects, 62%). Four patients (five defects, 19%) exhibited partially positive limited response (PH group). They reached on average 71.4 ± 13.6% of WAR and never exceeded 90% wound closure despite, in some cases, significantly prolonged treatment (up to 74 weeks). They showed less than 20% improvement over the period of first 9 to 20 weeks. Four patients (five defects, 19%) did not react to the treatment at all and were assigned to the unhealed group (UH group). In no case, an adverse secondary reaction to the AM application was observed. In cases when the defect responded well to the AM treatment, the epithelisation onset was very fast (after 2 AM applications), and the wound closure progressed rapidly towards complete healing. Typical wound healing in the course of treatment (D16) is presented in Figure 1A.

The period required for the defect's complete healing in the H group varied from 5 to 38 weeks (average 21.2 ± 12.2, median 16.5) and 2 to 30 AM applications (12.8 ± 7.9, 12.5) were needed. The WAR progress in the PH group was significantly slower, and its average showed the tendency to converge to a maximum value of approximately 88%. The data summarising outcomes for

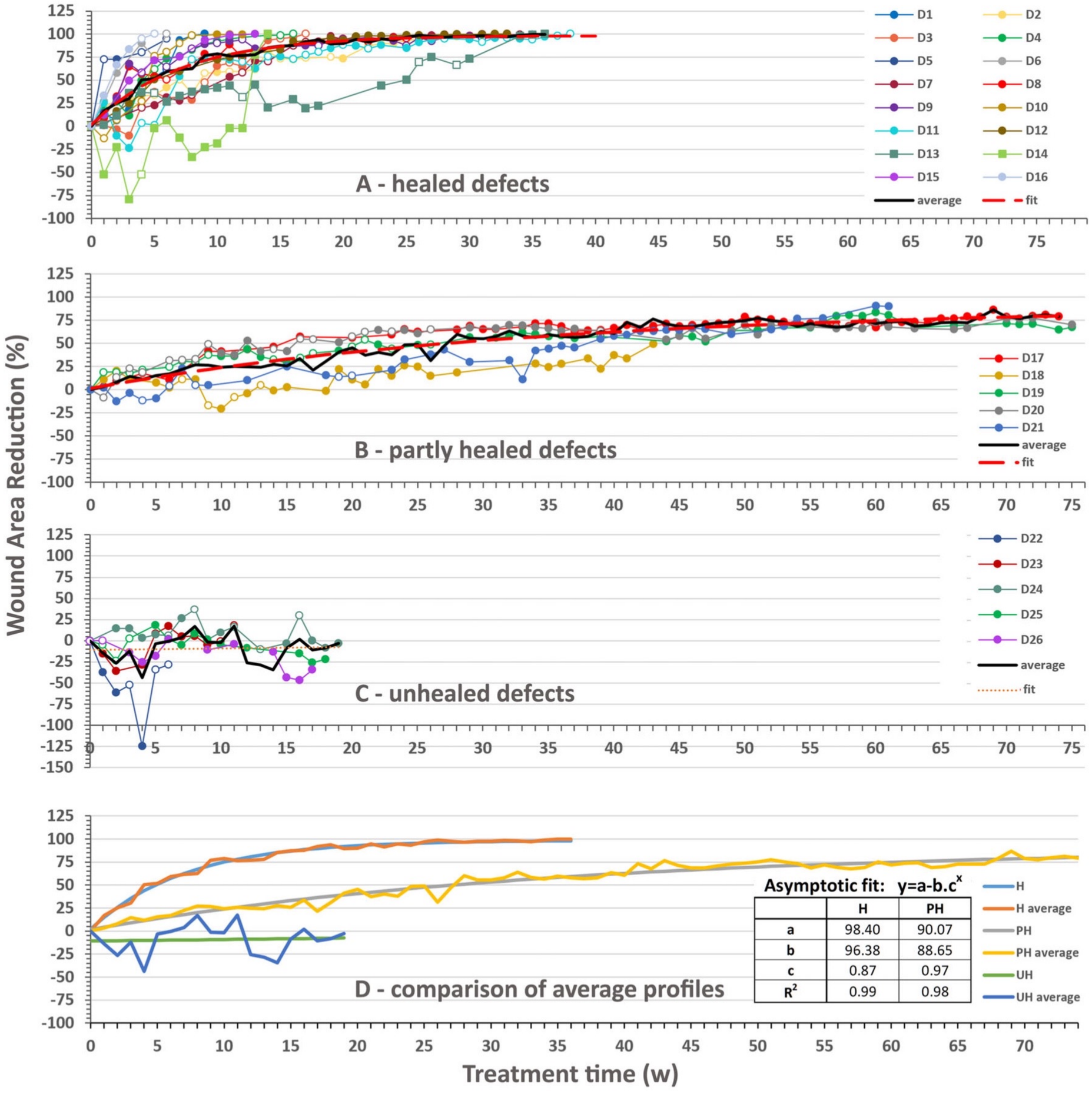

FIGURE 2 Wound closure evolution. WAR progress for healed A, partly healed B, and unhealed C, defects. D, comparison of the averages of the three groups together with fitted asymptotic functions and their parameters for H and PH and correlation coefficients (R^2). For A, B, and C, the closed and open markers reflect visits with or without AM application, respectively

individual defects are presented in Table 2. We have recorded the WAR profile for each defect and determined the average healing profiles separately for each group (H, PH, UH) (Figure 2). From the average WAR curve for healed defects (H) and its fit (regression coefficient $R^2 = 0.987$) (Figure 2A, D), we established that on average 50% of healing was achieved in 5 weeks of treatment and 70% in 10 weeks. All healed defects reached at least 50% of closure within the first 10 weeks of treatment (Figure 2A) with two exceptions: The defects D13, D14 (lines with square markers in Figure 2A) exhibited a profile significantly diverging from the rest of the defects in the group. They were characterised by delayed onset (12 and 17 weeks, respectively) of the AM stimulated healing and partial initial worsening. After this lag period, during which the healing profiles resembled those of the PH group, both defects started to progress and reached complete closure. The most prolonged healing in the H group lasted 44 weeks (defects D8 and D9).

Five defects (D17 to D21) healed partially, and despite the prolonged care period (up to 78 weeks) these defects progressed slowly without reaching the complete closure (Figure 1B, Figure 2B). The average WAR of these defects followed a different curve compared with the H group's characteristics, and approximately 27 weeks were necessary to reach 50% of closure (average). The average WAR value was 71% at the end of treatment. The course of the fitted curve is significantly flatter compared with the H group and predicts the maximum reachable WAR of approximately 90% (a = 88, Figure 2D).

Four patients (five defects, D22 to D26) did not respond to the AM treatment despite intense care, Figure 1C, Figure 2C. Their WAR values oscillated around 0, meaning that their size randomly changed around the baseline. The very approximate linear fit shows virtually no effect of the treatment on the wound size.

The degree of pain in all patients decreased independently of the healing progress from an average of 3.25 before the first AM application to 1.95, 1.22, and 0.47 after the first, fifth, and the tenth week of AM treatment, respectively, on a scale from 0 (no pain) to 10 (the worst pain) (Figure 3). No difference in pain relief was found between healed and unhealed patients.

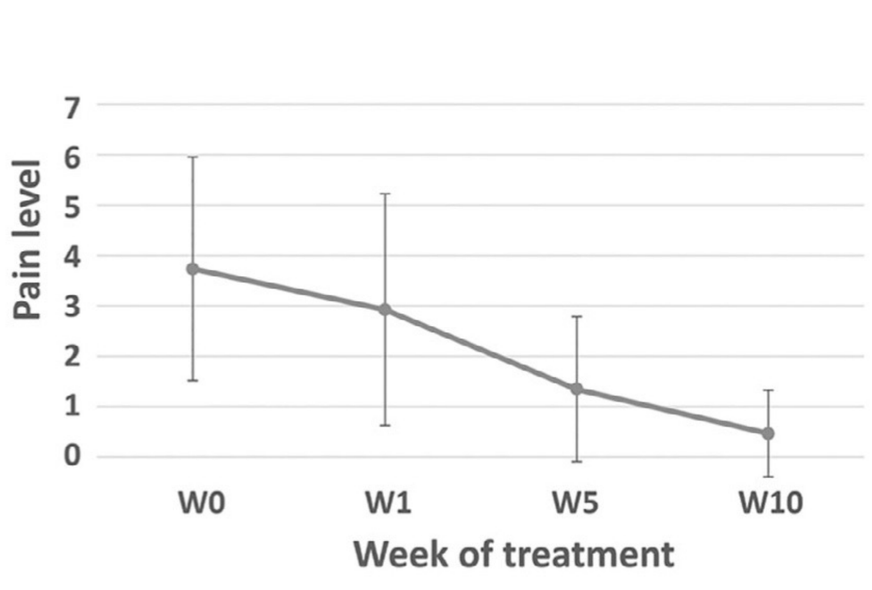

FIGURE 3 Pain level evolution during the AM treatment. Average value ± SD from all patients on a scale from 0 (no pain) to 10 (the worst pain) at week (W) 0, 1, 5, and 10 of treatment

8 | DISCUSSION

When AM is used for the treatment of NHW, several factors may affect the outcome: the wound aetiology, baseline size, period from onset to treatment start, type of AM used (cryo-preserved, dried, lyophilised, etc.), frequency of AM application, treatment period, and the individual sensitivity to the AM effect, which can be directly related to the general health status of the subject's organism, including age, and BMI and comorbidities of the subjects. In this multicentric study, we assessed the effect of cryo-preserved AM application on the healing of NHW. Apart from evaluating the general healing effect, one of the aims of the study was to understand if there is a way to predict the outcome of the AM stimulated healing process already at the early stages of the treatment. Although the logistics (long-term storage and the delivery in frozen state) related to the use of such material is more complex than that of, for example, dried or lyophilised tissues, cryo-preserved AM should preserve the majority of the growth factors and other molecules affecting the healing process in their active form and, therefore, promote the treatment efficiency.[7,27-29] Some studies, however, indicate that the quality of lyophilised AM levels that of cryo-preserved AM in terms of preservation of active molecular components[30] and efficiency in NHW treatment.[18]

The observed healing rate of 62% in our study is concordant with values reported in similar studies. In a multicentre, controlled, randomised, blinded, clinical trial, Lavery et al observed 62% successful healing rate (100% reepithelialisation at 12 weeks) for cryo-preserved AM compared with 21.3% success rate using SOC.[31] In a retrospective study evaluating 350 NHW from WoundExpert electronic health records, the rate of closure using cryo-preserved AM was found to be 59.4%.[32] Farivar and colleagues,[33] in a trial limited to 12 weeks and venous leg ulcers, reached 53% healing with a comparable set of NHW when using cryo-preserved AM and the average healing time of 10.9 weeks, which is markedly shorter compared with 25.5 weeks in our study. It should be noted, however, that the average NHW duration period before AM treatment in our patients was 88 weeks, which is considerably higher than in Farivar's study and other comparable studies using cryo-preserved AM.[24,31,34] Interestingly, in Ref. 33, 57% of unhealed defects showed WAR >50%, which is very similar to our 50% (five defects) representing the PH group. Another

multicentre trial reported a success rate of 48.4% (100% reepithelialisation at 8 weeks) for viable cryo-preserved placental membrane.[34]

In general, the reported in literature rate of complete wound closure using cryo-preserved AM are quite dispersed from 20%[23] through 46%,[31] 53%,[33] 84%[35] to 100%.[24] However, some studies were realised with limited AM application period reducing, thus, the potential healing completion had the treatment been continued. Time to complete closure appears to be also variable, ranging from 6 to 56 weeks.[23,24] Therefore, the extended healing period for some defects in the present work is in the range of values reported previously.

Some works report the healing efficiency's dependence on the baseline size.[32,34,36] In our study, although the average baseline size is superior in the UH group compared with H group, we could not prove its statistical significance. The average wound size before starting AM therapy (15.4 cm^2) was larger in our study than in other studies using cryo-preserved AM.[24,31,34,35]

The frequency of AM or AM-based derivatives application used in similar studies varies from frequent (2 to 3 days[37]) to scarce.[23] We set the standard application period to weekly at the beginning of treatment. In later phases (generally after 4 to 8 weeks), the AM application frequency was changed to bi-weekly and then modulated according to the wound reaction to the treatment and healing evolution.

AM treatment cost is rather high. Thus, the question at which state its application is adequate and what are the indications suggesting its efficiency is important. Existing data show that WAR of 50% after 4 weeks of SOC is a strong indicator of appropriate healing for diabetic foot ulcers.[38] WAR change in percent was reported as an indicator of a good prognosis for venous leg ulcers.[26,39] Failure to reach such rates by SOC suggests the need for initiating alternative and/or advanced treatments.[40]

When AM application is undertaken, an indicator of the probability of complete healing would be a valuable tool for deciding whether the treatment should be continued for an extended period or not. Analysis of our results allowed us to separate the wounds into three categories with different sensitivity to the AM treatment—H, PH, and UH. The wounds in the H group achieved, on average, 70% closure after 10 weeks and 50% after 5 weeks, which is similar to the values reported elsewhere.[24] All wounds in this group attained 50% closure in 10 weeks; therefore, it would seem adequate to establish these values as predictors for successful treatment. However, this criterion may exclude the cases that would have finally benefited from the AM application had the treatment not been aborted (D13, 14). The average WAR progress for NHW in PH and UH groups is different. The wounds completely insensitive to the AM application (UH group) are readily recognisable at the early stages of treatment (10 weeks at maximum) by the flat average progression line. To distinct NHW with the potential to heal completely (H) or to be only partially reduced over prolonged treatment (PH) is, however, more complicated. We have characterised the healing progress of these two groups by parameters of the fitted asymptotic function. The determined 'a' parameter defines the maximum reachable value of wound closure and thus can be used to predict the extent to which the wound would heal. Compared with the H group, the PH group shows significantly slower evolution with the indicated limit of only ~90% ('a' value), suggesting that these wounds will never reach complete healing when using this type of treatment, and probably it is of low interest to continue with rather expensive AM application. Instead, the treatment strategy should be reconsidered. Unfortunately, the data spread is wide, and therefore such distinction at the level of an individual patient can hardly be applied with high certitude before the weeks 12 to 13 of treatment. Interestingly, this value coincides with the time limit of most studies evaluating the effect of skin substitutes (for a complete overview, see Ref. 26.

Our results also show that the repeated and persistent application can eventually trigger the healing process even in defects not responding immediately to the AM treatment and not fitting into the above-stated values for H-type wounds. That was indeed the case of defects D13 and D14, which for an extended period exhibited only a minimal response to the treatment and reached the 50% closure only after 25 and 12 weeks, respectively, but finally healed completely. The important feature of AM is, besides healing acceleration and stimulation, its analgesic effect; pain relief has been perceived after first AM applications by all patients independently of wound healing. In any case, the AM application in NHW healing will always require a highly individual approach and should reflect previous wound treatment/healing history and the patient's general health condition.

9 | CONCLUSION

From our results, we conclude that cryo-preserved AM represents a safe and useful treatment with a strongly beneficial effect for managing NHWs. In our study, the AM application led to the complete healing of 62% of wounds. We have shown that it was possible to separate the NHW into three distinct groups with different healing characteristics (H, PH, U) according to their WAR profiles. This can then be used as a guideline for the prediction of the eventual outcome of the treatment.

ACKNOWLEDGEMENTS

The authors are thankful to Miluse Berka Mrstinova, MD. (Department of Obstetrics and Gynaecology, Motol University Hospital) for help in recruiting placental donors, to Mrs. Dagmar Hrabankova (Department of Transplantation and Tissue Bank, Motol University Hospital), MD. Viera Vesela and Mrs. Simona Krausova (Institute of Biology and Medical Genetics, Charles University, Prague) for technical assistance.

This work was supported by the NV18-08-00106 grant from the Ministry of Health of the Czech Republic, and by project Ministry of Education, Youth and Sports BBMRI_CZ LM2018125. Institutional support was provided by Progres-Q25, Charles University, First Faculty of Medicine.

CONFLICT OF INTEREST

The authors declare no conflicts of interest.

DATA AVAILABILITY STATEMENT

Data available on request from the authors.

ORCID

Katerina Jirsova https://orcid.org/0000-0002-4625-6701

REFERENCES

1. Martin P, Nunan R. Cellular and molecular mechanisms of repair in acute and chronic wound healing. *Br J Dermatol*. 2015;173(2):370-378.
2. Zelen CM, Serena TE, Denoziere G, Fetterolf DE. A prospective randomised comparative parallel study of amniotic membrane wound graft in the management of diabetic foot ulcers. *Int Wound J*. 2013;10(5):502-507.
3. Moore Z. Why is EWMA interested in implementation?. (Oral presentation). *20th Conference of the European Wound Management Association, Geneva, 2010*. Frederiksberg, Denmark: EWMA; 2010.
4. Frykberg RG, Banks J. Challenges in the treatment of chronic wounds. *Adv Wound Care (New Rochelle)*. 2015;4(9):560-582.
5. Jarbrink K, Ni G, Sonnergren H, et al. The humanistic and economic burden of chronic wounds: a protocol for a systematic review. *Syst Rev*. 2017;6(1):15.
6. Gibbons GW. Grafix([R]), a cryopreserved placental membrane, for the treatment of chronic/stalled wounds. *Adv Wound Care (New Rochelle)*. 2015;4(9):534-544.
7. Johnson A, Gyurdieva A, Dhall S, Danilkovitch A, Duan-Arnold Y. Understanding the impact of preservation methods on the integrity and functionality of placental allografts. *Ann Plast Surg*. 2017;79(2):203-213.
8. Malhotra C, Jain AK. Human amniotic membrane transplantation: different modalities of its use in ophthalmology. *World J Transplant*. 2014;4(2):111-121.
9. Parolini O, Alviano F, Bagnara GP, et al. Concise review: isolation and characterization of cells from human term placenta: outcome of the first international workshop on placenta derived stem cells. *Stem Cells*. 2008;26(2):300-311.
10. Pathak M, Olstad OK, Drolsum L, et al. The effect of culture medium and carrier on explant culture of human limbal epithelium: a comparison of ultrastructure, keratin profile and gene expression. *Exp Eye Res*. 2016;153:122-132.
11. Barr SM. Dehydrated amniotic membrane allograft for treatment of chronic leg ulcers in patients with multiple comorbidities: a case series. *J Am Coll Clin Wound Spec*. 2014;6(3):38-45.
12. Jirsova K, Jones GLA. Amniotic membrane in ophthalmology: properties, preparation, storage and indications for grafting—a review. *Cell Tissue Bank*. 2017;18(2):193-204.
13. Mamede AC, Carvalho MJ, Abrantes AM, Laranjo M, Maia CJ, Botelho MF. Amniotic membrane: from structure and functions to clinical applications. *Cell Tissue Res*. 2012;349(2):447-458.
14. Dua HS, Azuara-Blanco A. Amniotic membrane transplantation. *Br J Ophthalmol*. 1999;83(6):748-752.
15. Litwiniuk M, Bikowska B, Niderla-Bielinska J, et al. Potential role of metalloproteinase inhibitors from radiationsterilized amnion dressings in the healing of venous leg ulcers. *Mol Med Rep*. 2012;6(4):723-728.
16. McQuilling JP, Vines JB, Kimmerling KA, Mowry KC. Proteomic comparison of amnion and Chorion and evaluation of the effects of processing on placental membranes. *Wounds*. 2017;29(6):E36-E40.
17. Bennett JP, Matthews R, Faulk WP. Treatment of chronic ulceration of the legs with human amnion. *Lancet*. 1980;1(8179):1153-1156.
18. Ananian CE, Davis RD, Johnson EL, et al. Wound closure outcomes suggest clinical equivalency between lyopreserved and cryopreserved placental membranes containing viable cells. *Adv Wound Care (New Rochelle)*. 2019;8(11):546-554.
19. Zelen CM, Serena TE, Snyder RJ. A prospective, randomised comparative study of weekly versus biweekly application of dehydrated human amnion/chorion membrane allograft in the management of diabetic foot ulcers. *Int Wound J*. 2014;11(2):122-128.
20. Suzuki K, Michael G, Tamire Y. Viable intact cryopreserved human placental membrane for a non-surgical approach to closure in complex wounds. *J Wound Care*. 2016;25(Sup10):S25-S31.
21. Regulski M, Jacobstein DA, Petranto RD, Migliori VJ, Nair G, Pfeiffer D. A retrospective analysis of a human cellular repair matrix for the treatment of chronic wounds. *Ostomy Wound Manage*. 2013;59(12):38-43.
22. Bianchi C, Cazzell S, Vayser D, et al. A multicentre randomised controlled trial evaluating the efficacy of dehydrated human amnion/chorion membrane (EpiFix([R])) allograft for the treatment of venous leg ulcers. *Int Wound J*. 2018;15(1):114-122.
23. Mermet I, Pottier N, Sainthillier JM, et al. Use of amniotic membrane transplantation in the treatment of venous leg ulcers. *Wound Repair Regen*. 2007;15(4):459-464.
24. Valiente MR, Nicolas FJ, Garcia-Hernandez AM, et al. Cryopreserved amniotic membrane in the treatment of diabetic foot ulcers: a case series. *J Wound Care*. 2018;27(12):806-815.
25. Serena TE, Yaakov R, DiMarco D, et al. Dehydrated human amnion/chorion membrane treatment of venous leg ulcers: correlation between 4-week and 24-week outcomes. *J Wound Care*. 2015;24(11):530-534.

26. Snyder D, Sullivan N, Margolis D, Schoelles K. Skin substitutes for treating chronic wounds. Technology Assessment Program—Technical Brief 2020;Project ID: WNDT0818.
27. Duan-Arnold Y, Gyurdieva A, Johnson A, Jacobstein DA, Danilkovitch A. Soluble factors released by endogenous viable cells enhance the antioxidant and chemoattractive activities of cryopreserved amniotic membrane. *Adv Wound Care (New Rochelle)*. 2015;4(6):329-338.
28. Duan-Arnold Y, Gyurdieva A, Johnson A, Uveges TE, Jacobstein DA, Danilkovitch A. Retention of endogenous viable cells enhances the anti-inflammatory activity of cryopreserved amnion. *Adv Wound Care (New Rochelle)*. 2015;4(9):523-533.
29. Duan-Arnold Y, Uveges TE, Gyurdieva A, Johnson A, Danilkovitch A. Angiogenic potential of cryopreserved amniotic membrane is enhanced through retention of all tissue components in their native state. *Adv Wound Care (New Rochelle)*. 2015;4(9):513-522.
30. Dhall S, Sathyamoorthy M, Kuang JQ, et al. Properties of viable lyopreserved amnion are equivalent to viable cryopreserved amnion with the convenience of ambient storage. *PLoS One*. 2018;13(10):e0204060.
31. Lavery LA, Fulmer J, Shebetka KA, et al. The efficacy and safety of Grafix([R]) for the treatment of chronic diabetic foot ulcers: results of a multi-centre, controlled, randomised, blinded, clinical trial. *Int Wound J*. 2014;11(5):554-560.
32. Raspovic KM, Wukich DK, Naiman DQ, et al. Effectiveness of viable cryopreserved placental membranes for management of diabetic foot ulcers in a real world setting. *Wound Repair Regen*. 2018;26(2):213-220.
33. Farivar BS, Toursavadkohi S, Monahan TS, et al. Prospective study of cryopreserved placental tissue wound matrix in the management of chronic venous leg ulcers. *J Vasc Surg Venous Lymphat Disord*. 2019;7(2):228-233.
34. Ananian CE, Dhillon YS, Van Gils CC, et al. A multicenter, randomized, single-blind trial comparing the efficacy of viable cryopreserved placental membrane to human fibroblast-derived dermal substitute for the treatment of chronic diabetic foot ulcers. *Wound Repair Regen*. 2018;26(3):274-283.
35. Johnson EL, Saunders M, Thote T, Danilkovitch A. Cryopreserved placental membranes containing viable cells result in high closure rate of nonhealing upper and lower extremity wounds of non-diabetic and non-venous pathophysiology. *Wounds*. 2021;33(2):34-40.
36. Abdo RJ. Treatment of diabetic foot ulcers with dehydrated amniotic membrane allograft: a prospective case series. *J Wound Care*. 2016;25(Sup7):S4-S9.
37. Dehghani M, Azarpira N, Mohammad Karimi V, Mossayebi H, Esfandiari E. Grafting with cryopreserved amniotic membrane versus conservative wound care in treatment of pressure ulcers: a randomized clinical trial. *Bull Emerg Trauma*. 2017;5(4):249-258.
38. Sheehan P, Jones P, Caselli A, Giurini JM, Veves A. Percent change in wound area of diabetic foot ulcers over a 4-week period is a robust predictor of complete healing in a 12-week prospective trial. *Diabetes Care*. 2003;26(6):1879-1882.
39. Kantor J, Margolis DJ. A multicentre study of percentage change in venous leg ulcer area as a prognostic index of healing at 24 weeks. *Br J Dermatol*. 2000;142(5):960-964.
40. Kimmel HM, Robin AL. An evidence-based algorithm for treating venous leg ulcers utilizing the Cochrane database of systematic reviews. *Wounds*. 2013;25(9):242-250.

How to cite this article: Svobodova A, Horvath V, Smeringaiova I, et al. The healing dynamics of non-healing wounds using cryopreserved amniotic membrane. *Int Wound J*. 2022;19(5):1243-1252. doi:10.1111/iwj.13719

Appendix 6: Inter-placental variability is not a major factor affecting the healing efficiency of amniotic membrane when used for treating chronic non-healing wounds

Cell Tissue Bank
https://doi.org/10.1007/s10561-023-10096-y

FULL LENGTH PAPER

Inter-placental variability is not a major factor affecting the healing efficiency of amniotic membrane when used for treating chronic non-healing wounds

Vojtech Horvath · Alzbeta Svobodova · Joao Victor Cabral · Radovan Fiala · Jan Burkert · Petr Stadler · Jaroslav Lindner · Jan Bednar · Martina Zemlickova · Katerina Jirsova

Received: 31 January 2023 / Accepted: 24 April 2023

Abstract This study aimed to evaluate the efficacy of cryopreserved amniotic membrane (AM) grafts in chronic wound healing, including the mean percentage of wound closure per one AM application, and to determine whether the healing efficiency differs between AM grafts obtained from different placentas. A retrospective study analyzing inter-placental differences in healing capacity and mean wound closure after the application of 96 AM grafts prepared from nine placentas. Only the placentas from which the AM grafts were applied to patients suffering from long-lasting non-healing wounds successfully healed by AM treatment were included. The data from the rapidly progressing wound-closure phase (p-phase) were analyzed. The mean efficiency for each placenta, expressed as an average of wound area reduction (%) seven days after the AM application (baseline, 100%), was calculated from at least 10 applications. No statistical difference between the nine placentas' efficiency was found in the progressive phase of wound healing.

V. Horvath · P. Stadler
Department of Vascular Surgery, Na Homolce Hospital, Prague, Czech Republic
e-mail: vojtech.horvath@homolka.cz

P. Stadler
e-mail: Petr.Stadler@homolka.cz

A. Svobodova · J. Lindner
2nd Department of Surgery – Department of Cardiovascular Surgery, First Faculty of Medicine, Charles University and General University Hospital in Prague, Prague, Czech Republic
e-mail: alzbeta.svobodova@nemcl.cz

J. Lindner
e-mail: Jaroslav.Lindner@vfn.cz

J. V. Cabral · J. Bednar · K. Jirsova (✉)
Laboratory of the Biology and Pathology of the Eye, Institute of Biology and Medical Genetics, First Faculty of Medicine, Charles University and General University Hospital in Prague, Albertov 4, 128 01 Prague, Czech Republic
e-mail: katerina.jirsova@lf1.cuni.cz

J. V. Cabral
e-mail: victor.cabral@lf1.cuni.cz

J. Bednar
e-mail: jan.Bednar@lf1.cuni.cz

R. Fiala · J. Burkert
Department of Cardiovascular Surgery, Motol University Hospital, Prague, Czech Republic
e-mail: Radovan.Fiala@fnmotol.cz

J. Burkert
e-mail: Jan.Burkert@fnmotol.cz

J. Burkert · K. Jirsova
Department of Transplantation and Tissue Bank, Motol University Hospital, Prague, Czech Republic

M. Zemlickova
Clinic of Dermatovenerology, General Teaching Hospital and 1st Faculty of Medicine, Charles University, Prague, Czech Republic
e-mail: Martina.Zemlickova@vfn.cz

Published online: 25 May 2023

The 7-day average wound reduction in particular placentas varied from 5.70 to 20.99% (median from 1.07 to 17.75) of the baseline. The mean percentage of wound surface reduction of all analyzed defects one week after the application of cryopreserved AM graft was 12.17 ± 20.12% (average ± SD). No significant difference in healing capacity was observed between the nine placentas. The data suggest that if there are intra- and inter-placental differences in AM sheets' healing efficacy, they are overridden by the actual health status of the subject or even the status of its individual wounds.

Keywords Placenta · Amniotic membrane · Wound healing efficiency

Introduction

For years, the human amniotic membrane (AM) has become widely used as a bioactive dressing or the basic substrate for producing broadly distributed derivatives with beneficial healing properties (Fenelon et al. 2021; Nejad et al. 2021; Elkhenany et al. 2022). While AM transplantation was primarily adopted in ophthalmology for the reconstruction of the ocular surface (corneal ulcers, persistent epithelial defects, limbal stem cell deficiency, ocular neoplasia, pterygium), and for ocular surface wound healing (e.g., for chemical and thermal injuries, dry eye disease, recurrent corneal erosions or cicatrizing conjunctivitis such are Steven's Johnson syndrome, toxic epidermal necrolysis, pemphigoid or graft versus host disease) (Tsubota et al. 1996; Fuchsluger et al. 2005; Meller et al. 2011; Tabatabaei et al. 2017; Walkden 2020). Later its application has been extended to the problem of healing wounds other than that of the eye, and its use has been developing strongly over the last few decades (DiDomenico et al. 2016; Johnson et al. 2021). The primary material for AM acquisition, the placenta, is readily available and relatively abundant compared to other transplants (Jirsova and Jones 2017). AM's anti-inflammatory, anti-fibrotic, anti-microbial, neurotrophic, analgesic, anti-, and pro-angiogenic properties, along with the epithelization promotion, make it an ideal material for treating a wide variety of wounds (Wassmer and Berishvili 2020; Elkhenany et al. 2022). The rationale behind most of the mentioned effects has been characterized (Baradaran-Rafii et al. 2013), although the presence of substances, which can be responsible for the direct analgesic effect of AM, has only recently been suggested (Svobodova et al. 2023). The AM immunogenicity is very low; thus, the risk of rejection or incompatibility complication is practically non-existent (Adinolfi et al. 1982; Hori et al. 2006).

The efficiency of AM is assigned to the presence of extracellular matrix proteins, a variety of growth factors, and cytokines, the production of which can direct adhesion, migration, proliferation, and differentiation of epithelial and stromal cells, as well as the stem and progenitor cells of epithelial and mesenchymal origin (Koizumi et al. 2000a, b; Bomfim Pereira et al. 2016; Wassmer and Berishvili 2020; Ruiz-Canada et al. 2021).

However, this also suggests that the properties of the AM prepared for transplantation will be dependent on many factors that can influence the production, concentration, and activity preservation of these substances in the AM. AM quality can be influenced by factors related to the donor/placenta-specific variations (Hopkinson et al. 2006a, b; Krabcova et al. 2014; Deihim et al. 2016) and by the handling dependent/induced factors (Allen et al. 2013; Paolin et al. 2016). The formers are responsible for both donor-dependent (inter-placental) variations (Hopkinson et al. 2006a, b; Krabcova et al. 2014) and intra-placental sub-region variations of AM composition (Deihim et al. 2016; Litwiniuk et al. 2018; Moraes et al. 2021). They can be influenced by the donor's overall physiological status, genetic predisposition, the presence of pathology, or even by the week of pregnancy at which the placenta was retrieved (Skinner et al. 1981; Tossetta et al. 2014).

Studies evaluating the effect of intra- or inter-placental variations are relatively scarce. The evaluation of the properties of placental subregions was documented in several studies, describing the sub-regional differences from different aspects: the presence of stem cell markers (Lemke et al. 2017; Centurione et al. 2018; Garcia-Lopez et al. 2019), proliferation and differentiation capacity (Germain et al. 1992; Curtis et al. 1997; Farrugia et al. 2000; Han et al. 2008; Kim et al. 2011; Centurione et al. 2018), factors influencing wound healing and angiogenesis (Han et al. 2008; Gicquel et al. 2009; Lee et al. 2010; Banerjee et al. 2018; Litwiniuk et al. 2018) and other factors.

It was suggested that AM from placental and reflected sub-regions might have different potentials for tissue regeneration due to the different mitochondrial activity, which may be, in turn, crucial for clinical applications (Banerjee et al. 2015). Similarly, the study based on the evaluation of TGFβs (1,2,3) presence discovered significant differences in their concentration among individual donors proposing a potential modification of the healing effect based on the donor individuality (Hopkinson et al. 2006a, b; Han et al. 2008). Another study evaluated the placenta quality dependent on the pregnancy week retrieval (Skinner et al. 1981). Contrary, no significant difference in pluripotency markers concentration was found between the placental and reflected amnion (Garcia-Lopez et al. 2019), suggesting the homogeneous distribution of the pluripotency transcription factors, making all regions of AM equal in the regenerative processes effect. For an excellent review analyzing the data concerning the AM sub-regional differences, see Weidinger et al. (2020).

The studies evaluating the AM properties variations due to tissue processing are much more abundant as these parameters can be much better controlled. Tissue processing encapsulates the procedures employed through the AM graft preparation chain, from placenta retrieval, decontamination, AM preparation, and storage and treatment until the moment of transplantation (Aykut et al. 2015; Jirsova and Jones 2017). As the influence of these factors can be rather straightforwardly and rigorously evaluated, numerous studies were devoted to elucidating the effect of AM decontamination/sterilization procedure (Singh et al. 2006; Smeringaiova et al. 2017), graft structure and cellular viability and content modification (intact, or denuded AM) (Koizumi et al. 2000a, b; Hopkinson et al. 2006a, b; Duan-Arnold et al. 2015), the type of preparation and storage (freezing, air-drying, lyophilization) (Dhall et al. 2018; Memmi et al. 2022).

Finally, the effect of these factors on the effectiveness of the AM application is always additionally modulated by the individuality of the treated subject, i.e., by its physiological/pathological conditions, including its sensibility to the AM treatment at the moment of the AM application.

The closure kinetics of chronic wounds usually progresses in two phases; the first is characterized by relatively rapid progress and lasts for the first 5 to 20 weeks of healing with a closure level of more than 50%. The following phase of healing is characterized by a slower progression of wound closure with a less steep curve (Herbin et al. 1993; Venault et al. 2019; Becerra-Bayona et al. 2020). Herein, these two stadia are described as progressive (p-phase) and terminal (e-phase) (Svobodova et al. 2022).

In standard AM preparation for clinical use, several tens of AM sheets are typically prepared from one placenta without keeping exact track of the sub-region origin, except when the targeted region is very specific, e.g., the umbilical part (Cognard et al. 2022). Thus, the intra-placental variations are mostly impossible to survey in clinical applications. However, the track of AMs obtained from individual placentas is rigorous, as required by legislation, and therefore, should the inter-placental differences in AM healing features be prevailing the other factors, they could be potentially detectable by evaluating its healing effect, e.g., by assessing the wound closure rate (DiDomenico et al. 2016; Valiente et al. 2018; Johnson et al. 2021).

In this study, we evaluated the effect of the cryopreserved AMs retrieved from different donors on the efficiency of wound healing (wound closure), intending to understand whether the inter-placental variations could be dominant in wound healing progress or if they are suppressed by the processing/application chain and the individual patient status at the moment of application.

Materials and methods

The study followed the Ethics Committee's standards of three participating institutions (1st Medical Faculty of Charles University, General Teaching Hospital, University Hospital Motol, and Na Homolce Hospital, all in Prague) and adhered to the tenets set out in the Declaration of Helsinki.

AM grafts preparation

After obtaining informed consent from placenta donors, the placenta and blood for serological examination were retrieved. All donors were negative for hepatitis B and C, syphilis, and HIV, C-reactive protein was < 20 mg/l). The serology was repeated after 6 months. The AM grafts were prepared as described earlier (Svobodova et al. 2022). Shortly,

all placentas were obtained by elective cesarean section between 38 to 39 (from 38 weeks + 1 day to 39 weeks + 4 days) gestational week in the Motol University Hospital, Prague, from donors with no serious systemic or genetic diseases. Before further processing, placentas were visually inspected for injuries and visible pathologies. Then the tissue (placenta/AM) was decontaminated at room temperature using BASE•128 (Alchimia, Ponte San Nicolò, Italy) for 24 h (±2 h) at 37 °C. AM sheets were rinsed, stretched on Sanatyl support (Tylex, Letovice, Czech Republic), and cut into desired-sized patches (varying from 2×2 cm up to 7×11 cm). Finally, AM pieces were placed into Dulbecco's Modified Eagle Medium (Gibco™ DMEM 32,430,027, Thermo Fisher Scientific) in 50% glycerol (Dr. Kulich Pharma, Czech Republic) and stored at − 80 °C. After six months, tissues with negative microbiology and serology test results were released for grafting.

Patients

The presented study enrolled 16 patients suffering from chronic nonhealing wounds (lasting more than 6 weeks before AM application, range 6 to 1408 weeks, average 139 weeks). Twelve wounds were venous, one arterial, one diabetic origin, one wound was linked to fasciotomy, and one to physical trauma. The inclusion and exclusion criteria have been described previously (Svobodova et al. 2022), shortly, the inclusion criteria were: age ≥ 18 years, the presence of resistant NHW with a duration of more than 6 weeks, and wound extending through the entire thickness of the skin. Exclusion criteria were: tendon or bone exposure in the wound, allergy to antibiotics used for AM decontamination, transcutaneous oximetry value below 30 mmHg for patients with diabetes mellitus, known history of AIDS or HIV, ankle-brachial index (ABI) < 0.5, for all patients except those with diabetes mellitus, suspicious for cancer or history of radiation at the wound site, severe (uncontrolled) systemic disease, or planned surgical intervention in the next six months.

The average age of the patients was 66.8 years (33 to 82), with 4 females and 12 males. Altogether, 22 defects (D) were followed. Before starting the treatment using AM, the wound size varied between 0.99 and 50.51 cm^2, averaging 12.88 ± 14.54 cm^2. The wound resistance to treatments before the AM application spanned from 6 to 1408 weeks, averaging 12.88 weeks. The complete healing lasted from 5 to 105 weeks, averaging 31.14 weeks.

Input data selection and measurement

The efficiency of AM grafts obtained from 9 placentas was analyzed. The mean age of placenta donors was 34 years (26–38). AM sheets from each placenta were distributed to at least three patients, and at least ten AM sheets from individual placentas had to be used to include the placenta in the evaluation. All patients (16 in total) reached complete healing. The data from the p-phase only were evaluated (for the p-phase description, see the introduction and discussion section), which in most cases represents the first 10 to 20 weeks of the treatment. The efficiency score was evaluated as the relative wound closure; the wound size on the day of AM application was used as the baseline (100%), and the percentage of wound area change 7 days after the AM application was evaluated. The size of the wound was assessed as described previously (Svobodova et al. 2022). Briefly, the wound was photo-documented with a scale in the proximity of the wound. The wound size was determined by manually tracing the wound border on calibrated images with an automatic determination of the area using NIS-Elements software (Laboratory Imaging, The Czech Republic). The mean efficiency for each placenta, expressed as an average of wound area reduction (in %), was calculated from at least 10 applications.

Statistical analysis

First, the data sets for individual placentas were checked for the normality by Saphiro-Wilk's test. The results showed that not all sets were of normal distribution, so the Kruskal–Wallis test was applied to check if a statistically significant difference could be detected. Finally, Dunn's test for performing multiple pairwise-comparison between the means of individual placentas was used. All the evaluations were performed using the R and RStudio package (RStudio 2020).

Results

The results represent the analysis of AM efficiency on non-healing wound treatment over 5 years (2017–2022). The treatment of the "non-healing" wounds using AMs included in the study led to a complete wound closure at the end of the treatment. For the evaluation of the AM efficiency, only the p-phase of the healing progress was used (for details, see the Discussion section). Our evaluation of the AM efficiency shows that the 7-day average wound closure (% of wound surface) in the p-phase of healing after the application of cryopreserved AMs varied from 5.7 to 20.99% (medians from 1.07 to 17.75). The values for individual placentas are summarized in Table 1, and statistics are visualized in Fig. 1. These results suggest that the average wound closure rate when using cryopreserved AM for non-healing wounds is $12.17 \pm 20.12\%$ (average $\pm$ standard deviation) of the wound surface 7 days after AM application.

The records for individual defects treated by each placenta evaluated in this study are summarized in Table 2. The negative values represent a temporary worsening of the wound against the baseline. While the spread of the values measured after AM application was rather important for individual placentas (e.g., for placenta 4 ranging from − 38.20 to 72.73% of wound area closure one week after application, see Table 2), resulting in high values of standard deviations, the values of both mean and median were relatively coherent, ranging from 5.70 to 20.99 and 1.07 to 17.75 respectively.

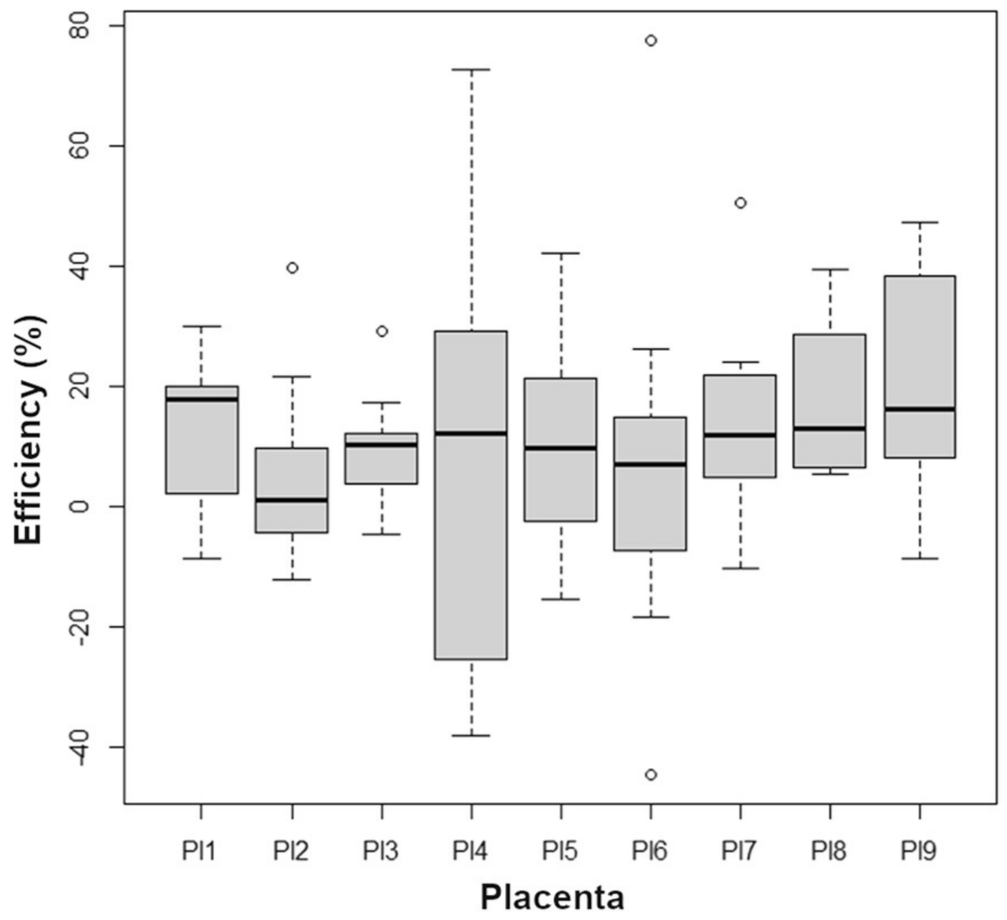

Fig. 1 A statistical representation of the efficiencies of AMs originating from different placentas

The results of Saphiro-Wilk's test revealed dispersed values for the normality of individual sets. Therefore, Levene's test was performed to decide whether parametric analysis (ANOVA) could be used. The resulting p-value of 0.008 indicated the data's non-normal character; thus, the Kruskal–Wallis test was applied. Its result showed no statistically significant difference ($p = 0.492$) between individual placentas. Therefore, it is legitimate to conclude that, in general, there is no important difference in the efficacy of AMs originating from different placentas on wound healing.

Table 1 The average healing efficiency of the placentas is expressed as wound area reduction in % seven days after AM application

	Average ± SD	Median	Saphiro-Wilk test p value
Placenta 1	13.67 ± 12.98	17.75	0.19
Placenta 2	5.70 ± 14.47	1.07	0.18
Placenta 3	10.13 ± 8.66	10.24	0.63
Placenta 4	6.83 ± 32.75	12.29	0.60
Placenta 5	12.13 ± 17.65	9.65	0.77
Placenta 6	7.26 ± 29.11	7.02	0.33
Placenta 7	13.46 ± 14.13	11.87	0.33
Placenta 8	18.06 ± 13.07	12.87	0.01
Placenta 9	20.99 ± 17.19	16.21	0.50

Discussion

In this study, we aimed to determine whether some significant differences in the healing efficiency of AM applied to non-healing wounds can be traced between AM sheets prepared from different placentas and to establish mean wound closure. As mentioned in the introduction, the existing studies are somewhat controversial concerning the inter- and intra-placental variation in the presence/concentration of wound healing factors (Avila-Gonzalez et al. 2015; Centurione et al. 2018). However, if such differences can be detected in the AM clinical applications for wound healing, it would help to orient more targeted studies on how to evaluate the placentas healing potential

Table 2 Effects of applications of AMs from selected placentas on individual defects seven days after application time

Placenta 1			Placenta 2			Placenta 3		
Change (%)	Defect	Application date	Change (%)	Defect	Application date	Change (%)	Defect	Application date
30.00	P1-D1	2017–10-05	− 1.32	P4-D1	2019–02-26	17.36	P6-D1	2018–07-31
14.01	P2-D1	2018–06-26	− 12.14	P4-D2	2019–02-26	11.38	P6-D1	2018–08-07
− 6.44	P3-D2	2018–07-10	− 6.25	P5-D1	2019–01-15	12.08	P2-D1	2018–07-10
30.00	P1-D1	2017–10-23	9.70	P6-D4	2019–01-02	29.23	P3-D2	2018–07-17
20.00	P1-D1	2017–10-28	− 1.25	P6-D4	2019–01-15	3.76	P3-D1	2018–07-17
20.00	P1-D1	2017–11-01	− 4.29	P5-D1	2019–01-02	11.80	P3-D1	2018–07-03
19.66	P3-D2	2018–07-24	39.66	P4-D2	2019–04-02	−4.72	P3-D2	2018–07-03
15.85	P3-D1	2018–08-07	21.71	P7-D1	2019–04-24	8.99	P5-D1	2018–09-11
2.24	P3-D2	2018–08-07	3.39	P8-D1	2019–04-24	9.09	P3-D2	2018–09-04
-8.60	P2-D1	2018–07-03	7.81	P8-D1	2019–04-17	2.30	P3-D1	2018–09-04
Placenta 4			Placenta 5			Placenta 6		
Change (%)	Defect	Application date	Change (%)	Defect	Application date	Change (%)	Defect	Application date
− 34.62	P5-D2	2018-10-16	8.73	P6-D4	2018-11-27	− 18.52	P8-D1	2019-04-10
− 8.48	P5-D1	2018-10-16	18.47	P5-D1	2018-12-11	− 13.60	P9-D1	2019-07-02
− 29.47	P5-D2	2018-10-02	4.07	P6-D4	2018-11-06	3.29	P9-D1	2019-07-09
− 38.20	P3-D1	2018-10-02	−2.45	P4-D1	2019-02-12	− 44.52	P9-D1	2019-06-11
19.37	P5-D2	2018-09-18	10.57	P6-D4	2018-11-13	− 0.90	P9-D1	2019-04-09
5.22	P3-D1	2018-10-16	−15.56	P5-D1	2018-11-13	7.02	P9-D1	2019-04-30
38.57	P6-D1	2018-09-25	42.25	P3-D1	2018-11-20	15.52	P8-D1	2019-04-30
19.77	P4-D1	2019-03-05	−5.17	P6-D4	2018-11-20	26.28	P7-D1	2019-04-30
21.66	P4-D2	2019-03-05	39.07	P5-D2	2018-10-30	14.04	P8-D1	2019-05-02
− 21.27	P5-D1	2018-10-02	21.34	P5-D1	2018-10-30	77.55	P8-D1	2019-05-07
36.66	P6-D1	2018-10-09				13.71	P4-D1	2019-06-25
72.73	P6-D2	2018-10-09						
Placenta 7			Placenta 8			Placenta 9		
Change (%)	Defect	Application date	Change (%)	Defect	Application date	Change (%)	Defect	Application date
10.21	P10-D1	2021-03-01	5.51	P14-D1	2022-03-15	16.28	P16-D1	2022-02-22
21.88	P11-D1	2021-03-22	36.50	P15-D1	2019-09-10	32.64	P16-D2	2022-02-22
14.41	P12-D1	2020-08-04	16.47	P14-D1	2022-03-01	4.38	P13-D1	2021-12-21
4.35	P11-D1	2021-04-12	9.66	P14-D1	2022-01-25	−8.61	P13-D1	2022-01-10
50.55	P12-D1	2020-10-27	5.89	P9-D1	2019-08-13	40.25	P16-D2	2022-02-15
23.55	P12-D1	2020-08-11	5.87	P4-D1	2019-07-23	0.67	P13-D1	2022-02-14
− 10.34	P11-D1	2021-03-17	12.87	P15-D1	2019-07-24	14.08	P13-D2	2021-12-13
24.06	P10-D1	2021-03-17	20.93	P15-D1	2019-07-29	11.99	P14-D1	2022-05-31
4.90	P11-D1	2021-03-01	7.31	P15-D1	2019-08-27	38.93	P16-D1	2022-02-01
− 4.11	P11-D1	2021-02-12	38.17	P9-D1	2019-08-27	37.73	P16-D2	2022-02-08
13.54	P10-D1	2021-04-12	39.44	P15-D1	2019-09-25	47.42	P16-D2	2022-01-03
19.15	P10-D1	2021-02-08				16.14	P14-D1	2022-05-17
9.64	P10-D1	2021-04-19						
6.67	P13-D1	2022-02-28						

P designates the subject number, *D* is the defect number of the given subject

(both in inter-placental and intra-placental respect) and perhaps avoid the use of less efficient placentas for their application, which could spare an important amount of preparative time and shorten the healing period.

Herein, we defined the placenta inclusion parameters at three different levels. First, the patient's positive reactive response to the AM application healing procedure was critical. Therefore, only patients with good healing progress and complete final healing were included. Second, only the first progressive phase of healing was included in the evaluation. As we reported previously, the healing progress of well-reacting patients in our clinical study could be fitted with asymptotic function (Svobodova et al. 2022). This is characterized by rather rapid progress in the initial phases, which is then progressively slowed down in the final healing period when the last few percent of the closure generally heal much slower than at the healing onset (Becerra-Bayona et al. 2020).

Moreover, the inaccuracies in the wound size determination increase with the smaller wound size and with the absolute differences in the wound size between the measurements. Therefore, our interest was to utilize the period when the wound size and its changes were the most important, typically in the first 10–20 weeks of healing. Furthermore, the patients with multiple wounds were preferred as this would allow us to, at least partly, evaluate the subject/defect status factor.

The rate of wound healing (% of wound closure per week) in the p-phase of our patients is consistent with the regularly observed one (Bull et al. 2022). Our results suggest that more than individual placentas' properties, patients' physiological status predominantly influences the wound closure progress. We suppose that important variation of obtained values found almost for each placenta (with one exception—Pl8) reflects the patient's or wound's immediate physiological/pathological condition. This is supported by the observation that the average healing efficiency of all 9 analyzed placentas did not statistically differ. However, it is necessary to consider the limitations of this study, such as the small number of placentas (9) and the variability in patients' parameters and their wounds.

The results show that although the average values of placenta efficiency may differ quite notably (more than double the value between Pl1 and Pl6), the analysis does not confirm the statistical significance. We have also observed case-by-case differences in reaction to the AM application. In some cases, we recorded different responses of two wounds of the same subject being treated by the AM from the same placenta. E.g., when treated with AMs from placenta 1 (Pl1), the reaction of the defects P3-D1 and P3-D2, which are the two defects of the same subject, was quite different even though they were treated on the same visit day (2018-08-07), closure 15.85 vs. 2.24%, respectively. A similar situation could be observed for the P5-D1 and P5-D2 (again two defects of the same patient) wherein two weeks, the defect P5-D1 changed its reaction from positive 21.34% (2018-10-30) to negative − 15.56% (2018-11-13) when treated by AMs from placenta 5 (Pl5). At the same time, the reaction of P5-D2 was twice as important as that of P5-D1 on the same application date (2018-10-30, 39.07% vs. 21.34%, respectively). Another example of reaction variation on the AM application can be detected for the defect P9-D1, which had a very different response on the AMs from placenta 6 in two months (2019-04-30 vs. 2019-06-11). All the data suggest that if there are intra- and inter-placental differences, they are overridden mainly by the actual health status of the subject or even the status of its individual wounds (due to the microbial, blood circulation, or other possible conditions, which may affect the healing process).

Acknowledgements This work was supported by the NV18-08-00106 grant from the Ministry of Health of the Czech Republic and by the Ministry of Education, Youth and Sports (BBMRI_CZ LM2018125). Institutional support (Charles University, Prague) was provided by the program Cooperatio: Medical Diagnostics and Basic Medical Sciences. The authors thank Mr. Lukas Balogh (Laboratory of the Biology and Pathology of the Eye, Institute of Biology and Medical Genetics) for his excellent technical assistance with data preparation.

Author contributions All authors contributed to the study's conception and design. Material preparation, data collection, and analysis were performed by VH, AS, JVC, RF, MZ, KJ. Statistical analysis was performed by JB. The first draft of the manuscript was written by VH, JB, and KJ; all authors commented on previous versions of the manuscript. All authors read and approved the final manuscript.

Funding Open access publishing supported by the National Technical Library in Prague.

Declarations

Conflict of interest The authors declare no conflict of interest.

References

Adinolfi M, Akle CA, McColl I, Fensom AH, Tansley L, Connolly P, Hsi BL, Faulk WP, Travers P, Bodmer WF (1982) Expression of HLA antigens, beta 2-microglobulin and enzymes by human amniotic epithelial cells. Nature 295(5847):325–327. https://doi.org/10.1038/295325a0

Allen CL, Clare G, Stewart EA, Branch MJ, McIntosh OD, Dadhwal M, Dua HS, Hopkinson A (2013) Augmented dried versus cryopreserved amniotic membrane as an ocular surface dressing. PLoS ONE 8(10):e78441. https://doi.org/10.1371/journal.pone.0078441

Avila-Gonzalez D, Vega-Hernandez E, Regalado-Hernandez JC, De la Jara-Diaz JF, Garcia-Castro IL, Molina-Hernandez A, Moreno-Verduzco ER, Razo-Aguilera G, Flores-Herrera H, Portillo W, Diaz-Martinez NE, Garcia-Lopez G, Diaz NF (2015) Human amniotic epithelial cells as feeder layer to derive and maintain human embryonic stem cells from poor-quality embryos. Stem Cell Res 15(2):322–324. https://doi.org/10.1016/j.scr.2015.07.006

Aykut V, Celik U, Celik B (2015) The destructive effects of antibiotics on the amniotic membrane ultrastructure. Int Ophthalmol 35(3):381–385. https://doi.org/10.1007/s10792-014-9959-z

Banerjee A, Weidinger A, Hofer M, Steinborn R, Lindenmair A, Hennerbichler-Lugscheider S, Eibl J, Redl H, Kozlov AV, Wolbank S (2015) Different metabolic activity in placental and reflected regions of the human amniotic membrane. Placenta 36(11):1329–1332. https://doi.org/10.1016/j.placenta.2015.08.015

Banerjee A, Lindenmair A, Steinborn R, Dumitrescu SD, Hennerbichler S, Kozlov AV, Redl H, Wolbank S, Weidinger A (2018) Oxygen tension strongly influences metabolic parameters and the release of interleukin-6 of human amniotic mesenchymal stromal cells in vitro. Stem Cells Int 2018:9502451. https://doi.org/10.1155/2018/9502451

Baradaran-Rafii A, Eslani M, Djalillian AR (2013) Complications of keratolimbal allograft surgery. Cornea 32(5):561–566. https://doi.org/10.1097/ICO.0b013e31826215eb

Becerra-Bayona SM, Solarte-David VA, Sossa CL, Mateus LC, Villamil M, Pereira J, Arango-Rodriguez ML (2020) Mesenchymal stem cells derivatives as a novel and potential therapeutic approach to treat diabetic foot ulcers. Endocrinol Diabetes Metab Case Rep. https://doi.org/10.1530/EDM-19-0164

Bomfim Pereira MG, Pereira Gomes JA, Rizzo LV, Cristovam PC, Silveira LC (2016) Cytokine dosage in fresh and preserved human amniotic membrane. Cornea 35(1):89–94. https://doi.org/10.1097/ICO.0000000000000673

Bull RH, Staines KL, Collarte AJ, Bain DS, Ivins NM, Harding KG (2022) Measuring progress to healing: a challenge and an opportunity. Int Wound J 19(4):734–740. https://doi.org/10.1111/iwj.13669

Centurione L, Passaretta F, Centurione MA, Munari S, Vertua E, Silini A, Liberati M, Parolini O, Di Pietro R (2018) Mapping of the human placenta: experimental evidence of amniotic epithelial cell heterogeneity. Cell Transpl 27(1):12–22. https://doi.org/10.1177/0963689717725078

Cognard S, Barnouin L, Bosc J, Gindraux F, Robin MC, Douet JY, Thuret G (2022) New devitalized freeze-dried human umbilical cord amniotic membrane as an innovative treatment of ocular surface defects: preclinical results. J Funct Biomater. https://doi.org/10.3390/jfb13030150

Curtis NE, Ho PW, King RG, Farrugia W, Moses EK, Gillespie MT, Moseley JM, Rice GE, Wlodek ME (1997) The expression of parathyroid hormone-related protein mRNA and immunoreactive protein in human amnion and chorio-decidua is increased at term compared with preterm gestation. J Endocrinol 154(1):103–112. https://doi.org/10.1677/joe.0.1540103

Deihim T, Yazdanpanah G, Niknejad H (2016) Different light transmittance of placental and reflected regions of human amniotic membrane that could be crucial for corneal tissue engineering. Cornea 35(7):997–1003. https://doi.org/10.1097/ICO.0000000000000867

Dhall S, Sathyamoorthy M, Kuang JQ, Hoffman T, Moorman M, Lerch A, Jacob V, Sinclair SM, Danilkovitch A (2018) Properties of viable lyopreserved amnion are equivalent to viable cryopreserved amnion with the convenience of ambient storage. PLoS ONE 13(10):e0204060. https://doi.org/10.1371/journal.pone.0204060

DiDomenico LA, Orgill DP, Galiano RD, Serena TE, Carter MJ, Kaufman JP, Young NJ, Zelen CM (2016) Aseptically processed placental membrane improves healing of diabetic foot ulcerations: prospective, randomized clinical trial. Plast Reconstr Surg Glob Open 4(10):e1095. https://doi.org/10.1097/GOX.0000000000001095

Duan-Arnold Y, Gyurdieva A, Johnson A, Jacobstein DA, Danilkovitch A (2015) Soluble Factors released by endogenous viable cells enhance the antioxidant and chemoattractive activities of cryopreserved amniotic membrane. Adv Wound Care (new Rochelle) 4(6):329–338. https://doi.org/10.1089/wound.2015.0637

Elkhenany H, El-Derby A, Abd Elkodous M, Salah RA, Lotfy A, El-Badri N (2022) Applications of the amniotic membrane in tissue engineering and regeneration: the hundred-year challenge. Stem Cell Res Ther 13(1):8. https://doi.org/10.1186/s13287-021-02684-0

Farrugia W, Ho PW, Rice GE, Moseley JM, Permezel M, Wlodek ME (2000) Parathyroid hormone-related protein(1–34) in gestational fluids and release from human

gestational tissues. J Endocrinol 165(3):657–662. https://doi.org/10.1677/joe.0.1650657

Fenelon M, Catros S, Meyer C, Fricain JC, Obert L, Auber F, Louvrier A, Gindraux F (2021) Applications of human amniotic membrane for tissue engineering. Membranes (basel). https://doi.org/10.3390/membranes11060387

Fuchsluger TA, Steuhl KP, Meller D (2005) Neurotrophic keratopathy–a post-LASIK case report. Klin Monbl Augenheilkd 222(11):901–904. https://doi.org/10.1055/s-2005-858800

Garcia-Lopez G, Avila-Gonzalez D, Garcia-Castro IL, Flores-Herrera H, Molina-Hernandez A, Portillo W, Diaz-Martinez NE, Sanchez-Flores A, Verleyen J, Merchant-Larios H, Diaz NF (2019) Pluripotency markers in tissue and cultivated cells in vitro of different regions of human amniotic epithelium. Exp Cell Res 375(1):31–41. https://doi.org/10.1016/j.yexcr.2018.12.007

Germain AM, Attaroglu H, MacDonald PC, Casey ML (1992) Parathyroid hormone-related protein mRNA in avascular human amnion. J Clin Endocrinol Metab 75(4):1173–1175. https://doi.org/10.1210/jcem.75.4.1400890

Gicquel JJ, Dua HS, Brodie A, Mohammed I, Suleman H, Lazutina E, James DK, Hopkinson A (2009) Epidermal growth factor variations in amniotic membrane used for ex vivo tissue constructs. Tissue Eng Part A 15(8):1919–1927. https://doi.org/10.1089/ten.tea.2008.0432

Han YM, Romero R, Kim JS, Tarca AL, Kim SK, Draghici S, Kusanovic JP, Gotsch F, Mittal P, Hassan SS, Kim CJ (2008) Region-specific gene expression profiling: novel evidence for biological heterogeneity of the human amnion. Biol Reprod 79(5):954–961. https://doi.org/10.1095/biolreprod.108.069260

Herbin M, Bon FX, Venot A, Jeanlouis F, Dubertret ML, Dubertret L, Strauch G (1993) Assessment of healing kinetics through true color image processing. IEEE Trans Med Imaging 12(1):39–43. https://doi.org/10.1109/42.222664

Hopkinson A, McIntosh RS, Shanmuganathan V, Tighe PJ, Dua HS (2006a) Proteomic analysis of amniotic membrane prepared for human transplantation: characterization of proteins and clinical implications. J Proteome Res 5(9):2226–2235. https://doi.org/10.1021/pr050425q

Hopkinson A, McIntosh RS, Tighe PJ, James DK, Dua HS (2006b) Amniotic membrane for ocular surface reconstruction: donor variations and the effect of handling on TGF-beta content. Invest Ophthalmol vis Sci 47(10):4316–4322. https://doi.org/10.1167/iovs.05-1415

Hori J, Wang M, Kamiya K, Takahashi H, Sakuragawa N (2006) Immunological characteristics of amniotic epithelium. Cornea 25(10 Suppl 1):S53-58. https://doi.org/10.1097/01.ico.0000247214.31757.5c

Jirsova K, Jones GLA (2017) Amniotic membrane in ophthalmology: properties, preparation, storage and indications for grafting-a review. Cell Tissue Bank 18(2):193–204. https://doi.org/10.1007/s10561-017-9618-5

Johnson EL, Saunders M, Thote T, Danilkovitch A (2021) Cryopreserved placental membranes containing viable cells result in high closure rate of nonhealing upper and lower extremity wounds of non-diabetic and non-venous pathophysiology. Wounds 33(2):34–40

Kim SY, Romero R, Tarca AL, Bhatti G, Lee J, Chaiworapongsa T, Hassan SS, Kim CJ (2011) miR-143 regulation of prostaglandin-endoperoxidase synthase 2 in the amnion: implications for human parturition at term. PLoS ONE 6(9):e24131. https://doi.org/10.1371/journal.pone.0024131

Koizumi N, Inatomi T, Quantock AJ, Fullwood NJ, Dota A, Kinoshita S (2000a) Amniotic membrane as a substrate for cultivating limbal corneal epithelial cells for autologous transplantation in rabbits. Cornea 19(1):65–71. https://doi.org/10.1097/00003226-200001000-00013

Koizumi NJ, Inatomi TJ, Sotozono CJ, Fullwood NJ, Quantock AJ, Kinoshita S (2000b) Growth factor mRNA and protein in preserved human amniotic membrane. Curr Eye Res 20(3):173–177

Krabcova I, Jirsova K, Bednar J (2014) Rapid cooling of the amniotic membrane as a model system for the vitrification of posterior corneal lamellae. Cell Tissue Bank 15(1):165–173. https://doi.org/10.1007/s10561-013-9388-7

Lee DC, Romero R, Kim JS, Yoo W, Lee J, Mittal P, Kusanovic JP, Hassan SS, Yoon BH, Kim CJ (2010) Evidence for a spatial and temporal regulation of prostaglandin-endoperoxide synthase 2 expression in human amnion in term and preterm parturition. J Clin Endocrinol Metab 95(9):E86-91. https://doi.org/10.1210/jc.2010-0203

Lemke A, Castillo-Sanchez JC, Prodinger F, Ceranic A, Hennerbichler-Lugscheider S, Perez-Gil J, Redl H, Wolbank S (2017) Human amniotic membrane as newly identified source of amniotic fluid pulmonary surfactant. Sci Rep 7(1):6406. https://doi.org/10.1038/s41598-017-06402-w

Litwiniuk M, Radowicka M, Krejner A, Sladowska A, Grzela T (2018) Amount and distribution of selected biologically active factors in amniotic membrane depends on the part of amnion and mode of childbirth. Can we predict properties of amnion dressing? A-proof-of concept study. Cent Eur J Imunol 43(1):97–102. https://doi.org/10.5114/ceji.2017.69632

Meller D, Pauklin M, Thomasen H, Westekemper H, Steuhl KP (2011) Amniotic membrane transplantation in the human eye. Dtsch Arztebl Int 108(14):243–248. https://doi.org/10.3238/arztebl.2011.0243

Memmi B, Leveziel L, Knoeri J, Leclere A, Ribes O, Despiaux MC, Bouheraoua N, Nordmann JP, Baudouin C, Borderie V (2022) Freeze-dried versus cryopreserved amniotic membranes in corneal ulcers treated by overlay transplantation: a case-control study. Cornea 41(3):280–285. https://doi.org/10.1097/ICO.0000000000002794

Moraes J, Costa MM, Alves PCS, Sant'Anna LB (2021) Effects of preservation methods in the composition of the placental and reflected regions of the human amniotic membrane. Cells Tissues Organs 210(1):66–76. https://doi.org/10.1159/000515448

Nejad AR, Hamidieh AA, Amirkhani MA, Sisakht MM (2021) Update review on five top clinical applications of human amniotic membrane in regenerative medicine. Placenta 103:104–119. https://doi.org/10.1016/j.placenta.2020.10.026

Paolin A, Trojan D, Leonardi A, Mellone S, Volpe A, Orlandi A, Cogliati E (2016) Cytokine expression and

ultrastructural alterations in fresh-frozen, freeze-dried and gamma-irradiated human amniotic membranes. Cell Tissue Bank 17(3):399–406. https://doi.org/10.1007/s10561-016-9553-x

RStudio (2020) RStudio: Integrated Development for R. RStudio, PBC, Boston, MA URL: http://www.rstudio.com/

Ruiz-Canada C, Bernabe-Garcia A, Liarte S, Rodriguez-Valiente M, Nicolas FJ (2021) Chronic wound healing by amniotic membrane: TGF-beta and EGF signaling modulation in re-epithelialization. Front Bioeng Biotechnol 9:689328. https://doi.org/10.3389/fbioe.2021.689328

Singh R, Gupta P, Purohit S, Kumar P, Vaijapurkar SG, Chacharkar MP (2006) Radiation resistance of the microflora associated with amniotic membranes. World J Microbiol Biotechnol 22(1):23–27. https://doi.org/10.1007/s11274-005-2890-8

Skinner SJ, Campos GA, Liggins GC (1981) Collagen content of human amniotic membranes: effect of gestation length and premature rupture. Obstet Gynecol 57(4):487–489

Smeringaiova I, Trosan P, Mrstinova MB, Matecha J, Burkert J, Bednar J, Jirsova K (2017) Comparison of impact of two decontamination solutions on the viability of the cells in human amnion. Cell Tissue Bank 18(3):413–423. https://doi.org/10.1007/s10561-017-9636-3

Svobodova A, Horvath V, Smeringaiova I, Cabral JV, Zemlickova M, Fiala R, Burkert J, Nemetova D, Stadler P, Lindner J, Bednar J, Jirsova K (2022) The healing dynamics of non-healing wounds using cryo-preserved amniotic membrane. Int Wound J 19(5):1243–1252. https://doi.org/10.1111/iwj.13719

Svobodova A, Vrkoslav V, Smeringaiova I, Jirsova K (2023) Distribution of an analgesic palmitoylethanolamide and other *N*-acylethanolamines in human placental membranes. PLoS ONE. https://doi.org/10.1371/journal.pone.0279863

Tabatabaei SA, Soleimani M, Behrouz MJ, Torkashvand A, Anvari P, Yaseri M (2017) A randomized clinical trial to evaluate the usefulness of amniotic membrane transplantation in bacterial keratitis healing. Ocul Surf 15(2):218–226. https://doi.org/10.1016/j.jtos.2017.01.004

Tossetta G, Paolinelli F, Avellini C, Salvolini E, Ciarmela P, Lorenzi T, Emanuelli M, Toti P, Giuliante R, Gesuita R, Crescimanno C, Voltolini C, Di Primio R, Petraglia F, Castellucci M, Marzioni D (2014) IL-1beta and TGF-beta weaken the placental barrier through destruction of tight junctions: an in vivo and in vitro study. Placenta 35(7):509–516. https://doi.org/10.1016/j.placenta.2014.03.016

Tsubota K, Satake Y, Ohyama M, Toda I, Takano Y, Ono M, Shinozaki N, Shimazaki JUN (1996) Surgical reconstruction of the ocular surface in advanced ocular cicatricial pemphigoid and stevens-johnson syndrome. Am J Ophthalmol 122(1):38–52. https://doi.org/10.1016/s0002-9394(14)71962-2

Valiente MR, Nicolas FJ, Garcia-Hernandez AM, Fuente Mora C, Blanquer M, Alcaraz PJ, Almansa S, Merino GR, Lucas MDL, Alguero MC, Insausti CL, Pinero A, Moraleda JM, Castellanos G (2018) Cryopreserved amniotic membrane in the treatment of diabetic foot ulcers: a case series. J Wound Care 27(12):806–815. https://doi.org/10.12968/jowc.2018.27.12.806

Venault A, Bai YW, Dizon GV, Chou HE, Chiang HC, Lo CT, Zheng J, Aimar P, Chang Y (2019) Healing kinetics of diabetic wounds controlled with charge-biased hydrogel dressings. J Mater Chem B 7(45):7184–7194. https://doi.org/10.1039/c9tb01662g

Walkden A (2020) Amniotic membrane transplantation in ophthalmology: an updated perspective. Clin Ophthalmol 14:2057–2072. https://doi.org/10.2147/OPTH.S208008

Wassmer CH, Berishvili E (2020) Immunomodulatory properties of amniotic membrane derivatives and their potential in regenerative medicine. Curr Diab Rep 20(8):31. https://doi.org/10.1007/s11892-020-01316-w

Weidinger A, Pozenel L, Wolbank S, Banerjee A (2020) Sub-regional differences of the human amniotic membrane and their potential impact on tissue regeneration application. Front Bioeng Biotechnol 8:613804. https://doi.org/10.3389/fbioe.2020.613804

Appendix 7: Discontinuous transcription of ribosomal DNA in human cells

PLOS ONE

RESEARCH ARTICLE

Discontinuous transcription of ribosomal DNA in human cells

Evgeny Smirnov[1]*, Peter Trosan[2], Joao Victor Cabral[2], Pavel Studeny[3], Sami Kereïche[1], Katerina Jirsova[2], Dušan Cmarko[1]

1 Laboratory of Cell Biology, Institute of Biology and Medical Genetics, First Faculty of Medicine, Charles University and General University Hospital in Prague, Prague, Czech Republic, **2** Laboratory of the Biology and Pathology of the Eye, Institute of Biology and Medical Genetics, First Faculty of Medicine, Charles University and General University Hospital in Prague, Prague, Czech Republic, **3** Ophthalmology Department of 3rd Faculty of Medicine, Charles University and University Hospital Kralovske Vinohrady, Prague, Czech Republic

* esmir@lf1.cuni.cz

OPEN ACCESS

Citation: Smirnov E, Trosan P, Cabral JV, Studeny P, Kereïche S, Jirsova K, et al. (2020) Discontinuous transcription of ribosomal DNA in human cells. PLoS ONE 15(3): e0223030. https://doi.org/10.1371/journal.pone.0223030

Editor: Michal Hetman, University of Louisville, UNITED STATES

Received: September 9, 2019

Accepted: January 24, 2020

Published: March 2, 2020

Peer Review History: PLOS recognizes the benefits of transparency in the peer review process; therefore, we enable the publication of all of the content of peer review and author responses alongside final, published articles. The editorial history of this article is available here: https://doi.org/10.1371/journal.pone.0223030

Data Availability Statement: URL to access data: https://osf.io/2v8am/?view_only=1d925a4e3ce845b599cdc7908edd0aa1.

Funding: The work was supported by research project BBMRI_CZ LM2018125, European

Abstract

Numerous studies show that various genes in all kinds of organisms are transcribed discontinuously, i.e. in short bursts or pulses with periods of inactivity between them. But it remains unclear whether ribosomal DNA (rDNA), represented by multiple copies in every cell, is also expressed in such manner. In this work, we synchronized the pol I activity in the populations of tumour derived as well as normal human cells by cold block and release. Our experiments with 5-fluorouridine (FU) and BrUTP confirmed that the nucleolar transcription can be efficiently and reversibly arrested at +4˚C. Then using special software for analysis of the microscopic images, we measured the intensity of transcription signal (incorporated FU) in the nucleoli at different time points after the release. We found that the ribosomal genes in the human cells are transcribed discontinuously with periods ranging from 45 min to 75 min. Our data indicate that the dynamics of rDNA transcription follows the undulating pattern, in which the bursts are alternated by periods of rare transcription events.

Introduction

Numerous studies show that genes in all kinds of organisms, from prokaryotes to mammals, can be transcribed in short bursts or pulses alternated by periods of silence (reviewed in Smirnov et al. [1]) The probability of such mode of expression was suggested long ago;[2] now it seems that the discontinuous transcription is a common feature of the gene expression, at least in mammalian cells.[3–12] The periodical switches of the promoter between the active and "refractory" states may be crucial in the efficient regulation of the gene expression.[13–17] General considerations suggest even more significant role of the phenomenon in the dynamic organization of the cell, since the pulsing mode of one process is likely to be a cause and a consequence of pulsing in other processes. Thus, RNA processing, which is closely linked to the RNA synthesis, seems to be discontinuous.[9] A spontaneous heterogeneity of gene expression occasioned by transcriptional fluctuations may influence cell behaviour in changing environmental conditions and in the course of differentiation.[18]

Regional Development Fund, project EF16_013/0001674, by the Grant Agency of Czech Republic (19-21715S) and by Charles University (Progres Q25 and Q28). SK acknowledges the financial support from the Czech Science Foundation Grant No. 1825144Y. The funders had no role in study design, data collection and analysis, decision to publish, or preparation of the manuscript.

Competing interests: The authors have declared that no competing interests exist.

The discontinuous character of transcription has been detected by various methods (reviewed in Smirnov et al. [1]) The number of transcripts produced in a certain (sufficiently short) period of time may be determined with high precision by single molecule RNA fluorescence in situ hybridisation (smFISH).[19–21] The results of such quantification alone provide indirect, but valuable information for modelling the expression kinetics in a cell population or tissue, when the studied gene is supposed to be transcriptionally active in all the cells. Methods based on the allele-sensitive single-cell RNA sequencing also allow to reveal and characterize the transcription bursting.[22] To monitor gene expression in real time, cells are transfected with constructs providing a fluorescent signal that corresponds to the expression of a particular gene. In a gene trap strategy, a luciferase gene is inserted under the control of endogenous regulatory sequences. Since both the luciferase protein and its mRNA are short-lived, the method allows to calculate the key parameters of the transcriptional kinetics. Probably the most popular *in vivo* method is based on the use of bacteriophages derived fluorescent coat proteins, such as MS2 or PP7, fused with GFP, which allows to visualize a bunch of the nascent RNA molecules accumulated around one gene.[4, 23, 24]

So far, the pulse-like transcription is well documented only in the genes transcribed by RNA polymerase II. It is not clear yet whether ribosomal DNA (rDNA) is also expressed discontinuously. In human cells, the clusters of multiple rDNA repeats, known as Nucleolus Organizer Regions (NORs), are situated on the short arms of the acrocentric chromosomes. Each repeat includes a gene coding for 18S, 5.8S and 28S RNAs of the ribosomal particles and an intergenic spacer.[25–30] In the interphase nucleus the rDNA provides the basis for the formation of nucleoli. The transcription by pol I and the first steps of rRNA processing take place in the special nucleolar units (FC/DFC) composed of fibrillar centers (FC) and dense fibrillar components (DFC).[31–42] The units correspond in light microscopy to the "beads" forming nucleolar necklaces,[43–46] and each unit is believed to accommodate a single transcriptionally active gene.[33, 39, 47, 48] The intensity of the rDNA transcription is usually very high throughout the entire interphase, especially at the S and G2 phases.[49] Now most of the methods used for the detection of the transcription fluctuation are hardly applicable to the ribosomal genes, since one cell usually contains hundreds of such genes. An alternative method was designed for direct measurements of rDNA transcription in the live cells by using the label-free confocal Raman microspectrometry. [50] This work revealed an undulatory character of the ribosomal RNA production in the whole nucleoli. In our earlier study on tumour-derived cells expressing a GFP-RPA43 (a subunit of pol I) fusion protein, we have observed specific fluctuations of the fluorescence signal in the individual FC/DFC units.[51] We also found high correlation of pol I and incorporated FU signals within the units. These data suggested that the ribosomal genes are transcribed in a pulse-like manner.

In the present work we used a different approach to the study of the discontinuous transcription of ribosomal genes in human cells. In our experiments with 5-fluorouridine (FU) and BrUTP, we found that the nucleolar transcription can be efficiently arrested at +4˚C and quickly restored at normal conditions. Based on this finding, we synchronized the pol I activity in the cell population by cold block and release. Then using specially designed software we measured the intensity of transcription signal (incorporated FU) in the nucleoli and individual FC/DFC units at different periods after the release. This enabled us to detect transcription fluctuations of ribosomal genes in tumour derived as well as normal human cells and to reveal special properties of this fluctuation.

Methods

Ethics

The study followed the standards of the Ethics Committees of the General Teaching Hospital and the First Faculty of Medicine of Charles University, Prague, Czech Republic (Ethics

Committee of General Univeristy Hospital, Prague approval no. 1570/11 S-IV (held on October 13, 2011, and updated January 18, 2018. The name of project: Pathogenesis of hereditary, degenerative and systemic diseases with manifestations in the eye, transplantology. Study of healthy and control tissue), and adhered to the principles set out in the Helsinki Declaration. We obtained human cadaver corneoscleral rims from 10 donors, which were surplus from surgery and stored in Eusol-C (Alchimia, Padova, Italy), from the Department of Ophthalmology, General University Hospital in Prague, Czech Republic, for the study. On the use of the corneoscleral rims, based on Czech legislation on specific health services (Law Act No. 372/2011 Coll.), informed consent is not required if the presented data are anonymous in the form."

Cell cultures

Human limbal epithelial cells (LECs) were obtained from XY cadaver corneoscleral rims after cornea grafting at University Hospital Kralovske Vinohrady, Prague, Czech Republic. The mean donor age ± standard deviation (SD) was 63.5 ± 6.5 years. Tissue was stored in Eusol-C (Alchimia, srl., Ponte San Nicolò, Italy) preservation medium at +4˚C. The mean storage time ± SD (from tissue collection until explantation) was 7.2 ± 3.6 days. The corneoscleral rims were prepared as described before.[52, 53] Shortly, corneoscleral rims were cut into 12 pieces and placed in a 24-well plate (TPP Techno Plastic Products AG, Trasadingen, Switzerland) on Thermanox plastic coverslips (Nunc, Thermo Fisher Scientific, Rochester, NY, USA). Explants were cultured in 1 ml of complete medium [1:1 DMEM/F12, 10% FBS, 1% AA, 10 ng/ml recombinant EGF, 0.5% insulin-transferrin-selenium (Thermo Fisher Scientific), 5 μg/ml hydrocortisone, 10 μg/ml adenine hydrochloride and 10 ng/ml cholera toxin (Sigma-Aldrich, Darmstadt, Germany)]. The culture media were changed every 2–3 days until the cells were 90–100% confluent (after 2–4 weeks).

HeLa cells were cultivated at 37˚C in Dulbecco modified Eagle's medium (DMEM, Sigma) containing 10% fetal calf serum, 1% glutamine, 0.1% gentamicin, and 0.85g/l $NaHCO_3$ in standard incubators. For the transcription synchronization, the cells were incubated in cold medium (+4˚C) for 1 h, then transferred to the normal conditions and fixed at different time points from 15 to 150 min with the interval of 15 min.

Plasmids and transfection

The GFP-RPA43 and GFP-Fibrillarin vectors were received from Laboratory of Receptor Biology and Gene Expression Bethesda, MD.[54] The constructs were transfected into HeLa cells using Fugene (Qiagen).

Labeling of the transcription sites

For visualization of the transcription sites, sub-confluent cells were incubated for 5 min prior to fixation with 5-fluorouridine (FU) (Sigma). The cells were fixed in pure methanol at -20˚C for 30 min and processed for FU immunocytochemistry. BrUTP (Sigma) was introduced into cells by the scratch procedure.[55, 56] Here we followed the same procedure as for the labelling of replication in the cited works. Briefly, the cells were grown on the coverslips; a drop of medium containing 20μg/ml BrUTP was applied upon each coverslip; then the latter was scratched by the tip of a syringe needle and incubated for 5 min at 37˚C. Thus permeabilized, the cells were incubated for 10 min in the usual medium and then fixed and processed as after the incorporation of FU.

Incorporated FU and BrUTP signal was visualized using a mouse monoclonal anti-BrdU antibody (Sigma) and secondary goat Cy3-conjugated anti-mouse antibody (Abcam).

Light microscopy

Confocal images were acquired by means of SP5 (Leica) confocal laser scanning microscope equipped with a 63×/1.4NA oil immersion objective. For *in vivo* cell imaging we used a spinning disk confocal system based on Olympus IX81 microscope equipped with Olympus UPlanSApo 100×/1.4NA oil immersion objective, CSU-X spinning disk module (Yokogawa) and Ixon Ultra EMCCD camera (Andor). The live cells were maintained in glass bottom Petri dishes (MatTek) at 37˚C and 5% CO_2 within a microscope incubator (Okolab).

Software and data analysis

For measurement and counting of the transcription and other signals corresponding to individual FC/DFC units in 3D confocal images, we developed a MatLab based software.[51] The program identifies each unit by creating a maximum intensity projection of the confocal stack and blurring the projection with a Gaussian filter (σ = 8–10 pixels), defining the blurred image with a value obtained by Otsu's method for automatic threshold selection. After that, the optical section whereupon the unit had maximum intensity was identified. The final result contains 3D coordinates of each unit, its size (full-width half-maximum), the value of χ^2, and integral intensities in the spheres with radii 1.0, 1.5, 2.0, 2.5, 3.0, 3.5, and 4.0 pixels. The values corresponding to 1.5 pixels seemed to be the most resistant to noise and were used for presentation of the data. FC/DFC units were counted after deconvolution with Huygens software.

For measuring signals in the entire nucleoli we used a custom ImageJ plugin available at https://github.com/vmodrosedem/segmentation-correlation.[45] Based on the confocal stacks, the program identifies the regions occupied by the cell nuclei as well as nucleoli, measures their areas (in pixels), and the intensities, both integral and average, of the signal within these areas.

Results

1. Effects of low temperature on the nucleolar transcription

In the control the incorporated FU is accumulated predominantly in the nucleolar beads which, according to our earlier study,[55] correspond to the FC/DFC units of the nucleoli (Fig 1). The transcription signal in the nucleoplasm appeared as multiple small foci of much lower intensity. After 15 min of incubation at +4˚C (without additional supply of CO_2), both HeLa and LECs lost the ability to incorporate 5-fluorouridin (FU). When the cells were returned to the normal conditions (37˚C, 5% CO_2), transcription was partly restored in 15 min, and in 30 min the FU incorporation did not visibly differ from the control (Fig 1).

Since incorporation of FU is preceded by its penetration in the cell and phosphorylation, we performed an additional experiment with another RNA predecessor, BrUTP, which was introduced in the HeLa cells by the scratch procedure (Fig 1B).[55, 56] When cells were permeabilized by scratching in the presence of BrUTP for 5 min and then immediately fixed (Fig 1B, left) or washed and incubated for further 10 min at +4˚C (Fig 1B, middle), there was no significant incorporation of the nucleotide. But when the permeabilization was followed by 10 min incubation in the normal conditions (Fig 1B, right), the cells situated along the scratch track displayed the transcription signal in the nucleoli and nucleoplasm. This result confirmed that the transcription was efficiently arrested in our experiments at +4˚C.

It is known that pol I and fibrillarin are particularly sensitive to stress, and their redistribution in the cell nuclei is a common symptom of nucleolar pathology. Therefore, to assess the effect of cold on the FC/DFC units, which are the centers of rDNA transcription and early rRNA processing, we transfected the cells with GFP-RPA43 or GFP-Fibrillarin. At the low

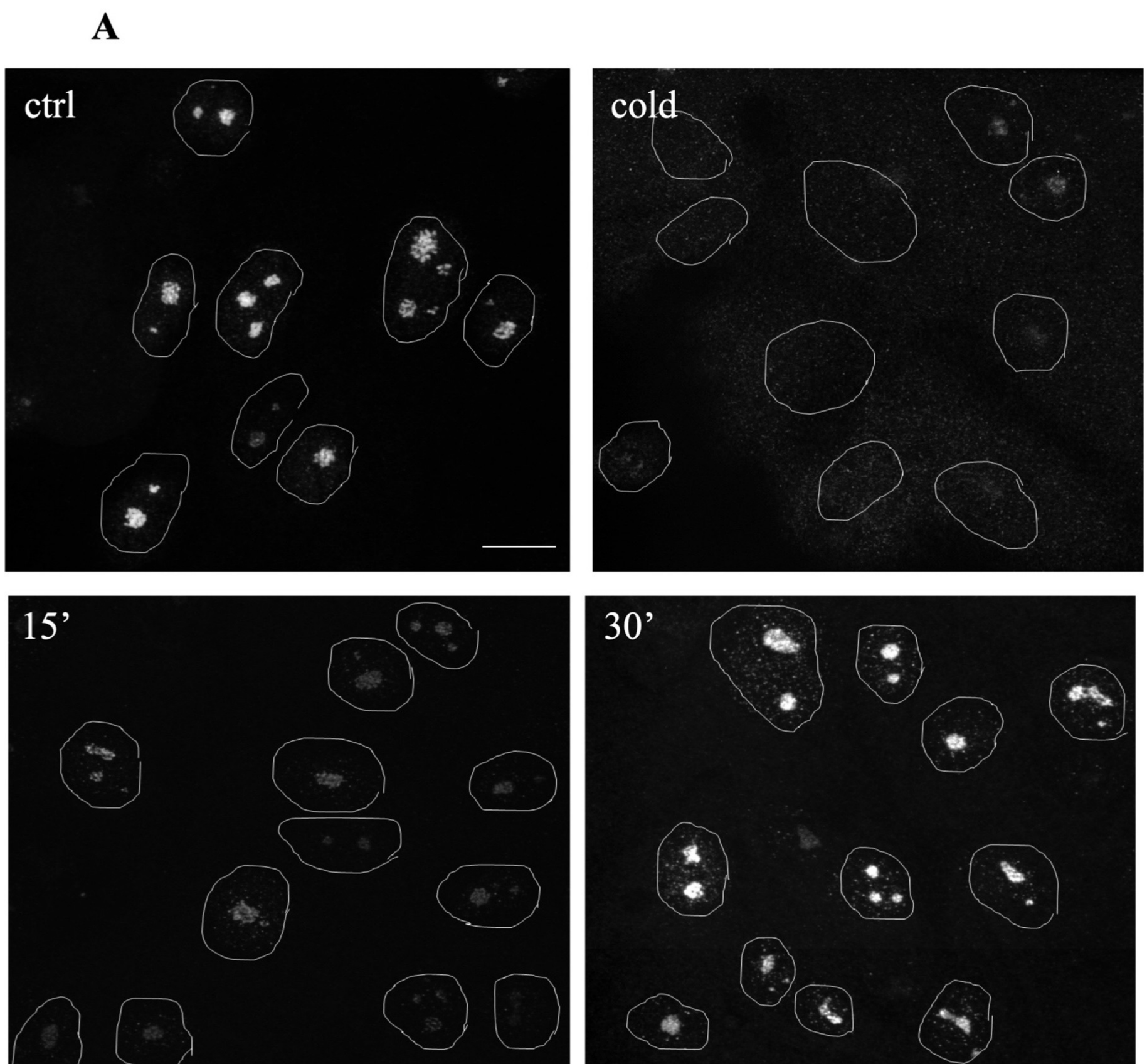
A
ctrl
cold
15’
30’
B
No incubation
Incubation at 4ºC
Incubation at 37ºC

Fig 1. (A) Transcription in HeLa cells is quickly inhibited at +4˚C and restored at the normal conditions. The transcription signal (FU incorporation) is accumulated in the nucleoli. The signal disappeared after 15 min of cold treatment (top right); when the cells were transferred to the normal conditions, the signal was partly restored in 15 min and appeared like in the control in 30 min (bottom). **(B) Incorporation of BrUTP.** No significant signal in the cells fixed after the permeabilization immediately (left) or following 10 min of incubation at +4˚C (middle); when permeabilization was followed by 10 min incubation at +37˚C, specifically labelled cells could be observed along the scratch track (right). Scale bar: 10μm.

https://doi.org/10.1371/journal.pone.0223030.g001

temperature the GFP-Fibrillarin signal did not change significantly, but the intensity of the RPA43 signal was decreased as average to about 60% of the control level (Fig 2).

Observation of the individual cells also showed that after transferring the cells from the cold to the normal conditions, the intensity of GFP-RPA43 signal in all FC/DFC units increased, although the number of the detectable units did not change (Fig 3).

These experiments show that low temperature causes a quick inhibition of the rDNA transcription, as well as significant though not complete depletion of the pol I pools in the nucleoli.

On the other hand, we observe a quick recovery of the cells without any lasting symptoms of pathology.

2. Synchronization of the nucleolar transcription in HeLa and human limbal cells by cold treatment

The experiments described in the previous section indicate that at the low temperature the ribosomal genes are brought to a silent state with a diminished RPA-GFP signal within the FC/DFC units which implies a decreased number of pol I complexes bound to the genes. This synchronization procedure was used for the study of the discontinuous expression of the rDNA in HeLa and LEC cells. Namely, the cells were incubated in cold medium (+4˚C) for 1 h, then transferred to the normal conditions and fixed at different time points from 15 to 150 min with the interval of 15 min. FU was added to the cultivation medium 5 min prior to each fixation. The transcription signal visualized by antibody was then measured in the nucleoli by means of the ImageJ plugin software (see Methods). The results are presented in Fig 4.

In all such experiments the intensity of the transcription signal increased during the first 30 min, then began to decrease. Altogether two cycles of rise and fall have been observed within the period of 150 min, the coefficient of variation (CV) was 0.26. The spectral analysis revealed a significant peak corresponding to the period of 60 min. Since the interval between the measurements was 15 min, the values of the period may be varying from 45 min to 75 min. An additional lower peak at 15 min probably reflected a high frequency noise. In the control, when the cells were kept at 37˚C and fixed at different time points as in the experiment, the fluctuations of the transcription signal intensity were irregular. CV was only 0.07, and the periodogram had two peaks of low amplitude (compare the left and right parts of the Fig 4). In two experiments the period of observation was extended to 210 min, but between 150 and 210 min the fluctuations of the transcription signal appeared irregular with the CV values 0.06, i.e. just like in the control, which indicated that the synchrony in the cell population was lost. These results showed that in HeLa cells the activity of pol I transcription machinery was synchronized by the cold treatment for the period of 150 min, but not longer.

The same experimental procedure was applied to the LECs (Fig 5). In this case the first two cycles were more pronounced and the difference between control and experiment was more significant (compare Fig 5 and Fig 4). Otherwise, the dynamics of the transcription activity after the cold treatment proved to be similar in the studied cell lines. In the LECs, the periodogram had a more distinct peak at 60 min, but the synchronization also did not last longer than 150 min. CV was 0.29, i.e. slightly higher than in HeLa cells. It seems worth mentioning that

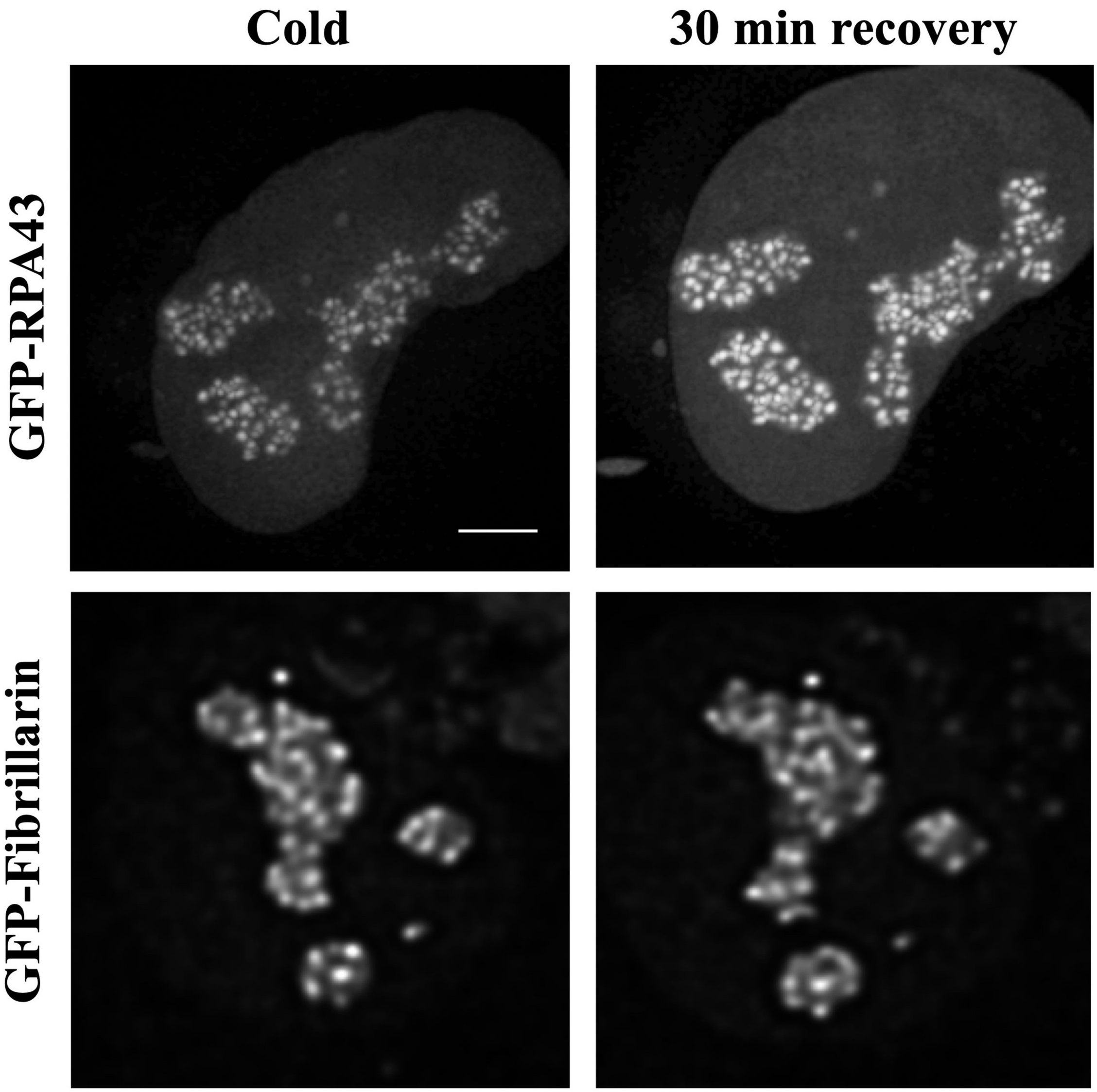

Fig 2. Following GFP-RPA43 and GFP-Fibrillarin signals in the transfected HeLa cells *in vivo*. The intensity of the GFP-RPA43 signal is reduced after 15min incubation at +4˚C (left, top) and restored after subsequent 30 min incubation at normal conditions (top, right). The GFP-Fibrillarin signal was not significantly affected by the cooling/warming procedure (bottom). Scale bar: 5μm.

https://doi.org/10.1371/journal.pone.0223030.g002

our attempt to synchronize the transcription in human fibroblasts failed, for only a few of these cells recovered quickly enough after the cold treatment.

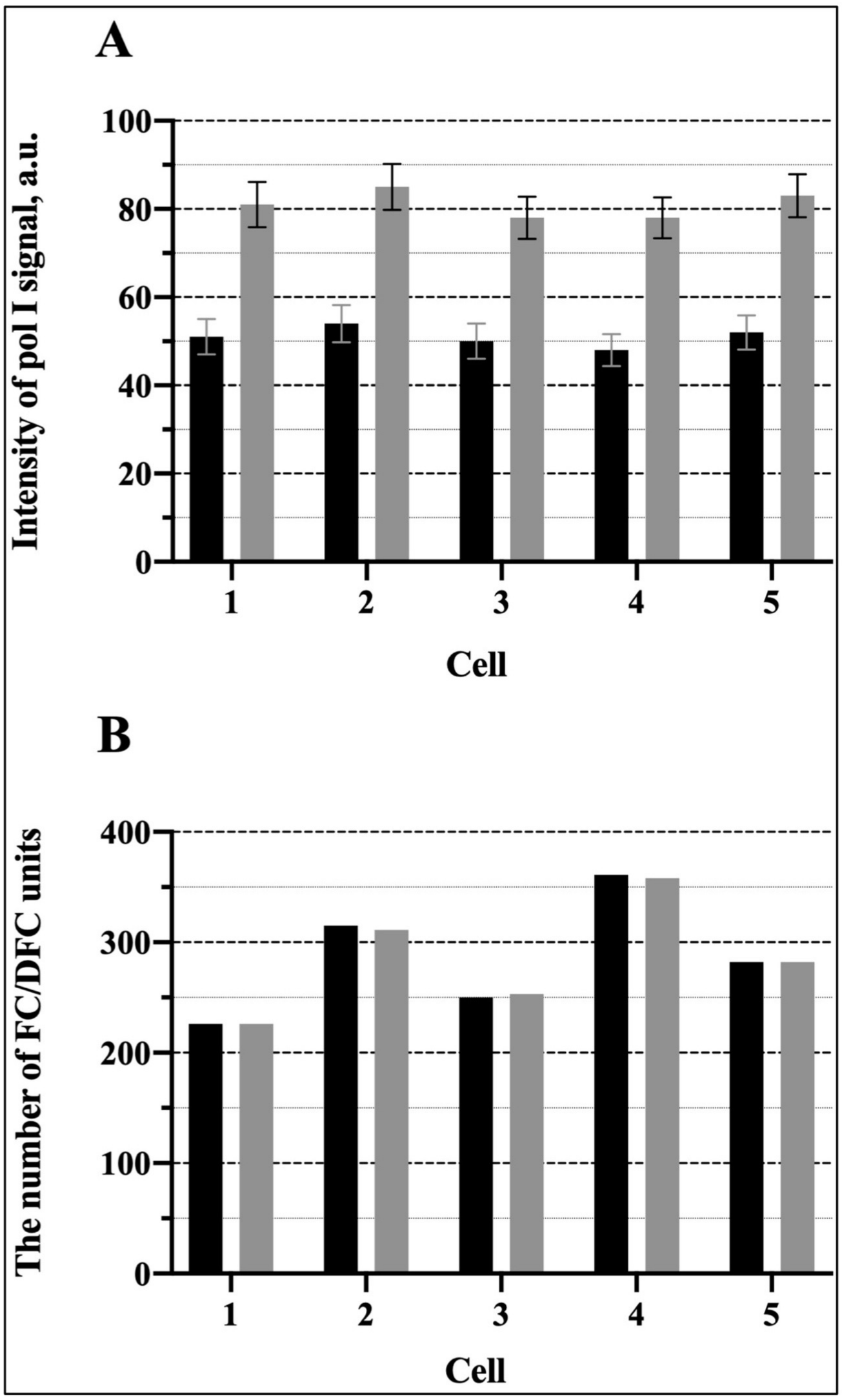

Fig 3. Effects of cooling/warming (as in Fig 2, top) on the FC/DFC units *in vivo* in the transfected HeLa cells. (A) intensity of the GFP-RPA43 signal in the individual units after 15min incubation at +4˚C (black columns) and after subsequent 30 min incubation at 37˚C (grey columns). Five cells were observed, and five selected units were followed in each cell. The error bars show SEM**. (B)** the total number of the GFP-RPA43 positive units in five cells after 15min incubation at +4˚C (black columns) and after subsequent 30 min incubation at 37˚C (grey columns). The experiment indicates that at the low temperature pol I escapes from the FC/DFC units.

https://doi.org/10.1371/journal.pone.0223030.g003

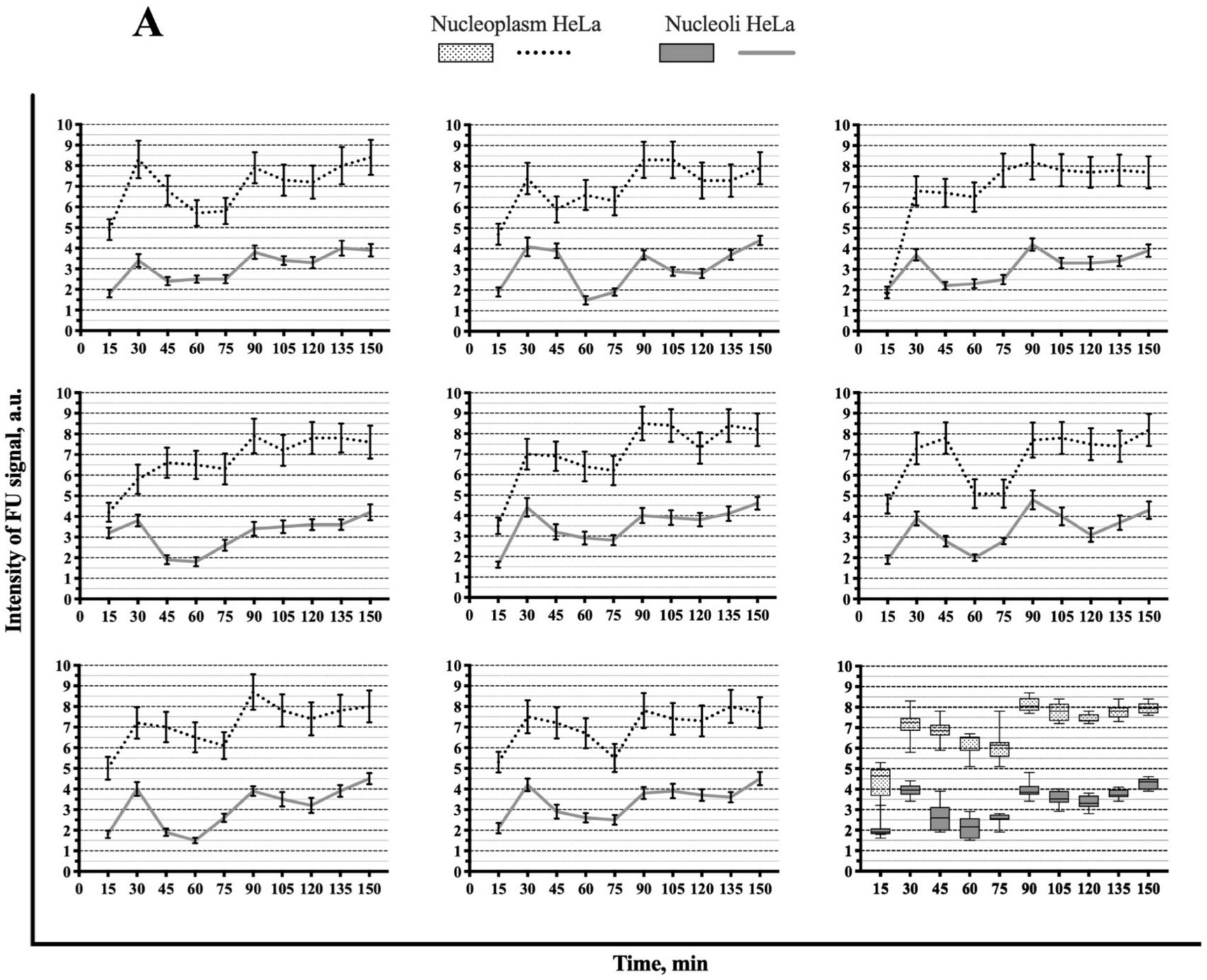
A
Nucleoplasm HeLa
Nucleoli HeLa
Intensity of FU signal, a.u.
Time, min

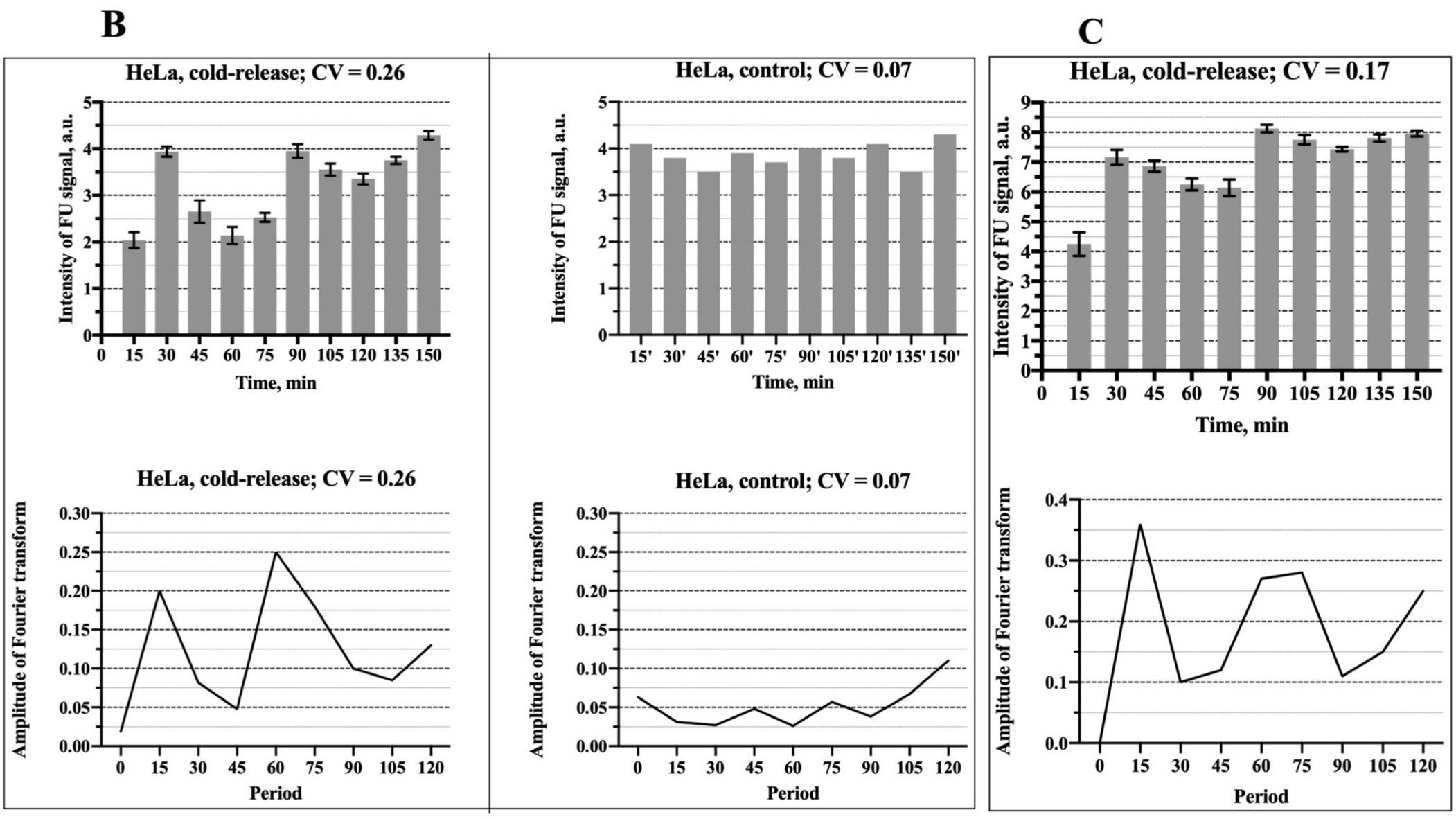
B
HeLa, cold-release; CV = 0.26
Intensity of FU signal, a.u.
Time, min
HeLa, control; CV = 0.07
Intensity of FU signal, a.u.
Time, min
C
HeLa, cold-release; CV = 0.17
Intensity of FU signal, a.u.
Time, min
HeLa, cold-release; CV = 0.26
Amplitude of Fourier transform
Period
HeLa, control; CV = 0.07
Amplitude of Fourier transform
Period
Amplitude of Fourier transform
Period

Fig 4. Fluctuation of the intensity of the transcription signal (incorporated FU) in the whole nucleoli and nucleoplasm of HeLa cells after release from the cold block. (A) Data of the individual experiments and the box-plot chart. **(B)** Mean values of the transcription signal intensity in the nucleoli after release from the cold block (left, top) and in the nucleoli of the control cells, i.e. without cold treatment (right, top) In the experiment the signal reaches maximal values at 30 min, 90 min, and 150 min. The graph shows mean values obtained from 50 cells in one experiment. Such experiment was repeated 8 times. CV- coefficient of variation. The error bars show SEM. The bottom graphs show the respective periodograms for the experiment (left) and control (right) calculated as amplitudes of the Fourier transforms. The x-axis represents the period (min). **(C)** Mean values of the transcription signal intensity in the nucleoplasm after release from the cold block (top) and the respective periodogram (bottom).

https://doi.org/10.1371/journal.pone.0223030.g004

Thus, our experiments indicated that transcription of the ribosomal genes proceeds in a wave-like manner, although the employed synchronization procedure is not equally efficient in various cells.

3. Fluctuation of the pol I signal in the cells synchronized by chilling

To confirm our result by an independent set of data, we used chilling shock to synchronize HeLa cells transfected with GFP-RPA-43 (see Fig 6). Measuring the intensity of the pol I signal in the nucleoli of the individual cells, we observed fluctuations similar to those of the transcription signal (Figs 4 and 5). The fluctuations had a relatively low amplitude, and the distinct undulations persisted for no longer than two hours, apparently because only a minor portion of the pol I molecules within FC/DFC units are engaged in the current transcription, as was indicated, for instance, in our earlier work.[51] Nevertheless, the initial increase of the signal intensity during the first 30 min after the cold treatment was followed by a noticeable decrease during the next half hour, which could not be attributed to the effects of recovery. Together with the other results of the present study (Figs 4 and 5) this indicates, that fluctuations of the transcription intensity and pol I levels in the nucleoli are synchronous.

4. Synchronization of the transcription in the nucleoplasm by cold treatment

When the LECs or HeLa cells were incubated at +4˚C, the transcription ceased completely in their nucleoplasm as well as in the nucleoli. Measurement of the total FU signal after transferring the cells from the cold to the normal conditions showed symptoms of synchronization: the signal in the nucleoplasm increased for 30 min and then began to decrease (Figs 4A, 4C, 5A and 5C). The average intensity of the transcription signal in the nucleoli and nucleoplasm positively correlated, with the correlation coefficients 0.65 for the HeLa cells and 0.74 for the LECs. But, as one could expect, the total expression of the nucleoplasmic genes was less synchronized. After the initial recovery and subsequent decrease, the signal became rather noisy. The CV was 0.17 and 0.19 in the HeLa and LECs respectively. The periodograms showed a not very distinct peak at 75 min as well as a sharper peak corresponding to higher frequencies. The second peak probably reflects a noisier character of the fluctuations in the nucleoplasm as compared to the nucleoli.

5. The FC/DFC units in the course of the transcription fluctuation

Since the measurement of the transcription signal in the whole nucleoli is significantly affected by the fluorescence between the FC/DFC units, we measured the signal also within the units. According to the data presented in the sections 2 and 3 (Figs 4 and 5), the intensity of FU signal in the nucleoli at 15 min and 30 min after the cold treatment may be taken as representatives of the two extreme states of the transcriptional fluctuation in the synchronized cells. Measurement of the FU signal in the individual FC/DFC units of the LECs and HeLa cells using the MatLab based software (see Methods) showed an approximately threefold increase

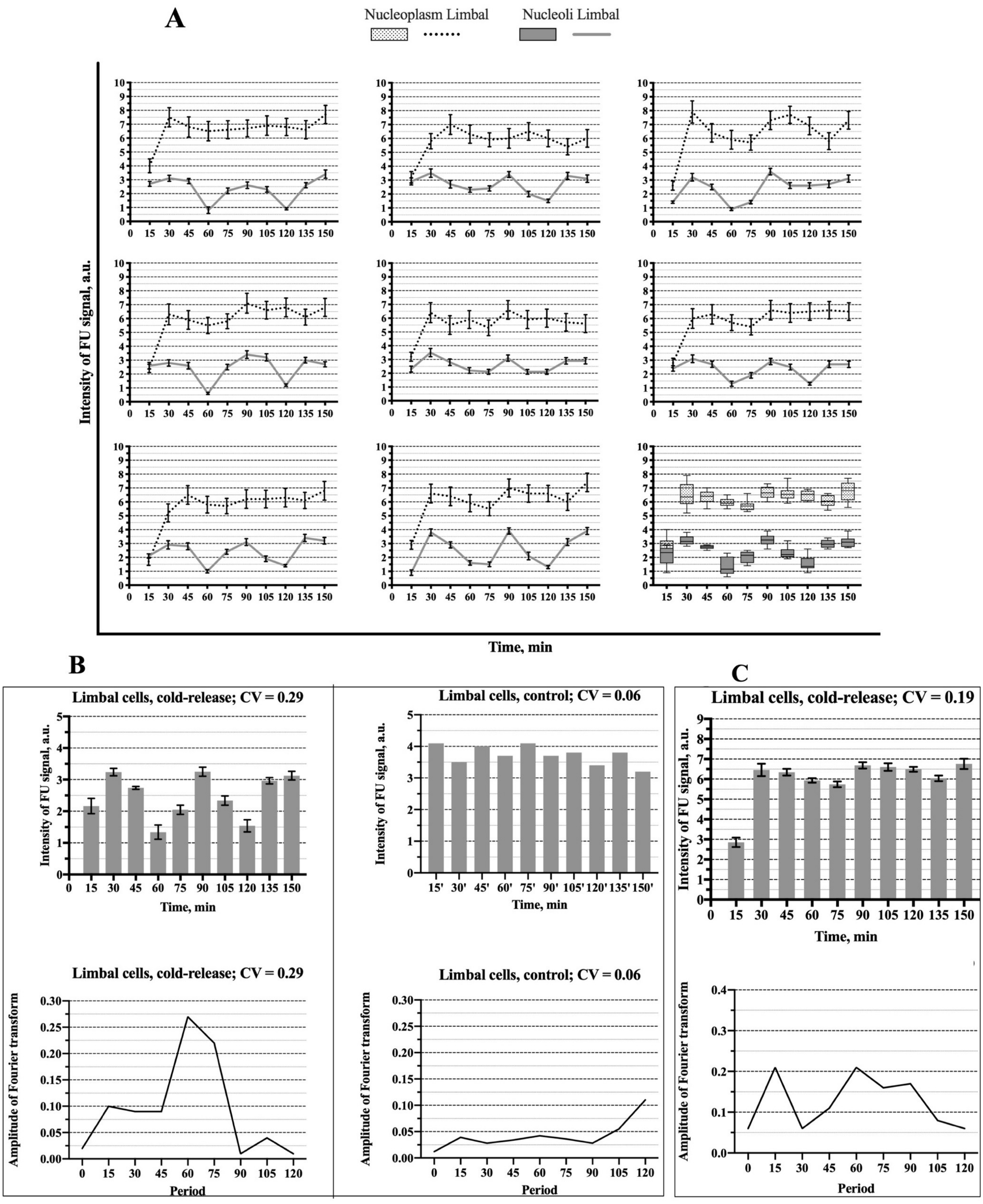

Fig 5. Fluctuation of the intensity of the transcription signal (incorporated FU) in the whole nucleoli and nucleoplasm of the limbal cells. **(A)** Data of the individual experiments and the box-plot chart as in Fig 4A. **(B)** Mean values of the transcription signal intensity in the nucleoli after release from the cold

block (left, top) and in the nucleoli of the control cells (right, top). The figure is analogous to the Fig 4. But in this case, the undulating pattern in the experiment (top, right) is more pronounced, and the periodogram related to the experiment (bottom, left) has a more distinct peak at 60 min. The data are obtained from 8 independent experiments, and in each of them 50 cells were measured. **(C)** Mean values of the transcription signal intensity in the nucleoplasm after release from the cold block (top) and the respective periodogram (bottom).

https://doi.org/10.1371/journal.pone.0223030.g005

of the signal intensity between 15 min and 30 min (Fig 7). But the transcription signal never disappeared from the cells completely, so that the average number of the FU-positive FC/DFC units did not change significantly (Fig 7B, right chart).

Discussion

In our experiments, when the human derived cells were incubated at +4˚C, transcription in their nuclei seemed to be arrested completely (Figs 1 and 7). At the same time the pol I signal in the FC/DFC units of the nucleoli was significantly reduced (Figs 2 and 6), whereas the amount of fibrillarin, which is an essential component of the early rRNA processing, did not change significantly (Fig 2). On the other hand, previous studies, including our own, indicate that the mobile fraction of pol I, apparently responsible for the actual transcription, constitutes less than a half of the entire pool of the enzyme in the units.[51, 54] Therefore, in all probability, the pol I complexes do not "freeze" on their matrices after the arrest of the transcription by the chill shock, but rather detach themselves and escape from the units. After returning to normal conditions, the pools of the enzyme are swiftly restored, and the rRNA synthesis in the cells is synchronized. This effect was used in our work for detection of the pulse-like transcription.

In our previous work we studied the fluctuations of pol I signal, but could not speak about the discontinuous transcription otherwise than hypothetically, since the dynamics of this signal does not necessarily reflect the transcription.[55] Therefore, only after developing the cold/release method of cell synchronization, we obtained the data related to the transcription fluctuations directly.

In thus synchronized HeLa and LEC cells, we observed a wave-like modification of the nucleolar transcription signal with two successive peaks (Figs 4 and 5). It should be mentioned, that the recovery process, which seemed to be limited to the first 30 min after the cold treatment, could not account for the observed dynamics, especially the regularly observed decrease of transcription intensity after the initial increase, as well as more or less distinct second peak. In both kinds of cells, the predominant fluctuation period estimated by the spectral analysis was about 60 min. A similar value of the period was obtained in our previous work for the fluctuations of the GFP-RPA43 signal.[51]. After the two distinct cycles, the waves were damped; probably because of their irregularity and variability in the individual cells. Nevertheless, our data indicate that the ribosomal genes are expressed discontinuously, with intervals of 45–75 min between the bursts.

In our review on the discontinuous transcription, we indicated what seemed to be four main patterns in which this phenomenon may be manifested: the typical busts; the undulating pattern; the regular pulsing; and the rare transcription events.[1] As mentioned above, the fluctuations observed in our study do not seem to belong to the regular type. Rare events also must be excluded, since rDNA transcription is very intensive throughout the entire interphase. The typical bursts are separated by the relatively long periods of silence. But we observed no diminishing of the number of FU positive (Fig 7B) or pol I positive (Fig 3) FC/DFC units in the course of the experiment, although the mean intensity of the incorporated FU signal in the individual units was greatly reduced at the points of minimal transcription activity (Fig 7B).

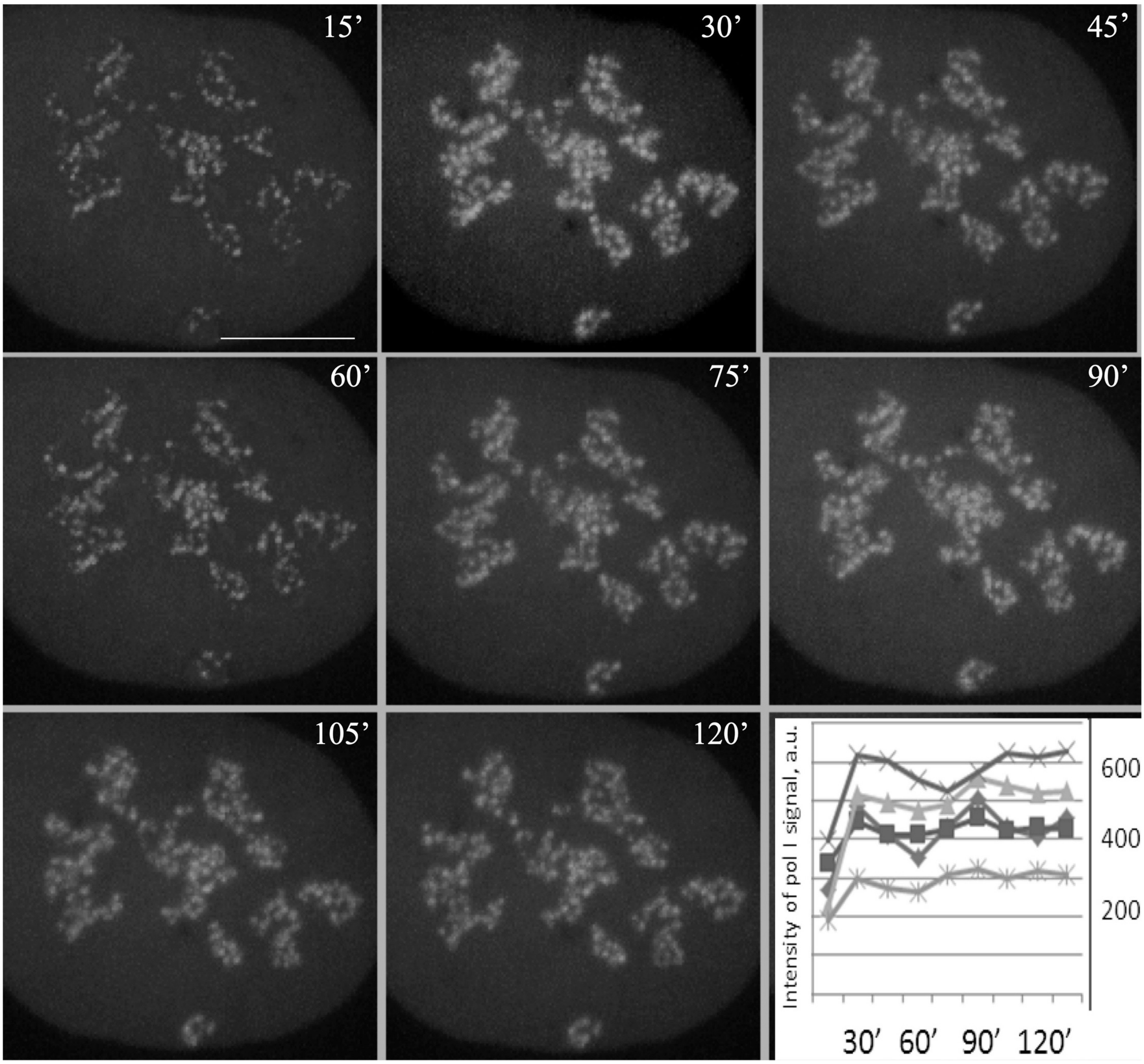

Fig 6. Fluctuation of the intensity of GFP-RPA43 signal in the nucleoli of HeLa cells after the cold treatment. The eight successive images of the same transfected cell photographed every 15 min after the release from the cold block. The intensity of the signal at 15 min as well as at 60 min after the release is visibly lower than at other points. The graph at the bottom right shows records of the pol I signal intensity in five cells at different time points after the release. Each curve represents one cell. All curves have two peaks at 30 min and at 90 min or close to it, as in the case of FU incorporation (Figs 4 and 5). Scale bar: 5μm.

https://doi.org/10.1371/journal.pone.0223030.g006

Therefore, the observed fluctuation of rDNA transcription most likely belongs to the undulating pattern, in which the bursts are alternated by periods of relatively rare transcription events.

Additionally, our method of synchronization allowed us to obtain averaged data concerning the fluctuations in the nucleoplasmic genes, since their expression was also inhibited by the cold treatment. After this procedure, the total transcription signal in the nucleoplasm

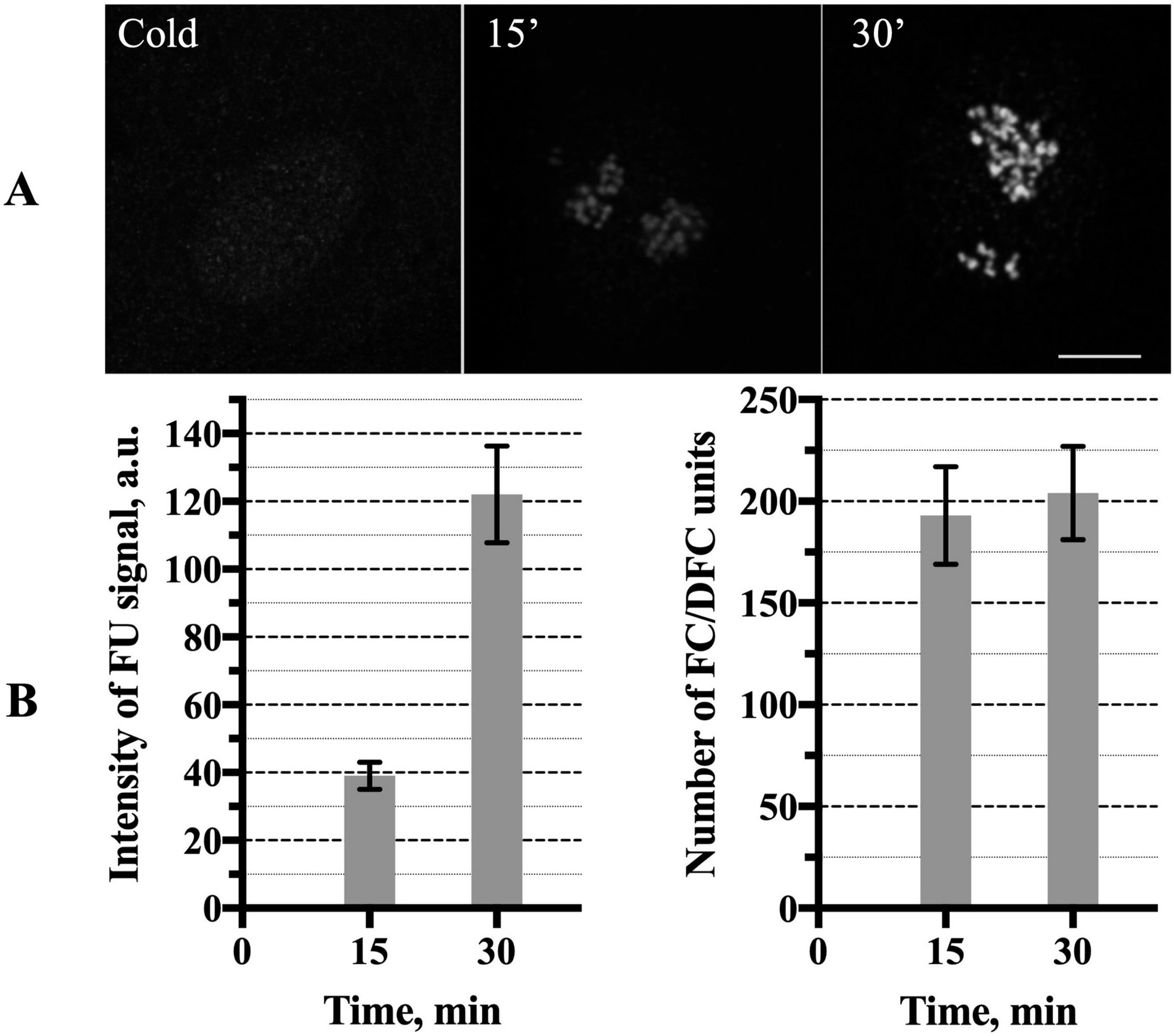

Fig 7. The transcription signal (incorporated FU) in the FC/DFC units of the limbal epithelial cells after the cold treatment. (A) no FU incorporation in the cells incubated at +4˚C for 15 min (left); a weak FU signal in the cell incubated at 37˚C for 15 min after the chilling (middle); 30 min; completely recovered FU signal in the cell incubated at 37˚C for 30 min after the chilling (right). Scale bar: 5 μm. **(B)** the average (from 50 cells) intensity of the FU signal in the individual FC/DFC units measured in the cells incubated at 37˚C for 15 min and 30 min after the chilling. The increase is statistically significant ($P < 0.0001$, according to the Student's t-test) (left). The average (from 50 cells) number of the FU positive FC/DFC units in the cells incubated for 15 min and 30 min at +37˚C after the cold treatment; the differences are statistically insignificant (right). The data show an initial quick recovery of the transcription in the units without changing their number (see Fig 5).

https://doi.org/10.1371/journal.pone.0223030.g007

showed symptoms of fluctuations with two discernible, though not very distinct, peaks (Figs 4A, 4C, 5A and 5C). Evaluating these results, we have to keep in mind that various nucleoplasmic genes in the same cell display a wide range of transcriptional kinetic behavior (reviewed in Smirnov et al. [1]).[4, 10, 57, 58] Moreover, some of these genes are expressed in typical bursts with long periods of silence, during which they cannot be detected by FU incorporation. We should also mention that the status of the nucleoplasmic RNA polymerases at the low temperature

was not examined in our experiments, and thus we do not know how efficiently the transcription was synchronized. Nevertheless, the presence of two significant peaks on the periodograms (Figs 4C and 5C) suggests that numerous genes in the nucleoplasm were transcribed in a pulse-like manner with periods close to 15 min and 75 min.

Thus, our results indicate that ribosomal genes in human cells are expressed discontinuously, and their transcription follows undulating pattern with predominant period of about 60 min.

Acknowledgments

The work was supported by research project BBMRI_CZ LM2018125, European Regional Development Fund, project EF16_013/0001674, by the Grant Agency of Czech Republic (19-21715S) and by Charles University (Progres Q25 and Q28). SK acknowledges the financial support from the Czech Science Foundation Grant No. 1825144Y. The funders had no role in study design, data collection and analysis, decision to publish, or preparation of the manuscript.

Author Contributions

Conceptualization: Evgeny Smirnov.

Data curation: Peter Trosan, Pavel Studeny, Katerina Jirsova.

Formal analysis: Evgeny Smirnov, Joao Victor Cabral, Sami Kereïche.

Investigation: Evgeny Smirnov, Joao Victor Cabral, Katerina Jirsova, Dušan Cmarko.

Methodology: Evgeny Smirnov, Peter Trosan.

Software: Sami Kereïche.

Supervision: Evgeny Smirnov, Dušan Cmarko.

Validation: Evgeny Smirnov, Joao Victor Cabral.

Writing – original draft: Evgeny Smirnov.

Writing – review & editing: Peter Trosan, Joao Victor Cabral, Pavel Studeny, Sami Kereïche, Katerina Jirsova, Dušan Cmarko.

References

1. Smirnov E, Hornáček M, Vacík T, Cmarko D, Raška I. Discontinuous transcription. Nucleus. 2018; 9 (1):149–60. https://doi.org/10.1080/19491034.2017.1419112 PubMed Central PMCID: PMC5973254. PMID: 29285985
2. McKnight SL, Miller OL. Post-replicative nonribosomal transcription units in D. melanogaster embryos. Cell. 1979; 17(3):551–63. https://doi.org/10.1016/0092-8674(79)90263-0 PMID: 113103
3. Bahar Halpern K, Tanami S, Landen S, Chapal M, Szlak L, Hutzler A, et al. Bursty gene expression in the intact mammalian liver. Mol Cell. 2015; 58(1):147–56. https://doi.org/10.1016/j.molcel.2015.01.027 PubMed Central PMCID: PMC4500162. PMID: 25728770
4. Chubb JR, Trcek T, Shenoy SM, Singer RH. Transcriptional pulsing of a developmental gene. Curr Biol. 2006; 16(10):1018–25. https://doi.org/10.1016/j.cub.2006.03.092 PubMed Central PMCID: PMC4764056. PMID: 16713960
5. Dar RD, Razooky BS, Singh A, Trimeloni TV, McCollum JM, Cox CD, et al. Transcriptional burst frequency and burst size are equally modulated across the human genome. Proc Natl Acad Sci USA. 2012; 109(43):17454–9. https://doi.org/10.1073/pnas.1213530109 PubMed Central PMCID: PMC3491463. PMID: 23064634
6. Golding I, Paulsson J, Zawilski SM, Cox EC. Real-time kinetics of gene activity in individual bacteria. Cell. 2005; 123(6):1025–36. https://doi.org/10.1016/j.cell.2005.09.031 PMID: 16360033

7. Nicolas D, Phillips NE, Naef F. What shapes eukaryotic transcriptional bursting? Mol Biosyst. 2017; 13 (7):1280–90. https://doi.org/10.1039/c7mb00154a PMID: 28573295

8. Nicolas D, Zoller B, Suter DM, Naef F. Modulation of transcriptional burst frequency by histone acetylation. Proc Natl Acad Sci USA. 2018; 115(27):7153–8. https://doi.org/10.1073/pnas.1722330115 PubMed Central PMCID: PMC6142243. PMID: 29915087

9. Raj A, Peskin CS, Tranchina D, Vargas DY, Tyagi S. Stochastic mRNA synthesis in mammalian cells. PLoS Biol. 2006; 4(10):e309. https://doi.org/10.1371/journal.pbio.0040309 PubMed Central PMCID: PMC1563489. PMID: 17048983

10. Suter DM, Molina N, Gatfield D, Schneider K, Schibler U, Naef F. Mammalian genes are transcribed with widely different bursting kinetics. Science. 2011; 332(6028):472–4. https://doi.org/10.1126/science.1198817 PMID: 21415320

11. Suter DM, Molina N, Naef F, Schibler U. Origins and consequences of transcriptional discontinuity. Curr Opin Cell Biol. 2011; 23(6):657–62. https://doi.org/10.1016/j.ceb.2011.09.004 PMID: 21963300

12. Wang Y, Ni T, Wang W, Liu F. Gene transcription in bursting: a unified mode for realizing accuracy and stochasticity. Biol Rev Camb Philos Soc. 2018. https://doi.org/10.1111/brv.12452 PMID: 30024089

13. Li C, Cesbron F, Oehler M, Brunner M, Höfer T. Frequency modulation of transcriptional bursting enables sensitive and rapid gene regulation. Cell Syst. 2018; 6(4):409–23.e11. https://doi.org/10.1016/j.cels.2018.01.012 PMID: 29454937

14. Ochiai H, Hayashi T, Umeda M, Yoshimura M, Harada A, Shimizu Y, et al. Genome-wide analysis of transcriptional bursting-induced noise in mammalian cells. BioRxiv. 2019. https://doi.org/10.1101/736207

15. Coulon A, Ferguson ML, de Turris V, Palangat M, Chow CC, Larson DR. Kinetic competition during the transcription cycle results in stochastic RNA processing. elife. 2014;3. https://doi.org/10.7554/eLife.03939 PubMed Central PMCID: PMC4210818. PMID: 25271374

16. Eldar A, Elowitz MB. Functional roles for noise in genetic circuits. Nature. 2010; 467(7312):167–73. https://doi.org/10.1038/nature09326 PubMed Central PMCID: PMC4100692. PMID: 20829787

17. Raj A, van Oudenaarden A. Nature, nurture, or chance: stochastic gene expression and its consequences. Cell. 2008; 135(2):216–26. https://doi.org/10.1016/j.cell.2008.09.050 PubMed Central PMCID: PMC3118044. PMID: 18957198

18. Chubb JR. Gene regulation: stable noise. Curr Biol. 2016; 26(2):R61–R4. https://doi.org/10.1016/j.cub.2015.12.002 PMID: 26811888

19. Bahar Halpern K, Itzkovitz S. Single molecule approaches for quantifying transcription and degradation rates in intact mammalian tissues. Methods. 2016; 98:134–42. https://doi.org/10.1016/j.ymeth.2015.11.015 PMID: 26611432

20. Femino AM, Fay FS, Fogarty K, Singer RH. Visualization of single RNA transcripts in situ. Science. 1998; 280(5363):585–90. https://doi.org/10.1126/science.280.5363.585 PMID: 9554849

21. Mueller F, Senecal A, Tantale K, Marie-Nelly H, Ly N, Collin O, et al. FISH-quant: automatic counting of transcripts in 3D FISH images. Nat Methods. 2013; 10(4):277–8. https://doi.org/10.1038/nmeth.2406 PMID: 23538861

22. Larsson AJM, Johnsson P, Hagemann-Jensen M, Hartmanis L, Faridani OR, Reinius B, et al. Genomic encoding of transcriptional burst kinetics. Nature. 2019; 565(7738):251–4. https://doi.org/10.1038/s41586-018-0836-1 PMID: 30602787

23. Bensidoun P, Raymond P, Oeffinger M, Zenklusen D. Imaging single mRNAs to study dynamics of mRNA export in the yeast Saccharomyces cerevisiae. Methods. 2016; 98:104–14. https://doi.org/10.1016/j.ymeth.2016.01.006 PMID: 26784711

24. Bertrand E, Chartrand P, Schaefer M, Shenoy SM, Singer RH, Long RM. Localization of ASH1 mRNA particles in living yeast. Mol Cell. 1998; 2(4):437–45. https://doi.org/10.1016/s1097-2765(00)80143-4 PMID: 9809065

25. Henderson AS, Warburton D, Atwood KC. Location of ribosomal DNA in the human chromosome complement. Proc Natl Acad Sci USA. 1972; 69(11):3394–8. https://doi.org/10.1073/pnas.69.11.3394 PubMed Central PMCID: PMC389778. PMID: 4508329

26. Long EO, Dawid IB. Repeated genes in eukaryotes. Annu Rev Biochem. 1980; 49:727–64. https://doi.org/10.1146/annurev.bi.49.070180.003455 PMID: 6996571

27. Moss T, Mars J-C, Tremblay MG, Sabourin-Felix M. The chromatin landscape of the ribosomal RNA genes in mouse and human. Chromosome Res. 2019; 27(1–2):31–40. https://doi.org/10.1007/s10577-018-09603-9 PMID: 30617621

28. Puvion-Dutilleul F, Bachellerie J-P, Puvion E. Nucleolar organization of HeLa cells as studied by in situ hybridization. Chromosoma. 1991; 100(6):395–409. https://doi.org/10.1007/bf00337518 PMID: 1893795

29. Raska I, Shaw PJ, Cmarko D. New insights into nucleolar architecture and activity. Int Rev Cytol. 2006; 255:177–235. https://doi.org/10.1016/S0074-7696(06)55004-1 PMID: 17178467

30. Sharifi S, Bierhoff H. Regulation of RNA polymerase I transcription in development, disease, and aging. Annu Rev Biochem. 2018; 87:51–73. https://doi.org/10.1146/annurev-biochem-062917-012612 PMID: 29589958

31. Bártová E, Horáková AH, Uhlírová R, Raska I, Galiová G, Orlova D, et al. Structure and epigenetics of nucleoli in comparison with non-nucleolar compartments. The Journal of Histochemistry and Cytochemistry. 2010; 58(5):391–403. https://doi.org/10.1369/jhc.2009.955435 PubMed Central PMCID: PMC2857811. PMID: 20026667

32. Bersaglieri C, Santoro R. Genome Organization in and around the Nucleolus. Cells. 2019; 8(6). https://doi.org/10.3390/cells8060579 PubMed Central PMCID: PMC6628108. PMID: 31212844

33. Casafont I, Navascués J, Pena E, Lafarga M, Berciano MT. Nuclear organization and dynamics of transcription sites in rat sensory ganglia neurons detected by incorporation of 5'-fluorouridine into nascent RNA. Neuroscience. 2006; 140(2):453–62. https://doi.org/10.1016/j.neuroscience.2006.02.030 PMID: 16563640

34. Cmarko D, Smigova J, Minichova L, Popov A. Nucleolus: the ribosome factory. Histology and Histopathology. 2008; 23(10):1291–8. https://doi.org/10.14670/HH-23.1291 PMID: 18712681

35. Cmarko D, Verschure PJ, Rothblum LI, Hernandez-Verdun D, Amalric F, van Driel R, et al. Ultrastructural analysis of nucleolar transcription in cells microinjected with 5-bromo-UTP. Histochemistry and Cell Biology. 2000; 113(3):181–7. https://doi.org/10.1007/s004180050437 PMID: 10817672

36. Koberna K, Malínský J, Pliss A, Masata M, Vecerova J, Fialová M, et al. Ribosomal genes in focus: new transcripts label the dense fibrillar components and form clusters indicative of "Christmas trees" in situ. The Journal of Cell Biology. 2002; 157(5):743–8. https://doi.org/10.1083/jcb.200202007 PubMed Central PMCID: PMC2173423. PMID: 12034768

37. Lam YW, Trinkle-Mulcahy L. New insights into nucleolar structure and function. F1000Prime Rep. 2015; 7:48. https://doi.org/10.12703/P7-48 PubMed Central PMCID: PMC4447046. PMID: 26097721

38. Scheer U, Benavente R. Functional and dynamic aspects of the mammalian nucleolus. Bioessays: News and Reviews in Molecular, Cellular and Developmental Biology. 1990; 12(1):14–21. https://doi.org/10.1002/bies.950120104 PMID: 2181998

39. Shaw PJ, McKeown PC. The Structure of rDNA Chromatin. In: Olson MOJ, editor. The Nucleolus. New York, NY: Springer New York; 2011. p. 43–55.

40. Sirri V, Urcuqui-Inchima S, Roussel P, Hernandez-Verdun D. Nucleolus: the fascinating nuclear body. Histochemistry and Cell Biology. 2008; 129(1):13–31. https://doi.org/10.1007/s00418-007-0359-6 PubMed Central PMCID: PMC2137947. PMID: 18046571

41. Raška I, Reimer G, Jarník M, Kostrouch Z, Raška K Jr. Does the synthesis of ribosomal RNA take place-within nucleolar fibrillar centers or dense fibrillar components? Biology of the cell. 1989; 65(1):79–82. PMID: 2539876

42. Correll CC, Bartek J, Dundr M. The Nucleolus: A Multiphase Condensate Balancing Ribosome Synthesis and Translational Capacity in Health, Aging and Ribosomopathies. Cells. 2019; 8(8):869.

43. Cheutin T, O'Donohue M-F, Beorchia A, Vandelaer M, Kaplan H, Deféver B, et al. Three-dimensional organization of active rRNA genes within the nucleolus. Journal of Cell Science. 2002; 115(Pt 16):3297–307.

44. Haaf T, Hayman DL, Schmid M. Quantitative determination of rDNA transcription units in vertebrate cells. Experimental Cell Research. 1991; 193(1):78–86. https://doi.org/10.1016/0014-4827(91)90540-b PMID: 1995304

45. Smirnov E, Borkovec J, Kováčik L, Svidenská S, Schröfel A, Skalníková M, et al. Separation of replication and transcription domains in nucleoli. J Struct Biol. 2014; 188(3):259–66. https://doi.org/10.1016/j.jsb.2014.10.001 PMID: 25450594

46. Haaf T, Ward DC. Inhibition of RNA polymerase II transcription causes chromatin decondensation, loss of nucleolar structure, and dispersion of chromosomal domains. Experimental Cell Research. 1996; 224(1):163–73. https://doi.org/10.1006/excr.1996.0124 PMID: 8612682

47. Tollervey D, Kiss T. Function and synthesis of small nucleolar RNAs. Curr Opin Cell Biol. 1997; 9(3):337–42. https://doi.org/10.1016/s0955-0674(97)80005-1 PMID: 9159079

48. Tollervey D, Lehtonen H, Jansen R, Kern H, Hurt EC. Temperature-sensitive mutations demonstrate roles for yeast fibrillarin in pre-rRNA processing, pre-rRNA methylation, and ribosome assembly. Cell. 1993; 72(3):443–57. https://doi.org/10.1016/0092-8674(93)90120-f PMID: 8431947

49. Iyer-Bierhoff A, Grummt I. Stop-and-Go: Dynamics of Nucleolar Transcription During the Cell Cycle. Epigenet Insights. 2019; 12:2516865719849090. https://doi.org/10.1177/2516865719849090 PubMed Central PMCID: PMC6537492. PMID: 31206100

50. Pliss A, Kuzmin AN, Kachynski AV, Baev A, Berezney R, Prasad PN. Fluctuations and synchrony of RNA synthesis in nucleoli. Integrative Biology: Quantitative Biosciences from Nano to Macro. 2015; 7 (6):681–92. https://doi.org/10.1039/c5ib00008d PMID: 25985251

51. Hornáček M, Kováčik L, Mazel T, Cmarko D, Bártová E, Raška I, et al. Fluctuations of pol I and fibrillarin contents of the nucleoli. Nucleus. 2017; 8(4):421–32. https://doi.org/10.1080/19491034.2017.1306160 PubMed Central PMCID: PMC5597295. PMID: 28622108

52. Brejchova K, Trosan P, Studeny P, Skalicka P, Utheim TP, Bednar J, et al. Characterization and comparison of human limbal explant cultures grown under defined and xeno-free conditions. Experimental Eye Research. 2018; 176:20–8. https://doi.org/10.1016/j.exer.2018.06.019 PMID: 29928900

53. Stadnikova A, Trosan P, Skalicka P, Utheim TP, Jirsova K. Interleukin-13 maintains the stemness of conjunctival epithelial cell cultures prepared from human limbal explants. Plos One. 2019; 14(2): e0211861. https://doi.org/10.1371/journal.pone.0211861 PubMed Central PMCID: PMC6370187. PMID: 30742646

54. Dundr M, Hoffmann-Rohrer U, Hu Q, Grummt I, Rothblum LI, Phair RD, et al. A kinetic framework for a mammalian RNA polymerase in vivo. Science. 2002; 298(5598):1623–6. https://doi.org/10.1126/science.1076164 PMID: 12446911

55. Smirnov E, Hornáček M, Kováčik L, Mazel T, Schröfel A, Svidenská S, et al. Reproduction of the FC/DFC units in nucleoli. Nucleus. 2016; 7(2):203–15. https://doi.org/10.1080/19491034.2016.1157674 PMID: 26934002

56. Schermelleh L, Solovei I, Zink D, Cremer T. Two-color fluorescence labeling of early and mid-to-late replicating chromatin in living cells. Chromosome Res. 2001; 9(1):77–80. https://doi.org/10.1023/a:1026799818566 PMID: 11272795

57. Golding I, Cox EC. RNA dynamics in live Escherichia coli cells. Proc Natl Acad Sci USA. 2004; 101 (31):11310–5. https://doi.org/10.1073/pnas.0404443101 PubMed Central PMCID: PMC509199. PMID: 15277674

58. Lionnet T, Czaplinski K, Darzacq X, Shav-Tal Y, Wells AL, Chao JA, et al. A transgenic mouse for in vivo detection of endogenous labeled mRNA. Nat Methods. 2011; 8(2):165–70. https://doi.org/10.1038/nmeth.1551 PubMed Central PMCID: PMC3076588. PMID: 21240280